ACOUSTICAL ANALYSIS AND DESIGN OF HORN TYPE LOUDSPEAKERS

A THESIS SUBMITTED TO
THE GRADUATE SCHOOL OF NATURAL AND APPLIED SCIENCES
OF
MIDDLE EAST TECHNICAL UNIVERSITY

BY

AYHUN ÜNAL

IN PARTIAL FULFILLMENT OF THE REQUIREMENTS
FOR
THE DEGREE OF MASTER OF SCIENCE
IN
MECHANICAL ENGINEERING

DECEMBER 2006

Approval of the Graduate School of Natural and Applied Sciences

Prof. Dr. Canan ÖZGEN
Director

I certify that this thesis satisfies all the requirements as a thesis for the degree of Master of Science

Prof. Dr. Kemal İDER
Head of Department

This is to certify that we have read this thesis and that in our opinion it is fully adequate, in scope and quality, as a thesis for the degree of Master of Science

Prof. Dr. Mehmet ÇALIŞKAN
Supervisor

Examining Committee Members

Prof. Dr. Samim ÜNLÜSOY (METU,ME) _____

Prof. Dr. Mehmet ÇALIŞKAN (METU,ME) _____

Prof. Dr. Tuna BALKAN (METU,ME) _____

Asst. Prof. Dr. Yiğit YAZICIOĞLU (METU,ME) _____

Prof. Dr. Yusuf ÖZYÜRÜK (METU,AEE) _____

I hereby declare that all information in this document has been obtained and presented in accordance with academic rules and ethical conduct. I also declare that, as required by these rules and conduct, I have fully cited and referenced all material and results that are not original to this work.

Name, Last name: Ayhun ÜNAL

Signature :

ABSTRACT

ACOUSTICAL ANALYSIS AND DESIGN OF HORN TYPE LOUDSPEAKERS

Ünal, Ayhun

M.S., Department of Mechanical Engineering

Supervisor: Prof. Dr. Mehmet ÇALIŞKAN

December 2006, 142 pages

Computer aided auto-construction of various types of folded horns and acoustic analysis of coupled horn and driver systems are presented in this thesis. A new procedure is developed for auto construction of folded horn shapes. Linear graph modeling technique is employed for specification of horn driver output in terms of diaphragm velocity or throat pressure. In the final phase of the design procedure, acoustic analysis of folded horns is carried by means of finite element analysis. A commercial software package MSC.ACTRAN is used to calculate directivity patterns and resulting acoustic pressure in the free field.

Horn geometry consisting of linear, exponential, hyperbolic and tractrix shapes is automatically constructed by parallel working of Delphi and finite element analysis program. The enclosure bordering the horn contours are considered rigid in the analyses. Maximum number of folding is limited to two. This study is made possible to evaluate the performance of these four types of horn contours for a specified range of frequencies.

Keywords: Horn Loudspeakers, Linear Graphs, Electro-Mechano-Acoustical Circuits, Acoustic Finite Element Analysis.

ÖZ

BOYNUZ TİPİ HOPARLÖRLERİN AKUSTİK ANALİZİ VE TASARIMI

Ünal, Ayhun
Yüksek Lisans Makina Mühendisliği Bölümü
Tez Yöneticisi: Prof. Dr. Mehmet ÇALIŞKAN
Aralık 2006, 142 sayfa

Bu çalışmada, çeşitli boynuz tipi hoparlörlerin bilgisayar destekli tasarımı ve sürücü ve hoparlörlerin bir bütün olarak akustik analizi sunulmaktadır. Katlamalı boynuz tipi hoparlörlerin geometrilerinin otomatik olarak oluşturulması için yeni bir yöntem geliştirilmiştir. Hoparlörler sürücüsünün çıktısının diyafram hızı veya giriş basıncı olarak belirlenmesi için çizge kuramı uygulanmıştır. Tasarım prosedürünün son aşamasında, katlamalı boynuz tipi hoparlörlerin akustik analizi için sonlu eleman analiz yöntemi kullanılmıştır. Yönelme biçimleri ve serbest alandaki akustik basınçları hesaplamak için ticari bir yazılım paketi olan MSC.ACTRAN kullanılmıştır.

Konik, üstel, hiperbolik ve traktriks şekilli, boynuz tipi hoparlörler geometrisi Delphi ve sonlu elemanlar analiz programlarının birlikte çalışması ile otomatik olarak üretilmektedir. Boynuz hoparlörleri sınırlayan kenarlar analiz sırasında katı olarak farz edilmektedir. Azami katlama sayısı ikiyle sınırlıdır. Bu çalışmayla dört tip hoparlörlerin belirlenen çalışma frekansları için performanslarını değerlendirmek mümkündür.

Anahtar Kelimeler: Boynuz Tipi Hoparlör, Çizge Kuramı, Elektro-Mekano-Akustik Devreler, Akustik Sonlu Eleman Analizi.

To My Family

ACKNOWLEDGMENTS

The author wishes to express his deepest gratitude to his supervisor Prof. Dr. Mehmet ÇALIŞKAN for his guidance, advice, criticism, encouragements and insight throughout the research.

The author would like to thank Alper YALÇINKAYA, Ferhan FIÇICI for their suggestions and comments.

The author would also like to thank Mehmet YENER, Bora KAT and Levent İPEK for their support and helps in software and hardware.

Finally the author wishes to thank to his family and Feriha ŞAHİN whose encouragement and support were invaluable throughout this study.

TABLE OF CONTENTS

LIST OF TABLES

TABLES

CHAPTER 5

APPENDICES

LIST OF FIGURES

CHAPTER 1

CHAPTER 3

CHAPTER 4

CHAPTER 5

APPENDICES

LIST OF SYMBOLS AND ABBREVIATIONS

SYMBOLS

a	Radius of horn mouth
A_a	A-Type active element
b_m	Mechanical damping of driver suspension in linear graph
B	Magnetic flux density in driver air gap
c	Speed of sound
C	Circumference
C_1, C_2	Constants
C_{AB}	Acoustical compliance of air in the back cavity
C_{AF}	Acoustical compliance of air in the front cavity
C_B	Acoustical capacitance of air in the back cavity in linear graph
C_F	Acoustical capacitance of air in the front chamber in linear graph
C_M	Mechanical compliance of the driver suspension (=1/k_M)
dx	Differential length
e_g	Driver voltage
f	Through variable
f_c	Cut-off frequency
f_s	Resonance frequency of driver in free-air
f_u	Desired upper frequency limit
F_{CM}, F_{EM}, ..	Forces on mechanical circuit
f_{bm}, f_{km}, f_{mm}	Forces on linear graph
h_a, h_b	Integrated through variable
h	Height
i_g	Driver current
k	Wave number (=ω/c)
K_{MD}	Mechanical stiffness of the driver suspension
k_m	Mechanical stiffness of the driver suspension in linear graph
l	Effective length of voice coil
L_T	Total length of horn
L_1	Axial length before the folding

L_F	Axial length of the folding part (Arc Length)
L_E	Voice coil inductance
m	Flare constant
M	Family parameter of horns
M_{MD}	Mechanical mass of driver diaphragm assembly
m_m	Mechanical mass of driver diaphragm assembly in linear graph
n	Polar coordinate flare constant
p, p(x,t)	Acoustic Pressure
plc	Placement factor
P_r	Power transmission ratio
P_{CA}, P_{CL}, P_{RA}	Pressures on acoustical circuit
P_{CB}, P_{CF}, P_{RB}	Pressures on linear graph
P_1, P_2	Driver Input Power
P_{NE}	Nominal electrical input power
q	Ratio of the cross sectional area (=S_2/S_1)
Q	Volume Velocity
Q_{CB}, Q_{CF}, Q_{RB}	Volume velocities on linear graph
Q(t)	Flow
Q_{ES}	Electrical Quality Factor
Q_{MS}	Mechanical Quality Factor
Q_{TS}	Total Quality Factor
r, r_1, r_2	Annulus of radius
$Ratio_{W/H}$	Width to height ratio of rectangular cross-section
r_M	Radius of mouth
r_T	Radius of throat
r_x	Radius at the distance x
R	Resistance
R_{AB}	Acoustical resistance of the back cavity
R_B	Acoustical resistance of the back cavity in linear graph
R_E	Voice coil resistance
R_{MD}	Mechanical resistance of driver suspension
R_T	Acoustical resistance term at throat

r_x	Radius at the distance x from the mouth
S(x)	Cross-sectional area
S_0	Initial Area
S_D	Area of diaphragm
S_t	Throat Area
S_M	Mouth Area
S_1, S_2	Cross-sectional area of the first and second conduit (pipe)
T(t)	Torque
U_D	Volume velocity emitted by diaphragm
U_F, U_L	Volume velocity on acoustical circuit
x, y, z	Cartesian coordinates
x_a, x_b	Integrated across variable
X	Reactance
X_T	Acoustical reactance term at throat
v	Across variables
v_D	Driver cone velocity
v_{bm}, v_{km}, v_{mm}	Velocities on linear graph
V_{AB}	Volume between planes A and B
$V_{A'B'}$	Volume between planes A' and B'
V_{as}	Equivalent volume of suspension
V_B	Volume of back cavity
V_F	Volume of front cavity
V_{rms}	Driver rms voltage
v_{EMF}	EMF voltage at transformer
v_{LE}	Voltage of inductor
v_{RE}	Voltage of resistor
$V_g(t)$	Voltage of driver voice coil in linear graph
V_{ga}	Amplitude of $V_g(t)$
V_{RE}	Voltage of resistor in linear graph
V_F	Front chamber volume
Z_{AL}	Radiation loading of the horn

ϕ	Velocity potential
w	Width
α	Attenuation term arising from the expanding geometry
β	Bulk modulus of elasticity
ε_{ac}	Acoustic Strain
ξ	Infinitesimal distance
λ	Wavelength
λ_c	Critical wavelength
μ	Damping coefficient
ψ	Single valued monotonic function
ρ_0	Density of air
θ	Polar angle (angle of bend)
$\Omega(t)$	Angular velocity
ω	Angular frequency (=2πf)

ABBREVIATIONS

1-D	One dimensional
2-D	Two dimensional
3-D	Three dimensional
B	Number of Branches
BEM	Boundary Element Method
CPU	Computer
EMF	Electro Motive Force
FDEC	Finite Difference Equivalent Circuit
FEA	Finite Element Analysis
FEM	Finite Element Method
MEM	Memory
N	Number of Nodes
Rms	Root Mean Square
SPL	Sound Pressure Level
SR	Sensitivity Rating
TQWT/QWT	(Tapered/) Quarter Wave Tube
TR	Turns Ratio

CHAPTER 1

INTRODUCTION

Horns are considered as acoustic transformers matching the impedance of air to that of the driver piston. Horns are used for increasing the radiation and control the direction of the radiation from a sound source such as loudspeaker. Driver assembly, front and back cavity and horn are the major parts of horn-loudspeakers (Fig. 1.1). Driver assembly consists of diaphragm (cone) and suspension system. The horn contour is the expansion (flare) rate of a horn.

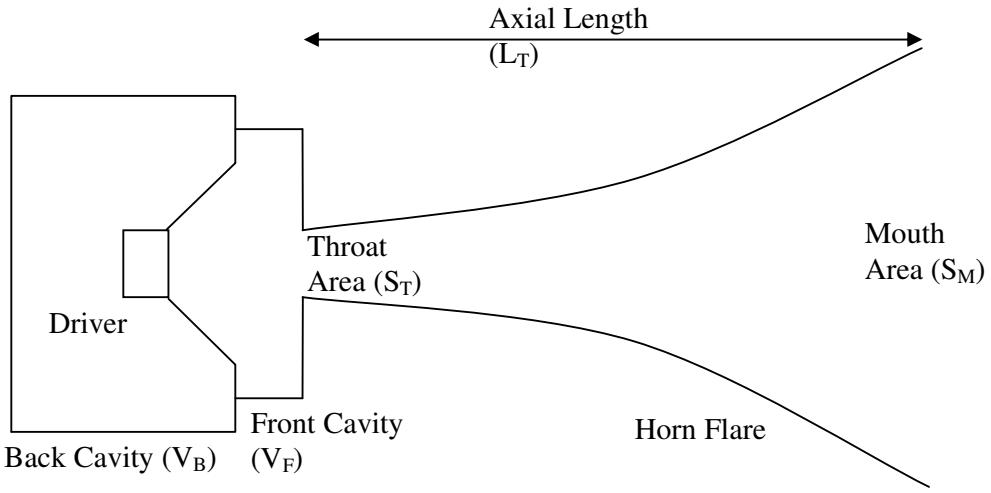

Fig. 1.1 Schematic drawing of a horn driver system

Loudspeakers are basic devices for generating sound through electrodynamic transformation. Electric impulse is transformed through some kind of mechanical system (for instance cone) into acoustic energy (also mechanical energy). Horn loudspeakers have been used to produce higher acoustical powers efficiently and to control the directivity pattern of radiated sound. One of the prominent advantages of

horn loudspeakers is their high efficiency. A horn system is a lot more efficient than any other type of enclosure due to impedance matching characteristics. A horn can be considered as an acoustic transformer. The horn permits the driver displacement to be small without sacrificing acoustic output. This means lower distortion and/or higher power handling. For example, while moving coil driver has a power transmission efficiency of 10-50% when it is horn loaded, the efficiency is less than 1% when used as a direct radiator. A horn will be effective in any given frequency range depending only on the size of its mouth and the rate of its flare. Acoustic size is a wave of a certain frequency that has a wavelength equal to the speed of sound divided by the frequency. If an object or dimension, like the diameter of the mouth of a horn, is the about the same as or larger than the wavelength of a given frequency, then that object or dimension is acoustically large at that frequency. The horn contour is the expansion (flare) rate of a horn. There are typically different equations mathematically describing the shapes of different flare types. The most appropriate curves for audio application are conical, exponential, hyperbolic, tractrix contours and permutations between them. Furthermore, cut-off frequency (or flare frequency) is the lower frequency limit of the horn-driver combination. The flare frequency really describes how fast the horn flare while the cut-off frequency describes how low in frequency the horn / driver's response is usable, but in typical horns these frequencies are fairly close. The throat of the horn can be as big as the transducer (driver) cone or smaller. Horn size is determined by the unalterable wavelength of sound. The lower the frequency is, the longer the wavelength. Because a horn loudspeaker takes up quite a bit of space and physical dimensions of unfolded bass horn (horns for low frequency) can be so large, which is non-practical, the horn should be stuffed into a box which may require folding the horn one or more times.

Traditionally, loudspeaker driver parameters are derived through electrical impedance measurement techniques. These parameters are commonly called Thiele/Small parameters, after Neville Thiele and Richard Small who are credited with developing industry-standard loudspeaker modeling techniques. One of the other methods to model electroacoustic transducers (loudspeakers) is to describe its basic system components using lumped elements which are analogous to those in

electrical networks. The subject of electro-mechano-acoustics is the application of electrical circuit theory to the solution of mechanical and acoustical problems. The lumped element system modeling is then represented using an equivalent electrical circuit representation. The goal of the equivalent circuit analysis is to solve for the velocity of the cone.

Up to now there have been many efforts to generate horn contours and geometry, indeed several commercial software have been developed. Furthermore, loudspeakers have modeled by using impedance and mobility analogies. Despite of all of these efforts, there is no full design and complete analysis process reported for horn speakers from beginning to end. These are distinct studies and almost all focused on whether construction of horn geometry or modeling the loudspeakers. In addition, it is very rare to come across construction of three dimensional (3-D) horn geometry especially folded horn geometries. Also there are no analyses open to the public use showing the effects of folding. In many texts, horn is accepted as infinite horn and its impedance is added to the equivalent circuit to realize complete acoustic analysis. In this thesis, it is aimed to achieve computer aided parametric design and acoustic analysis of horn loudspeakers as a whole for finite length horns of different contours. A new procedure is developed for auto construction of folded or non-folded finite length horn shapes. Some folding equations have been generated according to various horn flare. A different loudspeaker modeling technique, linear graph modeling technique, is also employed for the specification of horn driver output in terms of diaphragm velocity or throat pressure. Finally, complete acoustic analysis of (folded) horns is carried by means of acoustic finite element analysis.

The study consists of three main parts, namely (i) construction of various kinds of horn geometries automatically in accordance with basic acoustic design requirements, (ii) determination of electro-mechano-acoustical system outputs by using linear graph technique and finally, (iii) applying finite element analysis to obtain acoustical behavior of the constructed horns according to the first step due to an input diaphragm ring velocity calculated in the second step.

For step (i), cut-off frequency, types of cross-sectional area of the mouth and throat, maximum horn length are the primary designing parameters. A computer interface called as “Folded Horn Design” has been developed to facilitate the construction of the horn geometry by reducing the geometrical modeling time in a commercial finite element modeling (FEM) software. This interface works jointly with the FEM code and provides users opportunities such that they can change the primary design parameters. Horns will be modeled according to these specified parameters. Codes abide by acoustic design criteria have been written in Pascal language to achieve this parametric design. In accordance with these codes, secondary and major designing parameters such that flare rate, throat and mouth area of the horn, length of the horn can be calculated and whether the folding is required or not will be determined. Maximum number of folding is limited to two. After all, horn geometry consisting of linear, exponential, hyperbolic and tractrix shapes are automatically constructed by means of generation of a “*.proc file”. “*.proc file” is a procedure file which can be run automatically on MSC.Marc-Mentat from the simple button “construction” on the interface of Folded Horn Design. Construction of the finite element model of horns made the acoustic analyses possible for a specified range of frequencies.

In order to model the loudspeaker, linear graph modeling which has the ability to manage complex relationships between inputs and outputs is preferred in the second step (ii). Because of the fact that the usage of linear graph modeling can enhance simulation of the driver model and allow for accurate and simpler representations of real life scenarios between different mediums (electrical, mechanical and acoustical). The electrical and mechanical properties of the horn driver are modeled in terms of lumped parameters by linear graph modeling technique. Linear graph models express systems in terms of energy flow and can be used to identify key factors (state variables) that influence system behavior. For each physical domain (electrical, mechanical and/or acoustical in this case) the various parameters are grouped or ‘lumped’ and assigned to categories for 1-port elements if they supply store, or dissipate energy, and a 2-port element if they convert energy.

Numerical calculation of the acoustic field radiated from a loudspeaker is a computer-aided tool in loudspeaker design and development. The radiated sound field expression depends on the velocity distribution on the loudspeaker vibrating diaphragm. This velocity distribution is determined from lumped system linear graph modeling of driver system. Since analysis of the impedance and radiation properties of complex shaped acoustic horns is a very difficult task in the sense that the computational complexity, finite element analysis (FEA) can be used to analyze the acoustic radiation characteristics of any arbitrarily shaped object and the analysis of the acoustical properties of the horns are easily performed by finite element method. A commercial software package MSC.ACTRAN is used to calculate directivity patterns and resulting acoustic pressure in the free field. For example, the magnitude of the pressure field decays by the distance in radial direction. In polar direction the variations of the pressure field are called directivity, and these variations are typically constant with distance. In combination with a lumped-parameter linear graph model of the loudspeaker driver, the FEM model will be used to calculate the directivity and pressure distribution of the horns. The walls bordering horn contours are considered rigid in the analysis.

The material in this dissertation is organized in six chapters. The second chapter will briefly discuss some of the previous efforts and review of literature pertaining to horn and loudspeaker design.

Chapter 3 is describes the design considerations and horn flare equations. Methodology for the design and (auto-) construction of various kinds of horn geometries in accordance with basic acoustic design requirements will be developed. Horn geometries will be parametric and automatically constructed by proper algorithms and software prepared within the context of this chapter.

Chapter 4 is a detailed overview of loudspeaker modeling techniques. Two applications of loudspeaker modeling will be presented. One of them electro-mechano-acoustic circuit modeling and the other one is linear graph modeling. Driver cone velocity will be determined by using linear graph modeling technique.

Chapter 5 contains a series of acoustic finite element analysis that investigate the acoustical performance, sound pressure levels and directivity characteristics of the coupled horn and driver systems.

The final chapter is a summary and an evaluation of the work done in this thesis and offers some suggestions for future work that could be undertaken to design and analysis of horn type loudspeakers.

Appendices contain some parts of the source code developed during this study and some useful information related with the concerned topics.

CHAPTER 2

LITERATURE SURVEY

2.1. Horn Speakers

Since high power audio-frequency amplifiers are costly, it is a requirement to reduce the amplifier output to a minimum by use of high efficiency loudspeakers. Horn loudspeakers have been used to obtain large acoustic power and to control of the directivity pattern of radiated sound. A horn can be viewed as an acoustic transformer that couples the air at the surface of the diaphragm with the air outside of the horn, thus matching high pressure/low volume to low pressure/high volume. The name acoustic (impedance) transformer derives from this model of description. The horn contour is the expansion (flare) rate of a horn. There are few curves appropriate for audio application; these are conical, exponential, hyperbolic, tractrix contour and permutations between them depending on designer's needs. Parabolic horns are so inefficient that they are really of no practical use. Horns require compression drivers. These transducers produce high pressure but little displacement. The diaphragm therefore moves very little, which results in less distortion than a conventional radiating driver. Horn drivers need high magnet strengths to produce the high pressure.

It is not aimed to find new practical formula for the transmission of sound waves through different shaped horns, but because of changes of direction inherent in folded horns new approaches will be developed to find proper function at the folding parts. In this text, while construction of horn geometry, primary designs criteria and solutions for the equations of acoustical waves to the conditions of a boundary of arbitrary cross section S(x) will be applied. For some of the horn flare type (conical and exponential) plane-wave propagation along the propagation axis will be assumed. While for the tractrix horn the assumption is that, wavefront is spherical and of the same radius throughout the sound progression. In addition to these, for the

hyperbolic horn exact solution of the hyperbolic horn will be carried out. Below, contributors of horn equations and how they contribute will be discussed briefly.

2.2. Preliminary Studies on Horns

In the early days of sound reproduction, amplifiers supplied extremely modest powers and loudspeakers were not very efficient at all. A horn was advised to increase sound pressure of not very efficient driver. For example, Edison attached a tin horn to his phonograph in 1877 to couple the small vibrations of the diaphragm to the air load. Mainly straight conical horns were employed for the early horns, but the later gramophones of that period employed large flaring horns with either straight or curved axes depending on the overall length. After a while Lord Rayleigh analyzed the transmission of acoustic waves in pipes of varying section and gave the analysis of sound through a conical pipe [1]. Rayleigh also studied on bends in tubes of constant cross section and effects of these bends on transmitted sounds for varying range of wavelengths.

In the beginning of 1920s Webster [2], Hanna and Slepian [3] and Flanders [4] carried out theoretical analyses based on the work of Lord Rayleigh, but extending the work to the full audio range at domestic listening levels. These analyses were mainly based on exponential contour.

In 1919 Webster wrote the fundamental paper on the theory of audio horns [2]. This work was concerned with loading a diaphragm for maximum output. By applying the fundamental properties of acoustical waves to the condition of a boundary of arbitrary cross section S(x) and assuming plane-wave propagation along the axis of the device, Webster developed the fundamental horn equation:

$$\frac{1}{S(x)}\frac{d}{dx}\left(S(x)\frac{dp}{dx}\right)-k^2 p=0 \tag{2.1}$$

$$\frac{\partial^2}{\partial t} p(x,t) = c^2 \frac{1}{S(x)} \frac{\partial}{\partial x}\left(S(x) \frac{\partial}{\partial x} p(x,t) \right) \tag{2.2}$$

Webster had also worked out an approximate theory for other types of horn and had deduced that exponential was the optimum contour. Circular cross-section, straight axis and plane wavefronts were major assumptions. Webster's equation models the propagation of pressure waves in a horn assuming that no transverse modes exist. Under this assumption any point within the horn falls on some isophase surface which spans the cross section of the horn.

In 1927 Ballantine also expanded the theory by defining Bessel horns, adding them to the known conical and exponential forms [6]. He did this by transforming Webster's equation into Bessel's equation with the substitution of $S(x)=x^n$ in Eqn.(2.1). Ballentine's paper also contains an excellent discussion of the assumption behind the linearization of the fluid dynamic equations, which are necessary to derive the horn equation.

On the other hand Wilson [7] had independently derived the analysis of the exponential horn working from Rayleigh's treatise. According to his assumption the wavefront had a spherical shape and always cutting the contour of the horn wall and lateral axis of the horn at right angles This assumption, that initially flat wavefront at the throat and the curvature of the wavefront would gradually increase, satisfies also the condition specified Hanna and Slepian [3] and later by Crandall [8] that the wavefront as it emerges from the open end will be equivalent to that provided by a spherical surface, as opposed to that produced by a flat piston.

Voigt described TQWT/QWT (Tapered Quarter Wave Tube/ Quarter Wave Tube) uses like a transmission line design pipe length of 1/4 wavelength of driver's resonance frequency in 1930 [9]. TQWT and QWT stands for (tapered) quarter wave tube and are also referred as Voigt Pipes. By its shape TQWT is a conical horn with relatively high cutoff frequency. The driver is not placed at the apex of a horn as usual but rather at 1/3 of horn's length. Voigt had commenced his analysis on the

assumption that wavefront within the horn is spherical and of the same radius throughout propagation through the horn. His approach was based on the assumption that the entire wavefront must propagate at the speed of sound and constant throughout the horn. This requires that the horn contour should be the tractrix. The tractrix is sometimes called the tractory or equitangential curve. It is a curve well-known in the world of mechanics. According to Bos [10], the tractrix was first studied by Huygens in 1692, who gave it the name "tractrix". Later, Leibniz, Johann Bernoulli and others studied the curve. Different authors on loudspeaker horns have proposed different ideas about approximating a square or rectangular horn shape to the tractrix contour. Voigt preferred the section height to equal the diameter of the (round) tractrix. The area of a square horn is then 1.27 times larger than the tractrix contour, and the circumference, to which some researchers pay great attention, will be even larger compared to the circular circumference. To calculate from the circumference, on the other hand, would yield a smaller area from square horns than the circular tractrix, and since the square and rectangular shapes are compromises anyway, it seems safe not to complicate things more than necessary.

2.3. Works after the Webster Theory

Lindsay [11] employed the horn theory of Webster [2] for the connector in the form of $S=S_0\varphi(x)$. Transmission through conical connectors, Bessel connectors of higher order, exponential connectors and the connectors whose generating curve have a point of inflection had been analyzed.

In 1940 Freehafer [12] published an exact solution for a hyperbolic horn. It was the first formulation of a horn that was not based on Webster's equation. In 1946 Vincent Salmon returned to the plane-wave assumption and produced two significant papers on horn theory [13], [14]. He generalized the plane wave horn theory and unified estimating the performance of a given horn. He also obtained relations among the admittance components and the shape parameters. The first paper has a figure comparing the radiation impedance predicted by the exact theory of Freehafer's and the approximate Webster's equation. The two results differ by as

much as about 30% for a 30^{o} horn at ka=0.6. Geddes [11] discussed the possibility that this error is due to the approximate nature of Webster's equation and also dictated that Salmon was not concerned with, is that the two different wavefront shapes.

Mawardi [15] tried to solve Webster's equation for the arbitrary shape of horn contours and tried to develop generalized methods of solution. In order to solve Webster's equation for the approximate formulation of the propagation of sound waves in horns, he used two methods of approach. The first method considered a transmission line with variable parameters as the electrical analogue of the horn. This approach was especially useful in yielding generalized solutions for horns of finite length. Transmission line modeling of acoustic elements is a good compromise between accuracy and computational complexity. The second method, based on an investigation of the singularities of Webster's differential equation, lead to the discovery of a great number of new families of horns. Locanthi used this approach when he performed an analog computer simulation of horn-loaded compression drivers [19].

Applicability of (2.1, 2.2) for engineering analysis of the acoustic horn is somewhat explained by Eisner's 1964 discussion [18] on the history of (2.1, 2.2), wherein Eisner notes it was first developed and solved for an acoustic horn in a paper published in 1764 by Daniel Bernoulli [19]. All this history aside, details on the development of equations (2.1, 2.2) are readily available in basic textbooks on loudspeakers, e.g. Beranek [16] and Olson [17].

2.4. Follow up Studies on Horns

In 1927, the wider bandwidth of the Rice-Kellogg [5] direct radiator loudspeaker and availability of higher-power amplifiers all but removed the horn loudspeaker from home audio systems. After 1927, horn loudspeakers were only found in theater public announcement (PA) systems, until the introduction in the late '40s of the Klipschorn, which spawned a revival of horn loudspeakers in the '50s. The

introduction of high-power solid-state amplifiers and small bookshelf speakers in the '60s removed horns from home audio systems. In the early '90s, the hipe of SET tube amplifiers spurred a new interest in horn designs.

At the cut-off frequency (f_c), the throat reactance peaks, whereas the throat resistance is zero and rises to its maximum value above the cut-off frequency (Fig. 9.9, Beranek [16]). This frequency f_c is called the cut-off frequency because for frequency lower than this no power will be transmitted down the horn and theoretically, a bass horn should give response down to the flare frequency but, Edgar [26] observed that throat reactance (which rises as the flare frequency is approached) choked off the low end response of a horn before the flare frequency is reached. However, Wente and Thuras [20] at Bell Labs and Klipsch [21] independently found that throat reactance could be cancelled out by using sealed back chamber. Klipsch also stated that the volume of the cavity behind the cone is given by the throat area multiplied by the speed of sound divided by 2π times the cut-off frequency. This technique, which Plach [23] termed "reactance annulling", allows for bass response right down the flare frequency. Leach [24] showed that, for a number of exponential horn examples reactance annulling does not occur at the flare but a higher frequency. He eliminated this problem by choice of a hyperbolic horn rather than exponential horn [25]. After considering all above, Edgar [26] combined the Keele and Leach approach and presented formulae for calculating the theoretical optimum throat size and back chamber volume for a given driver/horn combination.

Horn-loaded loudspeakers, and particularly low frequency horn-loaded loudspeakers, are commonly used in applications where large, linear sound outputs are needed such as in sound reinforcement and active noise cancellation. For example, theater loudspeakers as large as or larger than eight feet in length and four feet by four feet in transverse physical dimensions were built in order to obtain reproduction of low frequencies in the audible range. Because low frequency horns can be very large, the physical dimensions of this kind of horn loudspeakers may be reduced by folding the horn. Olson [17] (pp. 206-209); Klipsch [22], Olson and Massa [27], Wente and Thuras [20], Hilliard [28] were the introduced some typical examples of the folding

the horn. Prior art low frequency folded exponential horn loudspeakers, such as those which are disclosed in the above-cited references, are, nevertheless, bulky and structurally complex due to the structure of the folded exponential horn which defines the sound path from the electroacoustic transducer to the volume into which sound waves are radiated.

Even when size of a horn is reduced with folding(s), they are still pretty big. In order to reduce horn size without loosing too much low bass performance, Klipsch brought up a matter that horn mouth is placed into a corner to increase the acoustical output of the horn mouth [21]. Klipsch was responsible for what is considered a mutually accepted stereotype of a classic corner horn, with apparently the highest name recognition associated with it. The Klipsch Corner Horn arrived in the mid 1940's, and is still currently being manufactured.

Sheerin [37] investigated the bends of a horn. Time-waveform measurements were taken at multiple points in a plane down the center of various bend shapes. These measurements were then processed to allow visualization of sound waves of various frequencies propagating through these bends. Finally he showed the deviation between experiencing performance and predictions.

A horn provides more sound pressure level (SPL) at a given listening area by increasing the directivity of the sound towards the listener. Early researcher generally paid very little attention to the directivity of the horn, but Sherrer and his design team at MGM (MGM turned to the Lansing Manufacturing Co. in Los Angeles that grew into the Altec Lansing Co. by 1941 and JBL in 1955, the industry leader in motion picture loud speakers) sound department worked on a development project that considered directivity control as a primary factor in horn design. By assuming the horn directional wide coverage could be obtained by using splayed array. It was a large two-way system that had much in common with an earlier system that had been designed for auditory perspective experiments at Bell Laboratories. The Shearer system used high-frequency multicellular horns driven by a driver with an annular slit phasing plug. On the other hand Keele considered the problem of designing a

horn that had both good loading and directivity control in his paper on constant directivity horn theory [29]. In this paper he proposed a horn in two sections. The section near the throat was exponential for good loading while the outer section was conical for good directivity control. This combined horn had two very sought after traits. It presented good loading to the driver to which it was attached allowing for an increase in the efficiency of the horn. It also maintained good directivity control over a wide range of frequencies. He had also investigated optimum size of a horn mouth [30] and for a number of different throat entry diameters and design coverage angles; the size of the aperture between the two sections of the waveguide was near its optimum size according to his work.

In 1977 Henricksen and Ureda [31] introduced what they called the Manta-Ray horn. It was named for its shape. This horn had good loading as well as good directivity control. However, it did suffer in some areas. One in particular was that it had rather severe astigmatism in the curvature of its wavefront. The radius of curvature for the wavefront was different for the horizontal and vertical planes. Accordingly, the shape of the wavefront from such a device could, at best, be ellipsoidal. While this doesn't seem to be the cause for concern when the horn is used by itself, when more than one horn is employed in an array it can be problematic. This astigmatism was common to a number of horn designs within the industry at the times.

J. Dinsdale [38] had outlined the physical principles underlying the operation of horns, and had shown how, provided basic rules were followed, sound reproduction of startling clarity and realism is possible from horns.

The assumption of a piston-like motion is valid only at low frequencies. At higher frequencies, this approximation may not hold, owing to the breakup modes of the driver diaphragm. However, this assumption is still beneficial for determination of loudspeaker's sound radiation. Generally, the starting point to compute the sound field at any spatial point inside a propagation medium is the evaluation of Rayleigh's surface integral [1], which is a statement of Huygens' principle that the total sound field at an observing field point P into the propagation medium is found by summing

the radiated hemispherical waves from all parts of the vibrating surface. It is difficult to solve analytically Rayleigh surface integral except in very special cases such as the acoustic pressure on the axis of a transducer. Various authors have proposed different theoretical approaches to transform this integral into an analytically tractable expression [32, 33]. Kaddour et al. [34] presented theoretical, computational and visualization solutions for the sound (pressure) field in air, produced by a loudspeaker, using a numerical method called Convolution Method (CM). This method uses the convolution product of the acceleration function of the radiating surface and the impulse response for a specific field.

Klippel [35, 36] has developed an acoustic transmission line model to describe finite-amplitude sound in horns and ducts with reflection by using conical one dimensional (1-D) elements. Each element is represented by a linear four-pole plus a nonlinear source of volume velocity, derived from the nonlinear wave equation in Lagrangian coordinates.

The derivation of Webster's equation carried out in Benade and Jansson [39] was exceptionally illuminating. Their method allowed any choice of acoustic wavefronts propagating in the bore as long as axial symmetry is preserved. One of the other recent researchers who worked on Webster's classic horn equation is Rienstra [40] and he rederived some generalizations systematically, as an asymptotic perturbation problem, from a number of modeling assumptions by the method of slow variation.

In recent years Geddes [41] and Putland [42] had put forth works on horns that have the properties of propagating a one-parameter acoustic wave. The motion of such a wave can be described by a single spatial coordinate. These types of horns have been referred to as waveguides. A good differentiation between a horn and a waveguide can be thought of as a horn being primarily concerned with the optimal loading of its driver, while a waveguide is primarily concerned with its directional characteristics.

Geddes [41] examined the mathematical foundation of the horn theory, analyzed the Webster's horn equation for the directivity-controlling devices and developed

another general formulation of the acoustic waveguide problem. He tried to determine boundary contour shape that will allow an accurate prediction of the acoustic variables, which are pressure contours, velocity vector, and acoustic impedance, at any point in the device; and find a way to determine the optimum shape.

Putland [49] seems to be the first author to actually specify the only three coordinate systems that produce exact solutions for one parameter wavefields: planar (1-D), cylindrical (2-D), and spherical (3-D). Putland noted that these and only these coordinate systems are capable of exactly specifying all the acoustic quantities (pressure, particle velocity, intensity, etc.) by a single spatial coordinate. When predicting and comparing the acoustical properties of horns it is a customary practice to formulate the propagation as a one-parameter plane wavefront problem. One-parameter waves, however, are possible only in rectangular, circular cylindrical and spherical coordinates, which correspond to pipes of uniform cross-section and conical horns, respectively. However, when particular attention is paid to the rapid flare near the mouth of a horn structure such as the tractrix, it also seems plausible to formulate the propagation on the basis of a one-parameter spherical wavefront theory. By visualizing the surfaces of constant phase as spheres of constant radii of a and the flow lines as tractrix having a generating arm of length of a; one-parameter wave equation and Ricatti impedance equation can be derived. Solutions to these equations have been obtained by wave perturbation and by analog computer techniques. Axial response and throat impedance measurements are compared with theoretical calculations postulating first a hemispherical and then a plane piston radiation pattern. It appears that the most satisfactory explanation lies somewhere in between these two limiting cases.

Traditionally, the air chamber is treated as a boundary value problem which results in the solution of the wave equation for the general case in which the horn throat enters the air chamber in any circumferentially symmetrical manner. The following specific cases were analyzed by Smith [43]; (1) the case in which the horn throat enters the air chamber by means of a single orifice, (2) the horn throat enters the air chamber by

means of a single annulus of radius r and width w, and (3) the horn throat enters the air chamber in “m” annuluses of radii r_1…..r_m and widths w_1…..w_m. His analysis revealed that the radial perturbation caused by the horn throat excites higher order modes. At the resonant frequencies of these modes the horn throat pressure becomes zero and the loudspeaker does not radiate. By suitable choice of annulus radii and widths the first "m" modes may be suppressed and the corresponding nulls in the output pressure eliminated.

It was shown by Holland et al. [44] that a horn of arbitrary flare rate can be analyzed by subdividing the horn into small sections of flare rate for which an analytical solution to equation (2.1 or 2.2) is available. Short sections of cylindrical, conical, or exponential curves may be fitted to some arbitrary and complex flare. The input and transfer impedances of each of these sections can be determined analytically from solutions to equation (2.1 or 2.2). These may be collected together as a sectioned transmission line model of varying impedance, from which the total input and transfer impedance may be calculated.

2.5. Loudspeaker Modeling

A horn loudspeaker consists of an electrically driven diaphragm coupled to horn. In order to analyze horn speaker system, diaphragm (cone) velocity of loudspeaker or sound pressure on the cone should be found. In this text these outputs will be found by applying lumped-parameter linear graph modeling and there are many attempts to generate equivalent circuit models in the literature. Various kinds of analogies similar to linear graph have been performed so far. The purpose is the application of electrical-circuit theory to obtain governing dynamic equations for mechanical and acoustical systems. Not only a schematic representation of the components and their connections make it possible to visualize and understand the system, but also the differential equations can be formed directly from these schematic diagrams.

2.6. Historical Development of Loudspeaker Modeling

Since the earliest days of electrical theory, electro-motive force became endowed with the mechanical force of hydraulic pressure and electric current had been thought as a mechanical velocity or the velocity of the fluid flow. Historically, the first analogy to be used between electrical and mechanical systems was the force–voltage analogy, as is readily seen in the early use of the term electromotive force. Firestone [45] and others established another consistent system of analogies based upon certain mathematical similarities between electrical current, force, and pressure on the one hand, and voltage, velocity, and fluid flow on the other. The older "classical" analogy is the "voltage-force-pressure" analogy while the Firestone analogy (originally called "mobility" analogy) is often referred to "current-force-pressure" analogy. Firestone also introduced the ideas of through and across variables which provide a unifying framework to extend analogies to other contexts, e.g., acoustic, thermal, fluid systems. On the other hand Olson used the impedance analogy in his books [17]. Typical example of this was the analogous circuit for a bass reflex loudspeaker. In 1954 Beranek [16] presented a very comprehensive acoustical circuit derivation. He used impedance analogy for the electrical side but for the mechanical side he preferred to mobility analogy and the voice coil acted as a transformer between the mechanical and acoustical circuits. So, whole domains could have been drawn as one circuit. In this work the diaphragm velocity, sound pressure and efficiency for the low frequency response were developed. In 1959, Novak [46] presented a generalized theory on the design and performance of vented and closed-box loudspeaker enclosures.

The usual procedure for the loudspeaker system design is calculation of the driver's fundamental electro-mechanical parameters by using Thiele-Small parameters. The Thiele-Small [47-53] approach is to first analyze the electro-mechanical behavior of a speaker voice coil, magnet, and cone, interacting with the cone suspension and the air in and outside the enclosure. The Thiele-Small method for speaker design considers the linear loudspeaker model driven by voltage sources and operating in a small signal environment. The resulting equation is mathematically identical to the

equation describing a purely electrical "equivalent circuit" consisting solely of resistors, capacitors and inductors. The sound produced by the loudspeaker can then be obtained via a relatively simple circuit analysis. The evolved theory of filter synthesis can be used to adjust circuit parameters to obtain a desired frequency response. The parameters can then be translated back into physical quantities, such as enclosure size, to build the loudspeaker. This procedure provides a scientific framework for the art of loudspeaker design. A very useful result is that after the speaker has been assembled, the electrical impedance at the speaker terminals can be measured and compared to the theory. In this method, the considered parameters are linear and valid only for small signals.

While the electrical circuit approach was very suitable for simple loudspeaker systems, complex acoustical loading was still difficult to include. In 1972 Howard [54] modeled complex-loading conditions by converting the acoustical properties into equivalent mechanical mass and compliance units and constructed analogous acoustical circuits.

Thiele [51, 52] demonstrated the possibility of fitting a speaker adjusting the power amplifier output resistance, making it positive or negative, according to the method proposed by Werner and Carrel [55].

2.7. Studies on Loudspeakers after Thiele/Small parameters

At low frequencies, where the wavelength is much longer than the largest physical dimension of the device, a distributed system can be lumped into idealized discrete circuit elements. Generally, the successful models of moving-coil loudspeakers in enclosures are based on equivalent circuits. These models have the convenient ability to represent the complete signal path, from electrical input to acoustic output, in a single circuit diagram. However, all such models are low-frequency approximations developed for the purpose of calculating and optimizing the bass roll off of the driver. Keele presented the first comprehensive and simplified design methodology for bass horns [56]. He showed most horn design parameters could be calculated

from Thiele/Small parameters for the driver. Leach [24] extended Keele's work by introducing losses into the model and constructed a standard equivalent circuit model of a horn such as described in Olson's book [17], but substituted a gyrator for the usual transformer between the electrical and mechanical sections of the model. He then made some simplifying assumptions, such as the output impedance of the driving source is negligible, and derives a set of equations based on Thiele / Small parameters. Earlier analyses of horn loudspeakers [16] driven from amplifiers with moderately high output impedances calculated the efficiency as the ratio of acoustic output power to maximum power available from the source. The set of equations lets one work from a given driver specification to design a horn to cover a specified frequency range or work from a horn specification to design the optimal driver. One thing to note is that the simplifying assumptions are significant. For example, Leach assumes an infinite exponential horn as the load. For very small (undersized) horn, Leach's equations will probably not predict the exact results. There is also no provision made for such things as folds in the horn, parallel side walls, etc.

Most of the earlier work in modeling low-frequency, voice-coil loudspeakers treated them as lumped-parameter linear systems as Beranek described [16] for loudspeakers without enclosures, Small [47], [48], and [49] for loudspeakers in sealed enclosures, Thiele [51], [52], and [53] for loudspeakers in vented enclosures, and [46] and [57] for loudspeakers in both sealed and vented boxes. The lumped-parameter loudspeaker model, although simple, captured much of the nonlinear behavior of the loudspeaker. In addition, the model formulation allowed a straightforward application of modern control system methods and lent itself well to modern parametric identification techniques. They are ground works and become industry standards, but they are not sufficient in analyzing today's high-performance loudspeakers, which are typically driven beyond their linear output range. More significant was the work by [58], [59], and [60], where lumped-parameter nonlinear models were analyzed.

In order to predict the internal resonances in the enclosure an equivalent-circuit model can be modified to account for the effects of damping materials added in an

effort to suppress resonances [47, 63]. However, when the original model is valid only at low frequencies, the version with added damping can do no more than predict the "side- effects" of damping on the low-frequency roll off; it cannot predict the degree to which the damping material achieves its primary purpose of suppressing resonances in the midband. These deficiencies are tried to overcome using the "finite-difference equivalent-circuit" (FDEC) model by Putland [64]. He offered an equivalent-circuit model of a loudspeaker which took account of the wave-like nature of the acoustic field in the enclosure and the effects of the resulting resonances on the system response. The differential equations describing an acoustic field have been approximated by the finite-difference method and the resulting difference equations have been written as the nodal equations of a three-dimensional L-C network. This was shown before, for Cartesian and cylindrical coordinates, by Arai [65] in 1960. Arai's method is valid for general curvilinear orthogonal coordinates.

Linear modeling of the driver and the horn is likely to fail at high drive levels. The various studies of nonlinearity in electroacoustic drive units have been summarized in the papers of Sherman and Butler [66, 67]. For horn loudspeakers, the modeling of driver nonlinearities has been discussed by Klippel [35, 36] and Schurer et al. [68].

In addition, Al-Ali [69] designed a low-frequency, feedback control method to improve the nonlinear performance of the loudspeaker system and he evaluated performance by developing a suitable distortion measure for use in design. Data from experiments performed on a variety of actual loudspeakers have been used to confirm that the methods can produce predictable and measurable improvements in the nonlinear performance of a low-frequency, voice-coil loudspeaker (attached to either vented or sealed enclosures). Furthermore, he studied on the linearizing effect of feedback using a linear controller of nonlinear systems.

A method to modify the mechanical characteristics of a loudspeaker (seen by the excitation source) through the amplifier output impedance has been considered by Stahl [78]. This method consists of making the power amplifier output resistance equal to the negative of the voice-coil resistance. In this way, the amplifier output

and voice-coil resistance cancels each other and the amplifier sees the loudspeaker mechanical circuit as a load. Normandin [79] has also exploited this method. The circuit proposed by Stahl was only able to generate a negative output resistance proportional to the voice-coil resistance, and not to the electric impedance. This fact restricted such a solution to the low frequency domain, since the voice-coil inductive reactance increases as frequency increases.

The radiated sound field expression depends on the velocity distribution on the loudspeaker vibrating diaphragm. This velocity distribution is determined from a complex computation and vibration analysis. Several authors have expanded the velocity potential in spherical Bessel and Legendre functions, or used alternative methods to calculate the sound radiation from a loudspeaker [70–77].

2.8. Recent Works

Since resent amplifiers have low output impedance, to design an enclosure means to determine its intrinsic characteristics (internal volume, tuning, and absorption, among others) to fit it with a loudspeaker or to adapt a loudspeaker to the enclosure, or even to adopt both the procedures. For this reason, the process concentrates only on the electro-acoustic side of the system. It does not consider the electric resistance of the connections and cables between the amplifier and speaker, which can lead to a considerable problem source [80]. Bortoni et al. [81] presented a comparative analysis through simulations of the sound pressure level and cone displacement of loudspeaker systems as an infinite baffle, a closed box, a vented box and band-pass enclosure driven by voltage and current sources, under small (linear) and large (non-linear) signals. The nonlinearities of the voice-coil, force factor and compliance of the loudspeaker were considered.

Knowledge about the interface of horn and driving electro-acoustical system and the description of the driving system are the keys to the simulation of horn driver and horn. Couples of investigations concerning this interface and the electro-acoustical source itself have been carried out by Behler and Makarski [82]. In this work, it was

shown that the two-port approach leads to reliable simulation results. Furthermore a measuring method to derive the driver's two-port parameters was presented, but this method suffered from the restricted frequency range of the used Kundt's tube. In order to extend the frequency range Makarski described two methods to obtain the two-port parameters without using any acoustical measurements [83]. Electrical impedance measurements and acoustical reference impedance as well known acoustical load were used for the both methods. The driver's two-port parameters were presented in this method using only electrical measurements and an acoustical reference impedance and this method was valid for wider frequency range.

2.9. Finite Element Models of Loudspeakers

After computers have allowed to the usage of complex models based on numerical approximation like finite element models, traditional horns can be analyzed with the boundary element method (BEM) or finite element method (FEM) instead of (or together with) analytical or simple numerical tools. Since just using simple numerical tools to analyze a folded horn is very complicated. Finite Element Method/Boundary Element Method become more and more interesting for the simulation of loudspeaker's enclosures and horn geometry as the performance of computers increases rapidly. BEM, also known as the Integral-equation method, it uses a discretisation of the surface of an object and a set of velocity or pressure boundary conditions to calculate an acoustic field, either into a free-field, or into an enclosed space. In this study FEM will be used to analyze constructed folded or non-folded horns.

A model was reported in 1984 by Sakai et al. [84], who used the finite-element method to calculate the acoustic impedance presented by the enclosure to the back of the diaphragm. Their model was fully three-dimensional and allowed the shape of a conical diaphragm with a specified semi-apex angle to be accurately represented. They also gave an equivalent-circuit model of the driver and enclosure, incorporating the enclosure impedance. However, instead of solving the circuit with the computed impedance in place, the authors used a mass-limited approximation to the circuit and

assumed that the radiated pressure is proportional to the diaphragm acceleration, obtaining a simple formula expressing the sound pressure level in terms of the impedance of the enclosure.

CHAPTER 3

CONSTRUCTION OF HORN GEOMETRY

In this chapter primary design criteria for acoustical waves confined to a solid boundary of arbitrary cross section S(x) will be developed. For some type of the horn flares (conical and exponential) plane-wave propagation along the propagation axis will be assumed. While for the tractrix horn the assumption is that, wavefront is spherical and of the same radius throughout the progression. In addition to these, for the hyperbolic horn exact solution of the hyperbolic horn will be carried out. The horn contour is the expansion (flare) rate of a horn. There are typically different equations mathematically describing the shapes of different flare types. The most appropriate curves for audio application are conical, exponential, hyperbolic, tractrix contours and/or permutations between them. Construction of horn geometry will be performed for the conical, exponential, hyperbolic and tractrix forms.

It is of significant importance to use as much as possible priori knowledge comprising of geometrical pattern, frequency response range (upper and lower frequency limits) and driver parameters. Frequency limits will be selected for the low to mid band horn speakers. From these parameters and conditions one can decide on the required horn length, mouth and throat sizes. If these dimensions (especially length) are out of given required range, a geometrical modification such as folding the horn should be performed. Horn geometries will be parametric and automatically constructed by proper algorithms and software prepared within the context of this chapter. A computer interface called as “Folded Horn Design” has been developed in Delphi to facilitate the construction of the horn geometry by reducing the geometrical modeling time in commercial finite element software. This interface works jointly with MSC.Marc-Mentat and provides users opportunities such that they can change the primary parameters and horns will be modeled according to these parameters.

3.1. Horns

Horns are considered as acoustic transformers matching the impedance of air to that of the piston. They convert acoustic energy at high pressure and low velocity (volumetric velocity) at the throat to energy at low pressure to high velocity at the mouth. Horns have been used for increasing the radiation and control the direction of the radiation from a sound source such as loudspeaker.

A horn system is a lot more efficient than any other type of enclosure. For the same sound pressure level (SPL), the driver in horn has smaller excursion than the driver in any other type of boxes or in open air. Therefore, the horn driver operates linearly and produces less distortion. The horn permits the driver displacement to be small without sacrificing acoustic output. This means lower distortion and/or higher power handling.

For a horn loudspeaker, directivity and high efficiency are very important design parameters. High efficiency can be achieved by various ways. One popular method is to design the system so that driving force works against resistance instead of reactance part of the vibrating diaphragm of driver. As a result, more power is radiated at low frequencies for a given source strength (cone velocity).

A horn consists of a tube of varying sectional area. When sound passes through a tube or conduit and if there is a change in the cross-sectional area, power transmission should be considered. Neglecting the viscous damping, power transmission ratio (P_r) is given by

$$P_r = \frac{4q^2}{\left(q^2+1\right)^2} \tag{3.1}$$

where, q^2 is the ratio of the two cross sectional area S_2/S_1 and S_1, S_2 are the cross-sectional area of the first and second conduit (Fig.3.1).

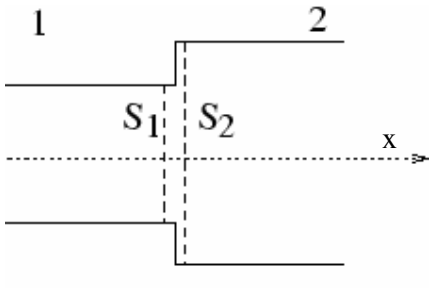

Fig. 3.1 Tube consisting of two different cross-sectional areas

The more gradually the transition from one cross-sectional area to the other, the better transmission of sound is achieved [11]. Sound transmission should be unity or approach to the unity as soon as possible for the working frequency range. This can be done by choice of conical, exponential, hyperbolic or tractrix form as seen in Fig.3.2.

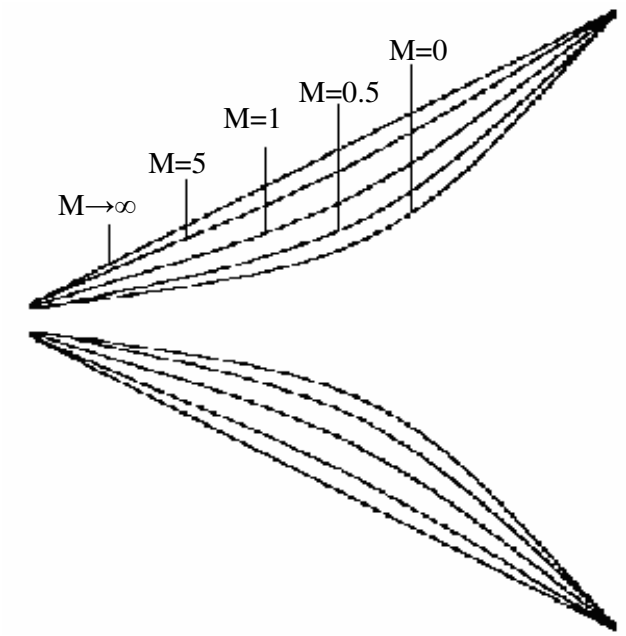

Fig. 3.2 Different flare types of horns. (M: family parameter, M=1 means exponential, M→∞ means conical, 0<M<1 Hyperbolic and M=0 means catenoidal)

For optimum loading of the driver, the impedance presented by the horn throat should be (close to) entirely resistive and of constant value throughout the working frequency range (Fig. 3.3). Below the cut-off frequency, the throat resistance is very low or zero and rises rapidly to its ultimate value of $S_t/\rho_0 c$ as the frequency increases over the cut-off frequency. (Where S_t is the throat area, ρ_0 is the density of air and c is the speed of sound.) Especially the one whose rate of taper (flare) is small near the throat region of the horn. From this point of view one can deduce from Fig.3.3 that exponential and hyperbolic contours suit better. However, non-linear distortion should be also taken into account before deciding. At the moment it can be said that for minimum distortion at given power per unit area, the conical horn is the best.

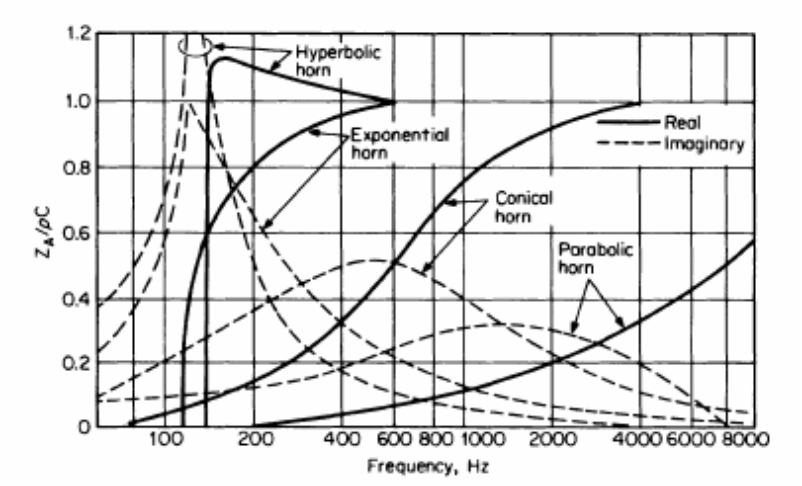

Fig. 3.3 Acoustical Resistance (Real) and Reactance (Imaginary) vs. Frequency curve at the throats of infinite horns, [38]

For horns the fundamental physical principles of mass and momentum conservation are expressed in terms of an acoustic pressure, *p(x, t)*, by the Webster equation (3.2)

$$\frac{\partial^2}{\partial t^2} p(x,t) = c^2 \frac{1}{S(x)} \frac{\partial}{\partial x}\left(S(x) \frac{\partial}{\partial x} p(x,t) \right) \tag{3.2}$$

which describes plane-wave propagation in a duct of slowly varying cross-sectional area, *S(x)*, where *c* is the speed of sound in the ambient medium. The fluid is compressible and ideal (homogeneous and non-viscous), adiabatic and low Mach number disturbances, small *p(x, t)* compared to the bulk modulus of the medium, and that the rigid tract walls are the linearizing assumptions.

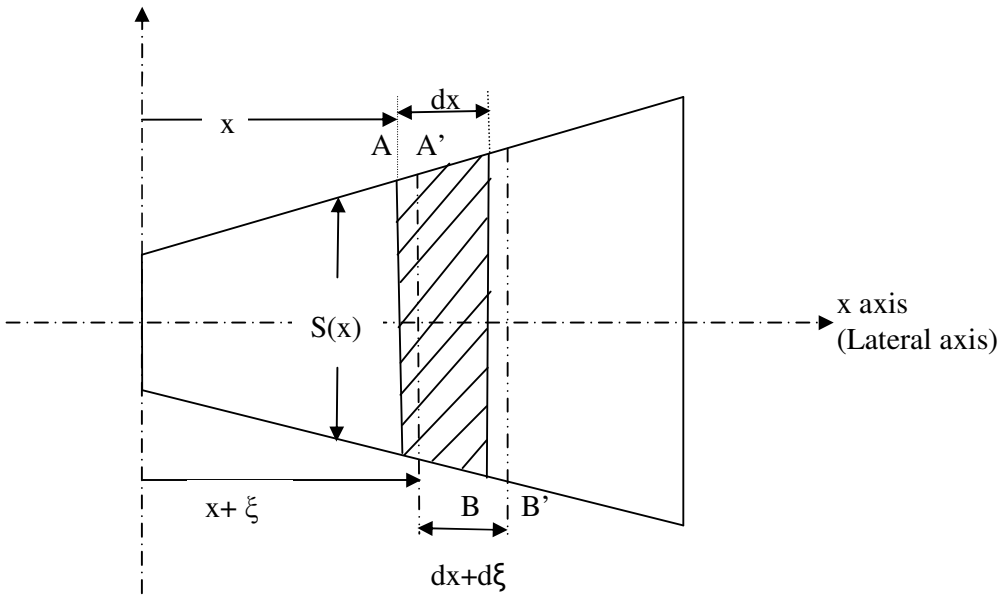

Fig. 3.4. Volume element S(x)dx of a horn

Consider the volume element of infinitesimal length dx and area S(x) within the horn (Fig. 3.4.). The small air volume between the planes A and B moves to a new position and now bounded by the planes A' and B'. The mass of air in these two volumes remains constant. In Fig. 3.4, it can be seen that the plane A has moved an infinitesimal distance (ξ) and that the original length of the volume has increased from dx to (dx + dξ). Clearly the original mass of air expands as it moves in the positive x direction to fill the increasing cross-sectional area of the horn. Fig. 3.4 shows the two positions for the small volume of air. By the way one should note that $dx > \xi > d\xi$.

The volumes V_{AB} and $V_{A'B'}$ correspond to first and second locations respectively can be expressed as;

$$V_{AB} = S(x)dx \tag{3.3}$$

$$V_{A'B'} = S(x+\xi)\left(dx + d\xi\right) \tag{3.4}$$

where

$$S(x+\xi) = S(x) + \left(\frac{\partial}{\partial x} S(x)\right)\xi \tag{3.5}$$

An expression for the pressure distribution in a horn can be derived for function of position and time. Using the above expressions for the two volumes, first the acoustic strain can be calculated, then multiplying the acoustic strain (ε_{ac}) by the bulk modulus of air (β), as defined in Kinsler and Frey [85], results in an expression for the pressure.

$$p(x,t) = -\rho c^2 \varepsilon_{ac}(x,t) \tag{3.6}$$

Where

$$\varepsilon_{ac}(x,t) = \frac{V_{A'B'} - V_{AB}}{V_{AB}} \tag{3.7}$$

After substituting the equations for the volumes, doing a little algebra and canceling the higher order terms, the acoustic pressure can be written as a function of the cross-sectional area and the displacement.

$$p(x,t) = -\frac{\rho c^2 \left(\left(\frac{\partial}{\partial x} S(x)\right)\xi(x,t) + S(x)\left(\frac{\partial}{\partial x}\xi(x,t)\right)\right)}{S(x)} \tag{3.8}$$

$$p(x,t) = -\frac{\rho c^2 \left(\frac{\partial}{\partial x} \left(S(x) \xi(x,t) \right) \right)}{S(x)} \tag{3.9}$$

Because the internal pressure decreases when the incremental volume increases as it moves from AB to A'B', a negative sign is included in the above equation 3.6 and so does equation 3.8. The forces acting on the volume AB generate the motion and the resulting change in position to A'B'. Figure 3.4 presents a free body diagram showing all of the forces acting on the small volume of air between planes A and B.

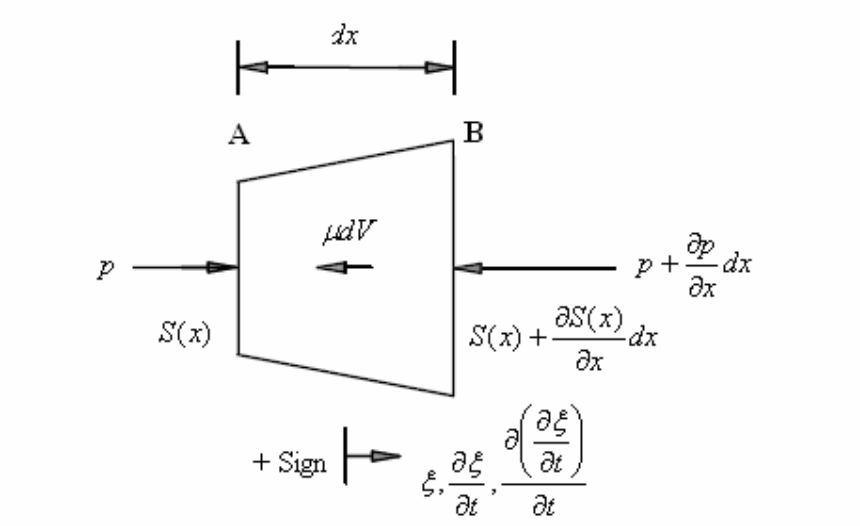

Fig. 3.5 Free body diagram of a small volume of air between planes A and B.

Summing the forces, and setting the result equal to the inertial acceleration, results in the equation of motion.

$$p(x,t)S(x) - \left(p(x,t) + \left(\frac{\partial}{\partial x} p(x,t) \right) dx \right) S(x) - \mu S(x) dx \left(\frac{\partial}{\partial t} \xi(x,t) \right) = \rho S(x) dx \left(\frac{\partial^2}{\partial t^2} \xi(x,t) \right) \tag{3.10}$$

μ is the damping coefficient acting on the volume. After some manipulation,

$$-\left(\frac{\partial}{\partial x}p(x,t)\right)-\mu\left(\frac{\partial}{\partial t}\xi(x,t)\right)=\rho\left(\frac{\partial^2}{\partial t^2}\xi(x,t)\right) \tag{3.11}$$

Substituting Equation (3.8 or 3.9) to eliminate the pressure term in Equation (3.11) produces the final differential equation of motion.

Throughout the text, the solution of several types of longitudinal section will be shown and corresponding horn geometry will be constructed. Exponential, conical, tractrix and hyperbolic type of horns with mouths of rectangular shapes are considered in the study.

3.1.1. Exponential Horn Contour

In order horn to be a satisfactory transformer, its cross-sectional area should increase gradually along its axis. Cross-sectional area of the ideal exponential horn increases logarithmically along its length from throat to mouth. For this shape, the cross-sectional area at any point along the x axis is given by the formula;

$$S(x)=S_T e^{mx} \tag{3.12}$$

and

$$S(0)=S_T \quad S(L)=S_M=S_T e^{mL} \tag{3.13, 3.14}$$

Where S: cross-sectional area at x in square meters

S_T: cross-sectional area of the throat in square meters

S_M: cross-sectional area of the mouth in square meters

m: flare constant (1/meter)

x: distance from throat in meters

Substituting Equation (3.12) for S(x) value to Equation (3.8) gives Equation (3.15);

$$p(x,t)=-\rho c^2\left(m\xi(x,t)+\left(\frac{\partial}{\partial x}\xi(x,t)\right)\right) \tag{3.15}$$

Putting Equation 3.15 into Equation 3.11 provides the final differential equation of motion for the exponential horn.

$$c^2\left(\left(\frac{\partial^2}{\partial x^2}\xi(x,t)\right)+m\left(\frac{\partial}{\partial x}(\xi(x,t))\right)\right)-\frac{\mu\left(\frac{\partial}{\partial t}\xi(x,t)\right)}{\rho}=\frac{\partial^2}{\partial t^2}\xi(x,t) \tag{3.16}$$

After some manipulation and using separation of variables techniques and setting the damping term μ to zero leaves the classic exponential horn wave equation found in most acoustics texts. The solution of displacement and pressure can be found as functions of times and position. Detailed calculation of the differential equation is not the aim of this text. In order to have detailed description, one can benefit King's [86] derivation.

$$\xi(x,t)=\left(C_1e^{((-\alpha-j\beta)x)}+C_2e^{((-\alpha+j\beta)x)}\right)e^{(j\omega t)} \tag{3.17}$$

$$p(x,t)=j\rho c^2\left(C_1(j\alpha+\beta)e^{((-\alpha-j\beta)x)}-C_2(-j\alpha+\beta)e^{((-\alpha+j\beta)x)}\right)e^{(j\omega t)} \tag{3.18}$$

where α is an attenuation term arising from the expanding geometry.

$$\alpha=\frac{m}{2} \tag{3.19}$$

$$\gamma=\frac{\sqrt{4\omega^2-m^2c^2}}{2c} \tag{3.20}$$

Up until now, wave equation is tried to be solved and calculations came to the important point in the name of determining mouth area. γ depends on the value of the frequency. If $(4\omega^2\text{-}m^2c^2)<0$ then γ is imaginary, resulting in an additional attenuation term but no power will be transmitted because acoustic impedance is entirely reactive. If $(4\omega^2\text{-}m^2c^2) > 0$ then γ is real and wave motion exists in the horn. The frequency at the limit of attenuation to wave motion is cut-off frequency and can be calculated from $(4\omega^2\text{-}m^2c^2) = 0$.

Since

$$\omega = 2\pi f \tag{3.21}$$

$$f_c = \frac{mc}{4\pi} \tag{3.22}$$

By knowing desired cut-off frequency the flare constant (m) can be calculated and the horn profile may then be constructed. Whether the horn mouth is circular or not (square), horn mouth should have a circumference large enough so that the radiation impedance is nearly resistive over the desired frequency range. In order to provide this, as Beranek [16] shown, the relationship $ka>1$ or $C/\lambda>1$ must hold. Where k is wave number, a is radius of mouth, C is circumference and λ is the wavelength. At this condition horn starts to efficiently transfer energy into the environment. He concluded this by finding mechanical impedance of the air load at the horn mouth, using plane circular piston mounted in an infinite surface assumption. If mouth area (S_M) is wanted to be find at this critical condition, $S_M= \lambda_c^2/4\pi$ should be solved. This is the minimum mouth area. But, there is one more thing such that all of this referring to the situation where the horn is suspended in a free space, meaning radiation into an angle of 4π solid radians. If the horn placed on the ground the mouth would only radiate into half a solid angle (2π solid radians), against a center of a wall π solid radian and in a corner formed by two walls and the floor only $\pi/2$ solid radians. The significance of this is the fact that, while minimum mouth area has been shown to be $\lambda_c^2/4\pi$ when suspended in free space, this value may be divided by a factor 2 when the solid angle is halved. This factor has an effect on radius in square root. So the final equation for the horn mouth radius (r_M) is,

$$r_M = \frac{c}{2\pi f_c \sqrt{plc}} \tag{3.23}$$

Where plc is the placement factor and 1 for free space, 2 for radiation on ground, 4 for radiation on ground near the wall, 8 for radiation in the corner.

While determining the throat area shunt capacitance is the important design criteria. When a cavity is placed between the diaphragm and throat, it behaves as a shunt capacitance across the throat itself. For high frequencies, the throat reactance approaches zero and the resistance approaches $\rho c/S_T$. As Dinsdale [38] mentioned, by making the cavity impedance equal to the throat impedance, the cavity-throat combination acts as low pas filter. i.e.

$$\frac{S_D^2 \rho c^2}{2\pi f_u V_F} = \frac{\rho c S_D^2}{S_T} \tag{3.24}$$

where S_D is the area of diaphragm, V_F is the volume of front cavity, S_T is the throat area, f_u refers to desired upper frequency limit.
Hence, the throat area of the horn can be calculated as,

$$S_T = \frac{2\pi f_u V_F}{c} \tag{3.25}$$

In this text throat area will be calculated in terms of the Thiele/Small driver parameters similar to Edgar [26] formula. Assuming the fact that $Q_{MS} >> Q_{ES}$, then $Q_{TS} \approx Q_{ES}$ for all frequency range.

$$S_T = \frac{2\pi f_s Q_{ES} V_{as}}{c} \tag{3.26}$$

where Q_{ES} is the electrical quality factor, Q_{MS} is the mechanical quality factor, f_s is the resonance frequency of driver in free-air and V_{as} is the equivalent volume of suspension (m^3)
The size of the compression chambers depends on the driver and the working frequency range. For compression chamber volume Keele's [56] formula can be performed during calculation which is simple practical formula for the use of fundamental electro-mechanical driver parameter, first derived by Klipsch [21]. V_B is the back volume (volume of compression chamber next to horn throat).

$$V_B = \frac{V_{as}}{\frac{f_c}{f_s Q_{TS}} - 1} \tag{3.27}$$

or, to obtain the correct rear cavity volume for reactance annulling V_B ($V_{as} \gg V_B$) can be calculated in terms of the Thiele/Small driver parameters. Keele mentioned a comparative listing of horn design equation for S_T and V_B in Table I [56].

$$V_B = \frac{V_{as} f_s Q_{TS}}{f_c} \tag{3.28}$$

Since r_M can be calculated from equation (3.23). Area of the mouth can be found either for the circular cross-section but then it can be turned to rectangular cross-section for the equivalent area and one can find corresponding width (w) and height (h) by knowing desired width to height ratio.

$$S_M = \pi r_M^2 \tag{3.29}$$

$$w = \sqrt{\frac{S_M}{Ratio_{W/H}}} \qquad \text{or} \qquad h = \sqrt{S_M Ratio_{W/H}} \tag{3.30}$$

Where $Ratio_{W/H}$ is the width-to-height ratio of the rectangular cross-section

All of the equations from equation (3.23) to equation (3.30) also valid for other type of flare profiles. Therefore while deriving the equation of different type of horns, these similar equations will not be repeated. Author will focus mainly on calculation of flare contour. Continuing from exponential contour, the last important parameter to find is axial length. After some modification on equation (3.14) and taking logarithm of both side results the following equation (3.31);

$$L_T = \frac{Ln(\frac{S_M}{S_T})}{m} \tag{3.31}$$

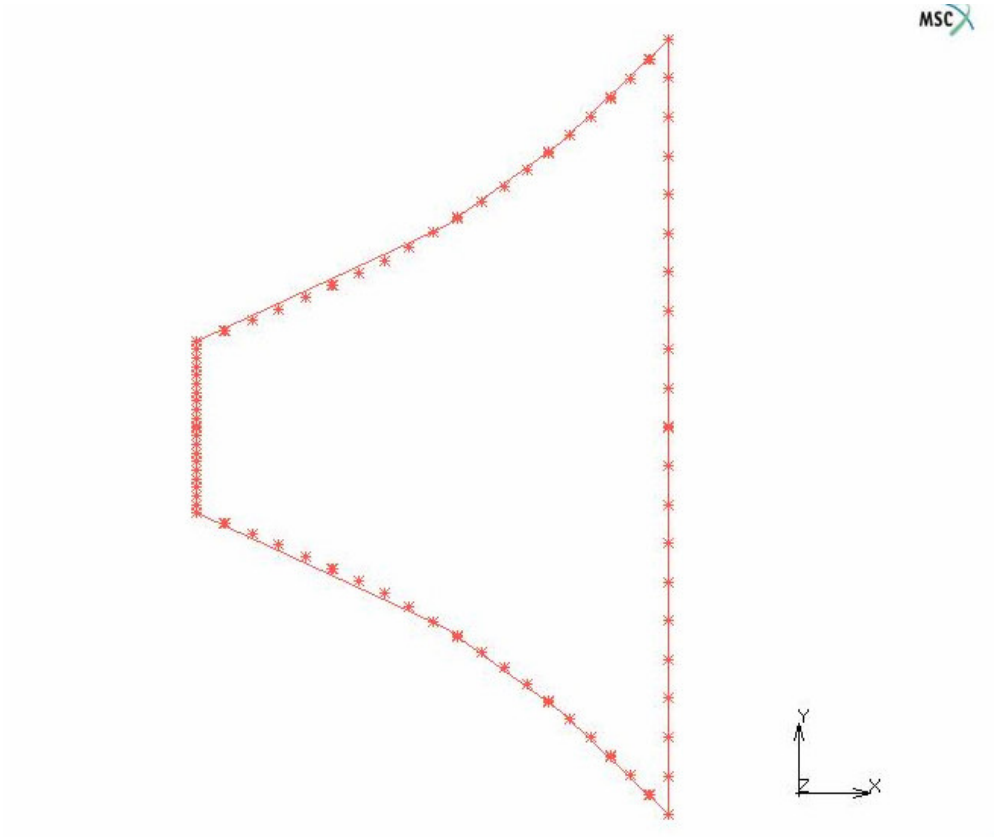

Fig.3.6 Top view of a non-folded exponential horn contour

3.1.2. Conical Horn Contour

The conical horn is the easiest one to calculate and stuff into a box, but it's also the least efficient. Conical contours are seldom employed for bass horns, because of the poor response and the impossibly long horns that result. This type of horn is a particular case of the Bessel horn and its shape is given by

$$S(x) = S_T \frac{x^2}{x_0^2} \tag{3.32}$$

An alternative approach to the previous analysis of the acoustic horn is to express equation (3.2) in terms of velocity potential ϕ, and by using the transformations

$$p = \rho \frac{\partial \phi}{\partial t} \tag{3.33}$$

And

$$\frac{\partial p}{\partial x} = \frac{\partial p}{\partial \phi}\frac{\partial \phi}{\partial x} = \left[\frac{\rho}{p}\frac{\partial p}{\partial t}\right]\frac{\partial \phi}{\partial x} \tag{3.34}$$

And finally the wave equation becomes

$$\frac{\partial^2 \phi}{\partial t^2} - c^2 \frac{\partial \phi}{\partial x}\frac{\partial}{\partial x}\left(\log S(x)\right) - c^2 \frac{\partial^2 \phi}{\partial x^2} = 0 \tag{3.35}$$

Inserting equation (3.32) to equation (3.35) for S(x) gives;

$$\frac{\partial^2 \phi}{\partial t^2} = c^2\left[\frac{\partial^2 \phi}{\partial x^2} + \frac{2}{x}\frac{\partial \phi}{\partial x}\right] = \frac{c^2}{x}\frac{\partial^2 (\phi x)}{\partial x^2} \tag{3.36}$$

In this text just the solution of this equation will be given, detailed calculation is out of purpose and can be found in basic acoustic books.

$$\phi = \frac{C_1}{x}e^{j(wt-kx)} + \frac{C_2}{x}e^{j(wt+kx)} \tag{3.37}$$

After putting velocity potential ϕ term into eqn. (3.33), the acoustic pressure at x can be found. For the case of a very long horn, Olson [17] gave the real and imaginary components at the acoustical throat.

So the acoustical resistance term R_T at the throat for the conical horn is

$$R_T = \frac{\rho c}{S_T}\left[\frac{(kx_0)^2}{1+(kx_0)^2}\right] \tag{3.38}$$

and the reactance term X_T is

$$X_T = \frac{\rho c}{S_T}\left[\frac{kx_0}{1+(kx_0)^2}\right] \tag{3.39}$$

Throat area and the mouth area calculated similar to exponential part. As mentioned before equation (3.23) to equation (3.30) are all applicable to all kind of horns. The difference is the fact that there is no specific cut-off frequency for the conical horn as exponential has, but one can mention about critical frequency range at which the resistance of the horn throat is bigger than the reactance of the horn throat. This can be also concluded from Fig. 3.3.

In order to $R_T > X_T$

$$(kx_0)^2 > kx_0 \rightarrow kx_0 > 1 \tag{3.40}$$

since

$$k = \frac{2\pi}{\lambda} \tag{3.41}$$

where k is the wave number and

$$\lambda = \frac{c}{f} \tag{3.42}$$

equation (3.40) corresponds to

$$\frac{2\pi f}{c} x_0 > 1 \quad \text{or} \quad f > \frac{c}{2\pi x_0} \tag{3.43}$$

So, if the desired frequency range is given, one can calculate corresponding x_0 (in fact minimum x_0). Higher the x_0 value, more resistive future the horn has. Due to the limiting condition of horn dimensions, it isn't meaningful to obtain very long horn. For most practical conical horns, this condition is not well satisfied, because it would require a very long horn. The accepted rule of thumb concerning horn length is that the horn will work as intended provided the horn is no shorter than 1/4 wavelength of Fc.

By knowing x_0 and r_T (radius of the throat) and r_M (radius of mouth), flare constant (m) and axial horn length (L_T) can be calculated as following,

$$m = \frac{r_T}{x_0} \tag{3.44}$$

$$L_T = \frac{(r_M - r_T)}{m} \tag{3.45}$$

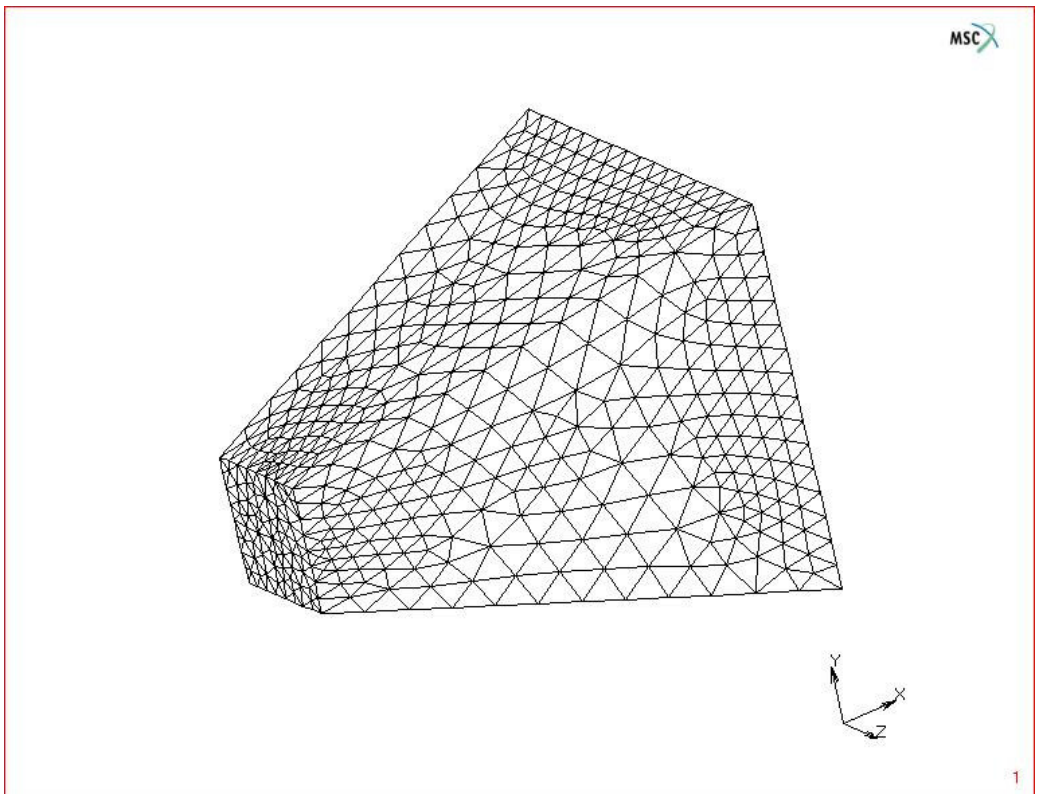

Fig. 3.7 Isometric view of a non-folded conical horn, constructed in MSC.Marc.

3.1.3. Tractrix Horn Contour

There are many discussions about the wavefront shapes within the horn and throughout the propagation through the horn. Some of the discussion based on the increasing of curvature from plane waves at the throat to a certain curvature at the mouth. But Voigt [9] claimed that wavefront within the horn must be spherical and of the same radius through the horn. His reasoning is, if the curvature increases from zero curvature at the throat to a certain curvature at the mouth, point in the axis

should travel faster than point at the wall. Thereafter, he concluded that the horn contour should be the tractrix.

The tractrix formulation is

$$x = r_M \ln\left(\frac{\left(r_M + \sqrt{r_M^2 - r_x^2}\right)}{r_x}\right) - \sqrt{r_M^2 - r_x^2} \tag{3.46}$$

Where, x is the distance from the mouth, r_x is the radius at the distance x from the mouth. To use this formula, choose your r_M, select a value for r_x of between zero and r_m, then calculate the distance from the mouth x (at this radius) and in order to find axial length *(L_T)*, r_T should be put into equation (3.46) instead of r_x. Since r_M can be calculated from equation (3.23) and r_T can be calculated from equation (3.26), there is only one unknown left in the equation which is L_T.

As Dinsdale [83] stated that tractrix has a dominant exponential term for the first half of its length from the throat to mouth, but thereafter it flares at an increasingly flaring rate until 180º included angle. The tractrix horn is the shortest one for a given throat and mouth dimensions. Again it can be turned into rectangular cross-section shape after setting the throat and mouth area by using equation (3.29 and 3.30). Fig. 3.8 shows the tractrix horn constructed in MSC.Marc.Mentat.

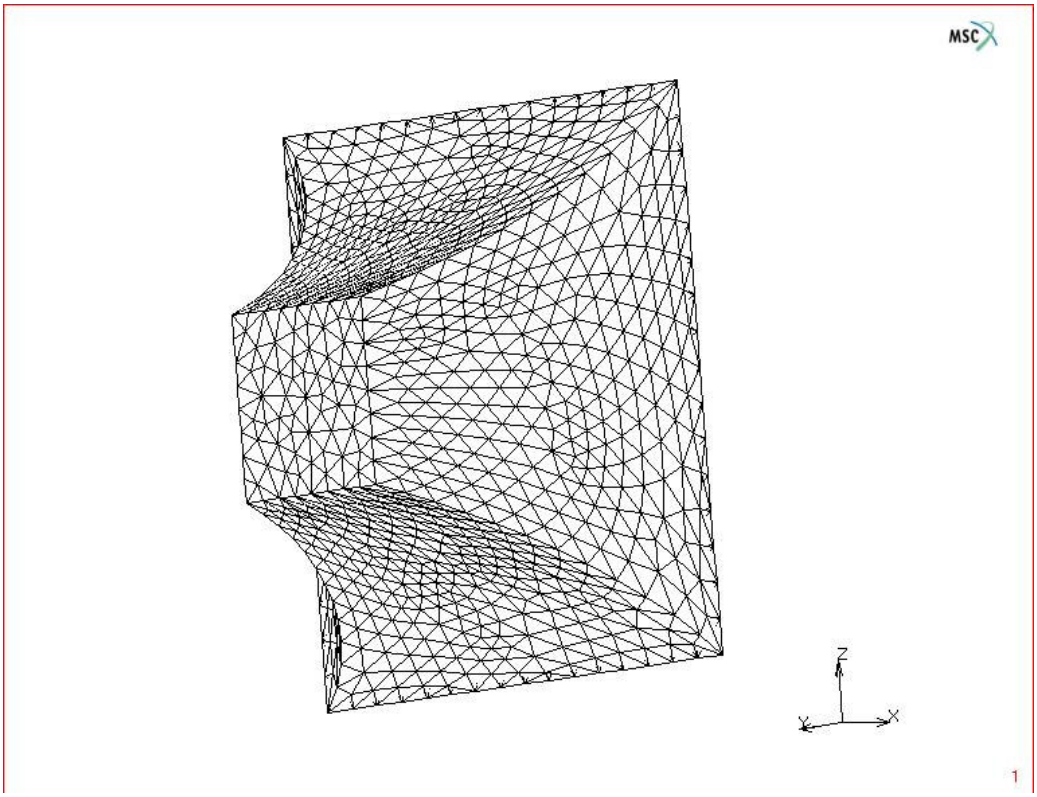

Fig.3.8 Isometric view of a tractrix horn, constructed in MSC.Marc.

3.1.4. Hyperbolic Horn Contour

In 1940 Freehafer [12] published an exact solution for a hyperbolic horn whose solution was not based on Webster's equation. After a while Salmon synthesized a new family of horns by using relations among the real and imaginary parts of the reciprocal of the horn impedance and the shape parameter.

By looking fig. 3.3 it can be said that throat resistance for the hyperbolic horn reaches the value of unity quicker than the other type of horns. From this aspect, for best loading conditions over the frequency range over the cut-off frequency hyperbolic horn should be preferred. However, non-linear distortion is higher for the hyperbolic, because hyperbolic horns have a tube that flares very little until it gets to the end where it flares suddenly. The problem with such a long tight flare is that as

sound pressures increase, the restricted passage for the air causes it to compress and distortion occurs.

The general hyperbolic horn contour formula is

$$S(x) = S_T\left(\cosh\frac{x}{x_0} + M\sinh\frac{x}{x_0}\right)^2 \tag{3.47}$$

Where x: axial distance from the throat in meters

x_0: reference axial distance from the throat in meters

M: family parameter whose value is between 0 and 1

and

$$fc = \frac{c}{2\pi x_0} \tag{3.48}$$

By knowing S_T and S_M from eqn. (3.26, 3.29) length of the horn can be calculated by a simple code written in Pascal language at Delphi (code 3.1, Appendix 1). After all hyperbolic horn construction can be completed as in Fig. 3.9.

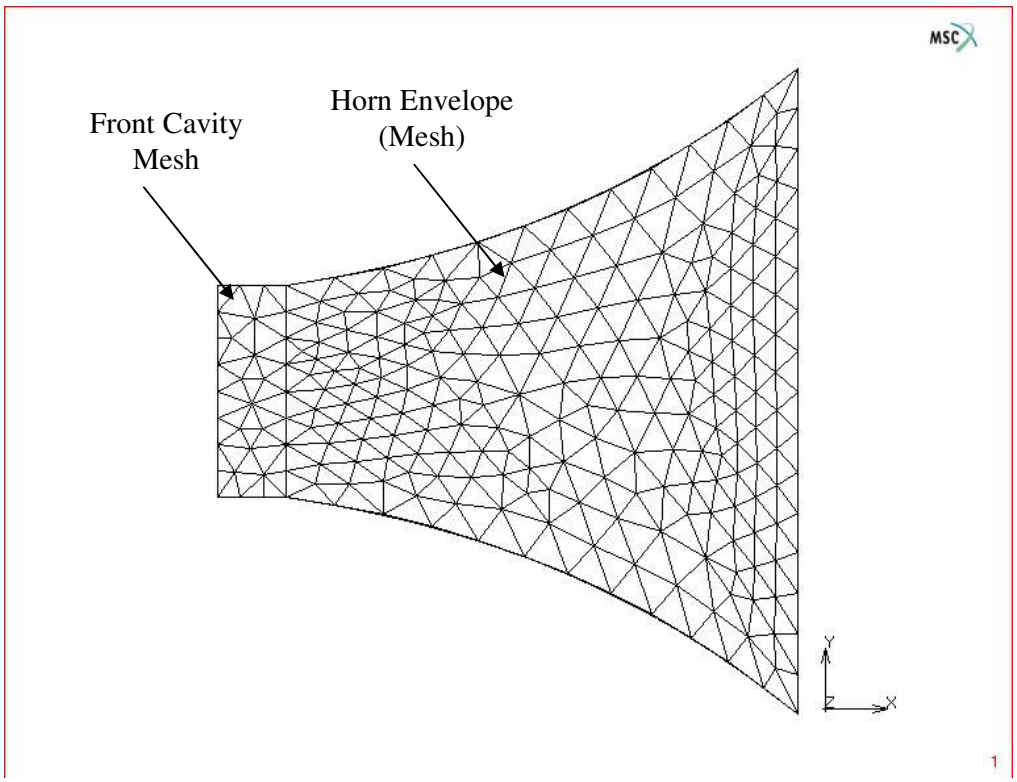

Fig. 3.9 Top view of a meshed surface of hyperbolic horn with front cavity, constructed in MSC.Marc

3.2. Foldings

Horn loudspeakers, and particularly low frequency horn loudspeakers, are commonly used in applications where large, linear sound outputs are needed such as in sound reinforcement and active noise cancellation. Because low frequency horns can be very large, the physical dimensions of this kind of horn loudspeakers may be reduced by folding the horn. There are many ways of folding horn. In this text, axial length is taking into account and horn will be folded to fit into a box having a limited axial dimension. If the bends are not sharp when their lateral dimensions approach half wavelengths, sound transmission will be efficient. Beranek [16, Fig.9.16] gave some data on the effect of bends of various types in rectangular ducts used in ventilating systems which are shown in Fig. 3.10.

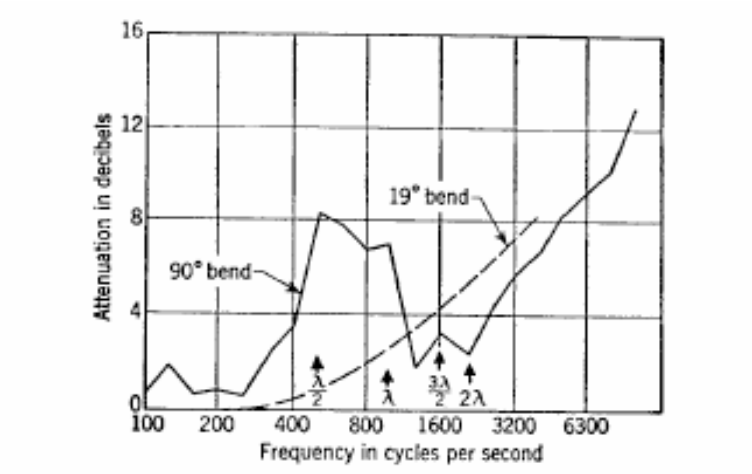

Fig. 3.10 Attenuation of sound due to the introduction of 19^o and 90^o bends as a function of frequency, [16].

Rayleigh [1] showed that bends in tubes of constant cross-section have no effect on transmitted sounds if the wavelength is larger than the diameter. According to Wilson [7] the horn diameter at bend must be less than 0.6 times the lowest wavelength. It is also applicable for rectangular cross-section such that, width should be less than 0.6 times the lowest wavelength.

The important factors taking into considerations are

a. At the bends, axial horn length needs to be modified through coordinate transformation from cartesian to polar coordinate.
b. A relation for this coordinate transformation should be developed while switching the coordinates
c. The arc length radius needs to be determined to calculate axial length of the horn at the bends. In fact, plane of cross-section turns around the axis and generally arc length radius (r) will be quarter of the corresponding plane width (or diameter if it is circular cross-section) R.
d. Cross-sectional area should be increased in accordance to horn contour in turning the bends, so the arc length radius does.

At the beginning of the bend, cross section (square) will be separated into 4 equal triangles (fig. 3.11). In fact they are trapezoid in shape. Initial the top length is zero and at the end top it reaches to the value of R_2. Cross-sectional area will be increased from S_1 to S_2 during bending.

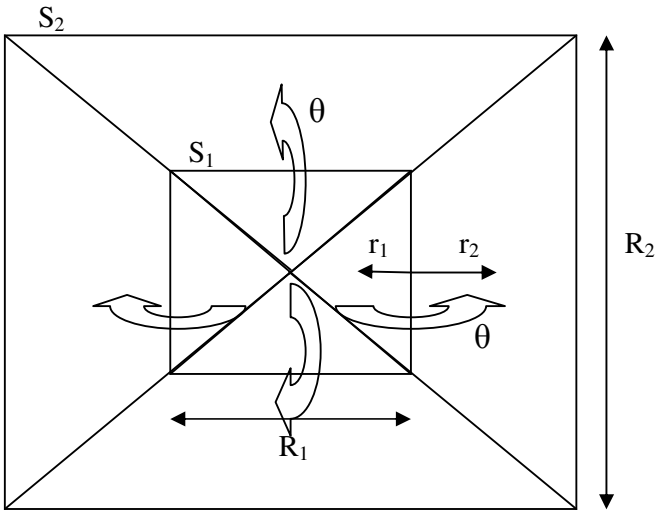

Fig. 3.11 Cross sectional view of horn at the beginning of the bending and at the end of the bending

3.2.1. Folding in the Exponential and Hyperbolic Horns

For exponential and hyperbolic horns exponentially increasing curves are tried to be fitted into polar equation. Then, arc length of the propagation curve will be found. It is also the corresponding axial length for that particular turn. Finally cross sectional areas will be compared.

$$r_1 = \frac{R_1}{4} \tag{3.49}$$

$$r(\theta) = r_1 e^{(n\theta)} \tag{3.50}$$

Where θ: polar angle (angle of bend)

n: polar coordinate flare constant

The arc length L_F (axial length of the folding part) can be found from,

$$L_F = \int_0^{\pi} \sqrt{r^2(\theta) + \left(\frac{dr(\theta)}{d\theta}\right)^2}\, d\theta \tag{3.51}$$

For exponential horn, if there is no folding, S_2 will be,

$$S_2 = S_T e^{m(L_1+L_F)} = S_1 e^{mL_F} \tag{3.52}$$

For hyperbolic horn, if there is no folding, S_2 will be,

$$S_2 = S_T \left(\cosh\left(\frac{L_1 + L_F}{x_0}\right) + M \sinh\left(\frac{L_1 + L_F}{x_0}\right)\right)^2 \tag{3.53}$$

Where L_1: Axial length before the folding

L_F: Axial length of the folding part

For π radian turn one can find final radius (r_2) by using eqn. (3.50)

$$r_2 = r_1 e^{n\pi} \tag{3.54}$$

And

$$R(\theta) = 4r(\theta) \tag{3.55}$$

Then area S_2 can also found as following;

$$S_2 = R_2^2 - R_1^2 \tag{3.56}$$

Comparing eqn. (3.52) or (3.53) with eqn. (3.56) gives the corresponding n value. By knowing n value, radius of curvature can be found for different rotation angle from eqn. (3.50), so do x, y, z components of the horn contour. Finally, corresponding single-folded hyperbolic or exponential horn can be obtained as in Fig. 3.12.

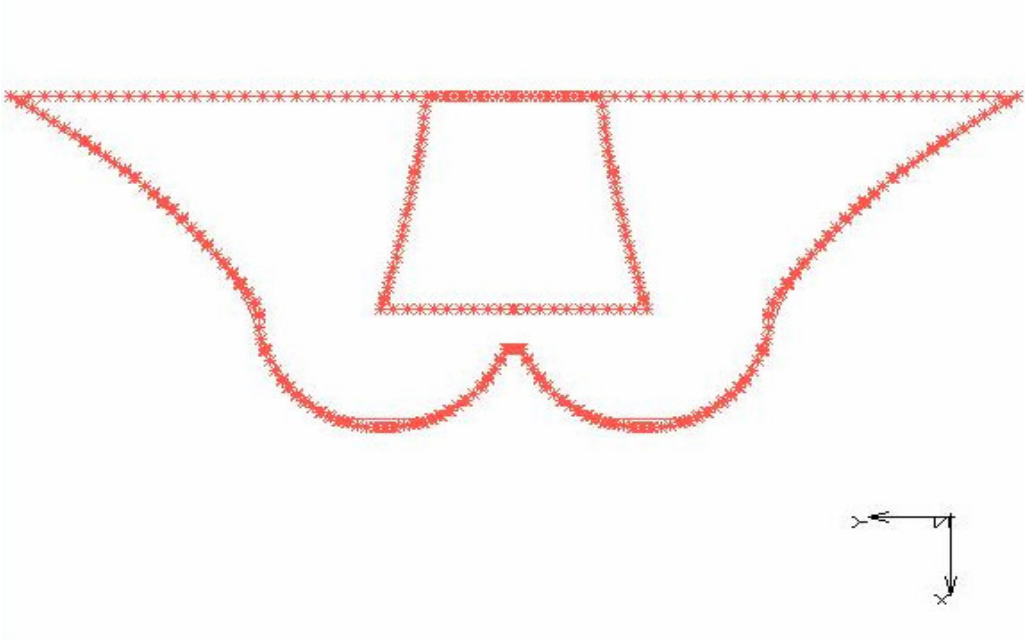

Fig.3.12 Single folded hyperbolic horn contour.

3.2.2. Folding in the Tractrix and Conical Horns

Bending contour calculation of conical horns are very similar to previous section except radius of curvature formula, such that

$$r(\theta) = r_1(n\theta + 1) \tag{3.57}$$

For the tractrix case, it's a little different since tractrix requires inverse calculation and tractrix horn contour equation gives directly axial distance from the mouth. So that, required bending length can be stated before and suitable radius of curvature can be found from both tractrix formula and arc length formula. After all equate them and try to error go to zero.

For example, let the bending length (L_F) is

$$L_F = \frac{L_T}{5} \tag{3.58}$$

By using equation (3.46) for L_F, then R_2 and R_1 can be calculated, so do r_2 and r_1. Part of the calculation code written in Delphi is given in Appendix (Appendix 1, code 3.2).

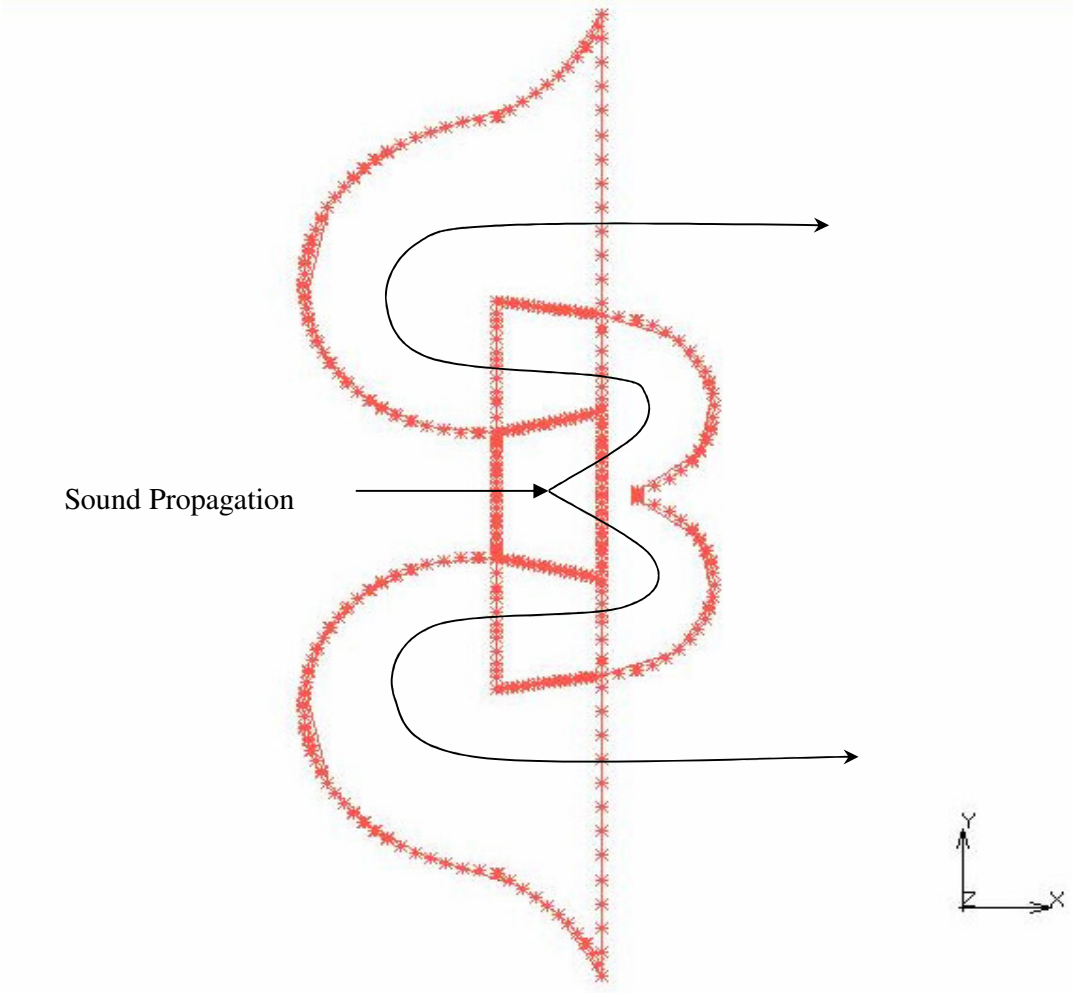

Fig. 3.13 Top view of double folded tractrix horn contour.

3.3. Distortions

There are some types of distortion in horn loudspeakers due to internal cross-reflections and standing waves set up within the horn.

The air overloaded distortion is caused by the non-linear relationship between pressure and volume of the air in the throat of the horn as it undergoes adiabatic compression and expansion. A sound wave of large amplitude cannot be propagated in air without change in the wave form. The volume change for an increase in pressure will be less than the volume change for an equal decrease in pressure. Beranek showed that for large change of volume, the pressure built up in the throat of the horn is no longer sinusoidal (Fig.3.14) even tough displacement of diaphragm is sinusoidal [16, Fig.9.11] and he has also derived the relationship for 2nd harmonic distortion at the throat of an infinite exponential horn. If the horn were cylindrical pipe, the distortion would increase the wave progressed towards the mouth. In the case of exponential horn (flaring horn), the amplitude of the pressure wave decreases as the wave travels away from the throat. In order to have low distortion the horn should flare out rapidly to reduce to pressure amplitude, so that the second harmonic distortion does not increase linearly with distance. From this point of view, conical horns will generate the least distortion since it flares out rapidly.

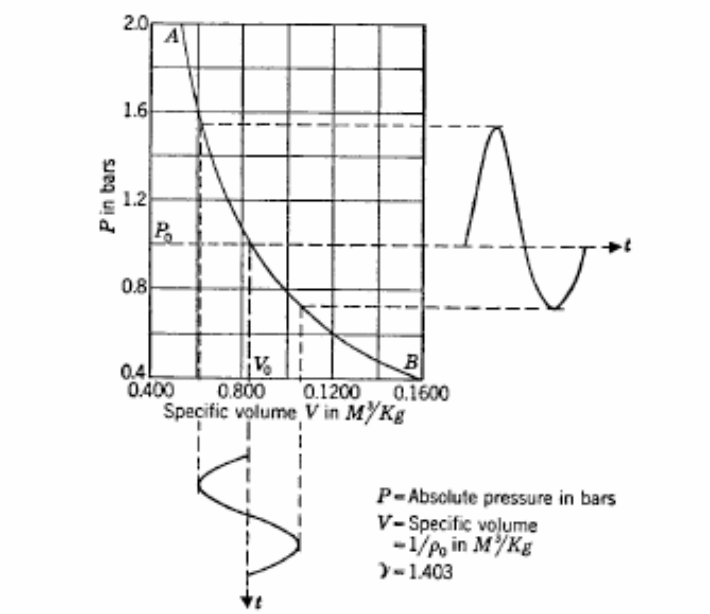

Fig.3.14 Adiabatic pressure/volume relationship for air.[16].

Olson [17] stated that delivering large sound outputs with small distortion may require large throat which should also suitably coupled to large diaphragm to obtain high efficiency. He also showed that at low frequencies where the amplitude of the diaphragm is large that volume of the air chamber becomes alternatively zero and two times the normal value, the acoustical reactance of the acoustical capacitance is very large compared to acoustical resistance of the horn.

Furthermore, stiffness of suspension systems of diaphragm may not be a constant, but a function of the amplitude. The materials of the horn can also resonate and they are also accentuated if the horn is folded, when wavefronts will be distorted at the bends. These are the other factor create distortion. It's good to choose properly compliance of the suspension system and the compliance of the air chamber, so that high efficiency obtained.

3.4. FEM Geometry of Horns

The previous sections have dealt in some detail with the basic theory of the various kinds of horn. In this study, a computer interface (Fig.3.15) called as "Folded Horn Design" has been developed in Delphi to facilitate the construction of the horn geometry by reducing the geometrical modeling time in a commercial FEA program. This interface works jointly with MSC.Marc-Mentat and provides users opportunities such that they can change the primary parameters and horns will be modeled according to these parameters. Cut-off frequency, types of cross-sectional area of the mouth and throat, maximum horn length are the primary designing parameters. The interface takes the essential geometric design parameters of the chosen horn as inputs and calculates all the necessary data in conformity with the previously mentioned horn design procedures. Codes abide by acoustic design criteria have been written in Pascal language to achieve this parametric design. In accordance with these codes secondary and the major designing parameters such that; flaring rate, throat and mouth area of the horn, length of the horn can be calculated and whether the folding is required or not will be determined. Maximum number folding is limited to two. After calculating the required data, the interface creates a *.proc file which includes

horn geometry creation commands and sends this file to MSC.Marc-Mentat. "*.proc file" is a procedure file which can be run automatically at Mentat from the simple button "construction" on the "Folded Horn Design" interface.

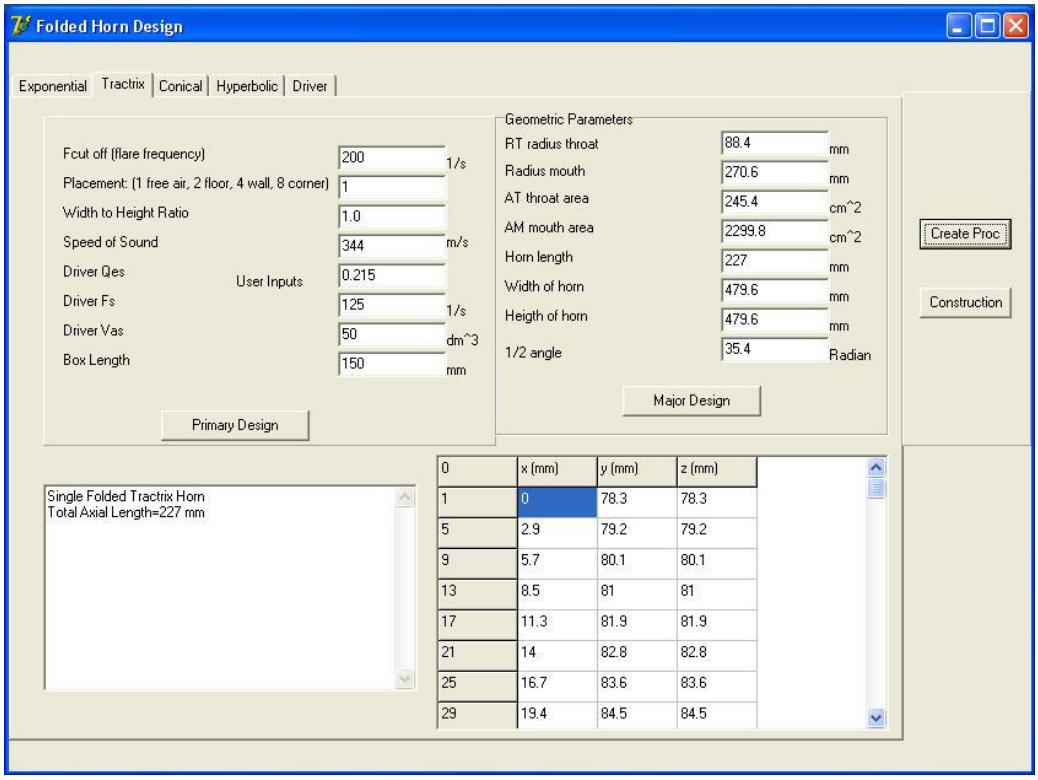

Fig. 3.15 Computer interface generated by using Delphi

Users have the possibility of changing primary design parameters easily by inserting desired values to the "User Inputs" panel on the interface. These parameters are called as 'Variable parameters'. In this work, these variable parameters are divided into three groups, which are main driver parameters, geometrical limitation of box and acoustical parameters such as speed of sound and cut-off frequency. After the appropriate values inserted, primary calculation will start as soon as the click on the "Primary Design" button and at the right panel major parameters of the horn, namely mouth area, throat area, axial length, flare constant if applicable will then be shown.

Furthermore, at the left screen some useful information will be seen, such that how many times it requires folding and total length after folding and etc. At the right bottom table one of the horn contour coordinates can be seen after the “Major Design” button is pressed. At this point horn is ready to be constructed, so “*.proc file” can be constituted by means of “create proc” button. Finally, this file can be run automatically at Mentat with the help of “construction” button and construction of FEM geometry (Fig.3.16) will be completed.

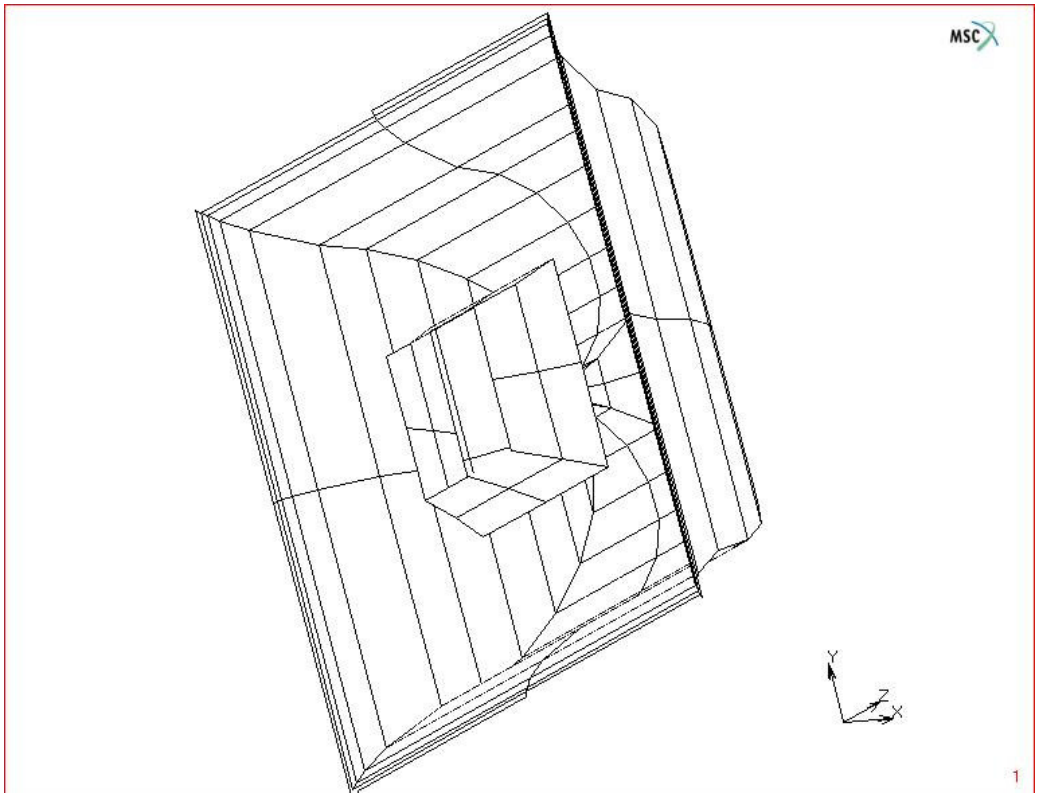

Fig.3.16 FEM geometry of single folded tractrix horn.

CHAPTER 4

LUMPED PARAMETER SYSTEM MODELING OF HORN DRIVERS

This chapter discusses modeling of the loudspeaker driver. Horn loudspeakers usually consist of a moving-coil driving unit coupled to horn. Moving coil driving unit has a diaphragm attached to a cylindrical coil of wire that is suspended in a fixed magnetic field. For the purposes of horn loudspeaker system analysis and design, it has been found advantageous to model the driver in terms of lumped parameters. A good model of a real system may be characterized by its simplicity and also its ability to provide all the necessary information about the system. In the lumped parameter system models the real system such as horn driver is modeled as a collection of finite number of simple components. All of these components can either store or dissipate or transform energy and they are assumed to have only one property value for each component. The behavior of components and their interconnections will then be described by linear algebraic and/or linear differential equations.

Throughout this chapter, after some analogies mentioned a little, lumped parameter electro-mechano-acoustical equivalent system and the corresponding linear graph of the driver will be depicted. The main objective sought in the analysis is to find diaphragm velocity or sound pressure at the throat.

4.1. Analogies

While working with multi-domain systems like the loudspeaker, transformation from one domain to the other is required. For example, the equivalent electric circuit can be constructed by transformation of mechanical and acoustical systems into electrical domain. The following variable classification based on the type of measurement will be used to classify physical variables:

a. Across variables (v)
b. Through variables (f)

In the analysis of loudspeaker driver units it is popular to develop analogies. There existed several types of analogy. Most common ones are impedance and mobility analogies. For the mobility analogy; voltage, velocity, angular velocity and volume velocity are treated as analogous to each other. Also current, force, torque and pressure are analogous variables. On the other hand, for the impedance type analogy; current, velocity, angular velocity and volume velocity are analogous to each other. Whereas voltage, force, torque and pressure are analogous variables. With respect to distinction between through and across variables; across variables are voltage, velocity, angular velocity and pressure, while through variables are current, force, torque and volume velocity. For this type of analogy, it can be said that it's a mixture of mobility and impedance type analogy, such that for the electrical and acoustical domain it's similar to impedance type but for the mechanical case it's similar to mobility type of analogy.

In this chapter successively electro-mechano-acoustical circuits will be constructed then linear graph will be constructed. While constructing an electro-mechano-acoustical equivalent circuit, for the mechanical part mobility analogy will be used and for the electrical and acoustical part impedance analogy will be used. On the other hand, for the linear graph modeling through and across variables analogy will be preferred.

4.2. Electro-Mechano-Acoustical Circuits

Analogies mentioned in previous section are used to construct equivalent electrical circuits for acoustical and mechanical systems. The purpose is the application of electrical-circuit theory to obtain governing dynamic equations for mechanical and acoustical systems. Not only a schematic representation of the components and their connections make it possible to visualize and understand the system, but also the differential equations can be formed directly from these schematic diagrams. Before the construction of lumped element equivalent electro-mechano-acoustical circuit, it's better to designate simplified physical model of horn-loaded moving-coil loudspeaker driver (or compression driver) (Fig.4.1).

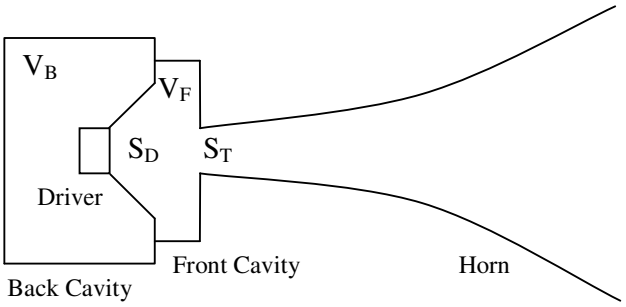

Fig.4.1 Simplified model of a horn-driver system

Vibrating diaphragm (cone) of a moving coil loudspeaker is appreciably larger than the voice coil to enhance the efficiency of radiation at low frequencies. The time required for a displacement of the cone center to propagate the rim is small compared to the period of vibration at low frequencies, so that the cone may be assumed to vibrate as a rigid surface. Nearly all modern power amplifiers used for loudspeakers are regarded as low output impedance and constant voltage type. Thereby, output impedance of the driving source is assumed to be negligible.

Loudspeaker impedance character is an important matter, for the aspect of the power transfer and stability characteristics of the loudspeaker. The impedance curve of a basic loudspeaker displays a peak at the first (bass) resonance frequency. The electrical equivalent of the mechanical resonance of the cone and suspension at the bass resonance is a series resonant circuit for the impedance type of analogy. It shows minimum value of mechanical impedance at the resonance, as constant force produces the maximum velocity or displacement at that frequency.

A moving-coil loudspeaker driver can be modeled with lumped-parameter characteristics and with coupling between the electrical, mechanical, and acoustical domains. There are two components transforming energy between two medium. The first one is the coupling between the electrical domain and the mechanical domain

due to the alternating Lorentz force acting on the voice coil. And the second one involves the coupling between the mechanical and acoustical domains due to the motional coupling of the cone and the air adjacent to the cone. For the first type coupling, a transformer will be used, not the gyrator, since the voltage in the electrical loop scales with the velocity (voltage in the mechanical loop). If all domains were constructed based on the impedance analogy, the circuit would be different like Leach's complete electro-mechano-acoustical circuit [25, Fig. 2.] and the first coupling transformer would be turned into gyrator.

The voice coil of a driver is initially modeled as a resistor R_E in series with an inductor L_E in the electrical part with the impedance analogy. The moving-coil driver connected to a driver of voltage e_g which supplies a current i_g. The diaphragm and suspension system are modeled in the mechanical part with the mobility analogy as a damped mass-spring system (with mass M_{MD}, compliance C_{MD}, and resistance R_{MD}). In the mechanical part, across variable is driver velocity (v_D) and through variable is force (f_D). In the acoustical part, after applying the impedance analogy, R_{AB} and C_{AB} represent the acoustical resistance and compliance of the box of volume V_B and C_{AF} is the acoustical compliance of the front chamber (V_F). The radiation loading of the horn is Z_{AL} (Fig. 4.2).

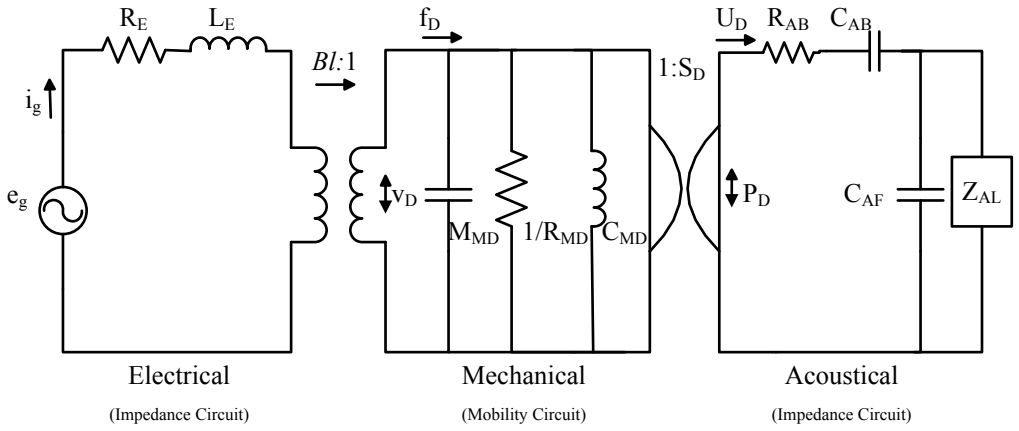

Fig. 4.2 Complete electro-mechano-acoustical circuit of horn loudspeaker system.

Behind the diaphragm, there is a space (cavity) that can be filled with soft acoustical material and in mid frequency range this space adds the system a compliance C_{AB} and the resistance R_{AB}. This back volume resistance and reactance combines with the radiation loading of the horn throat since the diaphragm must develop power both to its front and its back. Therefore, in the acoustical part of the circuit these terms are shown as series branch. While air space compliance C_{AF} in front of the diaphragm is parallel to the horn loading.

This circuit can be simplified to a single-domain representation by carrying the other domain parts of the circuit into the one domain part by means of impedance transformation from a transformer or gyrator.

For example, acoustic parts are converted through the area gyrator into the mechanical mobility analogy then all the mechanical mobility parts are carried through the transformer into the electrical impedance analogy. The result is shown in Fig. 4.3. In a similar manner, electrical and mechanical parts can be transformed into the acoustical part, given in Fig. 4.4.

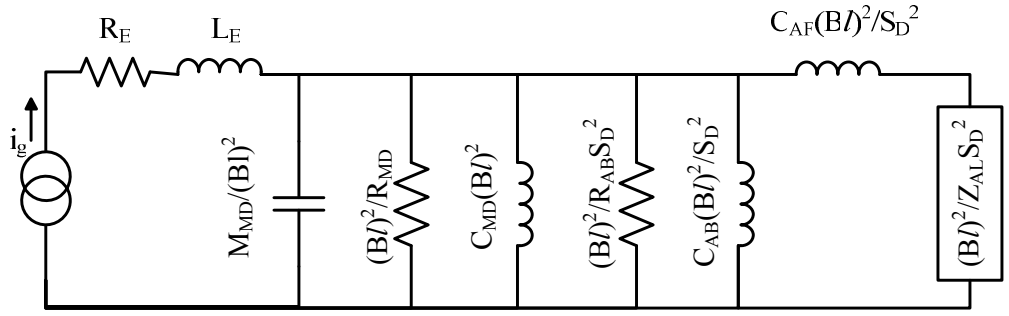

Fig. 4.3 Complete mobility type electrical equivalent circuit of horn speaker system

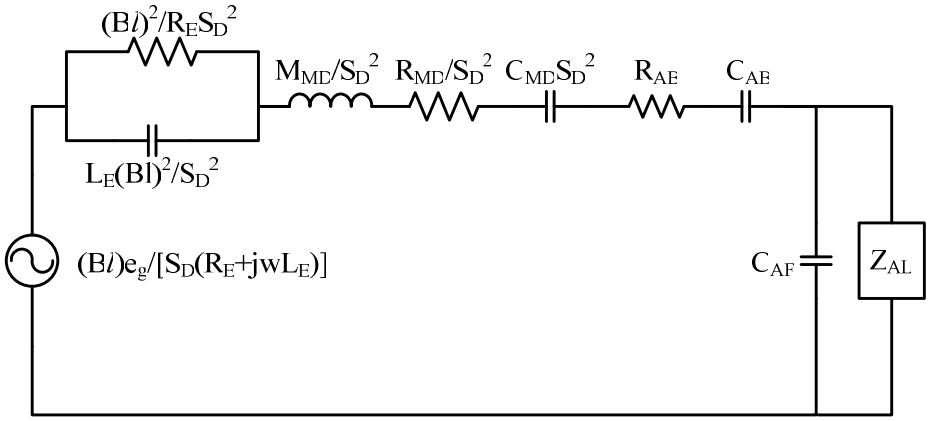

Fig. 4.4 Complete impedance type acoustical equivalent circuit of horn speaker system

Note that impedance Z is the inverse of mobility z. One circuit is known as the dual of the other circuit. While converting a circuit from one analogy to the other type, series element should be converted to parallel elements; capacitor is converted to inductor and vice-versa.

4.2.1. Electrical Circuit

The electrical part shows the moving coil driver connected to a generator of voltage e_g which supplies a current i_g.

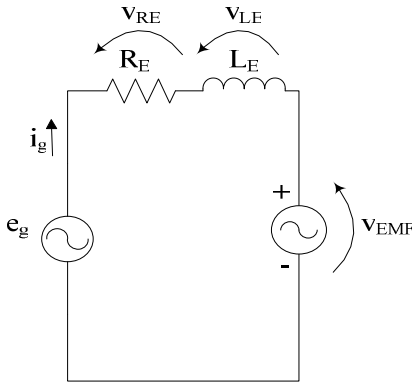

Fig. 4.5 Electrical circuit

Equations for the electrical system:

$$v_{R_E}(t) = R_E i_g(t) \tag{4.1}$$

$$v_{L_E}(t) = L_E \frac{di_g(t)}{dt} \tag{4.2}$$

By using Kirchoff's Voltage Law

$$e_g(t) = v_{R_E} + v_{L_E} + v_{EMF} = R_E i_g(t) + L_E \frac{di_g(t)}{dt} + Blu(t) \tag{4.3}$$

4.2.2. Electro-Mechanical Transducer (Ideal Transformer)

Electro-magnetic part converts electrical energy into mechanical case by means of transformer element. If both mechanical and electrical domain are constructed by impedance analogy this transformer element is gyrator if electrical part is made with impedance and mechanical circuit made with mobility analogy then it will be transformer.

A permanent magnetic material produces a constant strength magnetic field B. When an electric current $i_g(t)$ is supplied to the voice-coil, it produces an electro-magnetic force $F_{EM}(t)$ acting on the voice-coil and the mechanical system attached to voice coil. The length of the wire on the voice coil called *l* and assumed constant. When the voice-coil moves in the magnetic field, a EMF voltage $v_{EMF}(t)$ proportional to the velocity $u(t)$, is produced across the terminals.

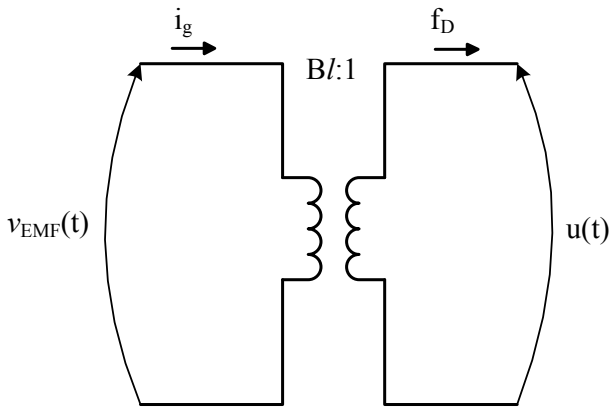

Fig. 4.6 Electro-magnetic transducer (transformer)

$$F_D(t) = Bli_g(t) \tag{4.4}$$

$$v_{EMF}(t) = Blu(t) \tag{4.5}$$

4.2.3. Mechanical Circuit

The mechanical system is shown for the mobility analogy.

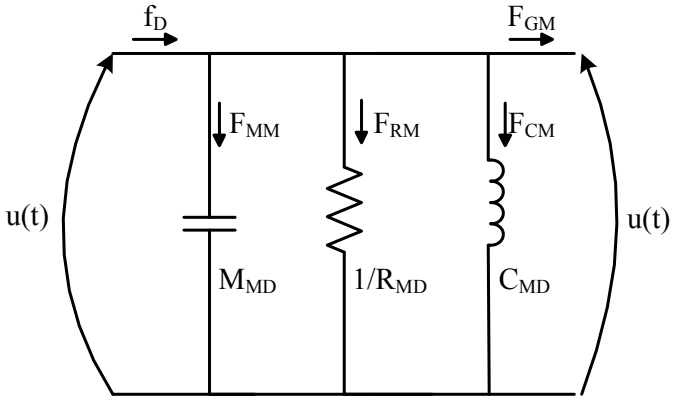

Fig. 4.7 Mechanical circuit

Equations for the mechanical system:

$$F_{CM}(t) = -\frac{1}{C_{MD}}\int u(t)dt \tag{4.6}$$

$$F_{RM}(t) = -R_{MD}u(t) \tag{4.7}$$

$$F_{MD}(t) = M_{MD}\frac{du(t)}{dt} \tag{4.8}$$

From Kirchoff's Current Law;

$$f_D(t) = F_{MD}(t) + F_{RM}(t) + F_{CM}(t) + F_{GM}(t) \tag{4.10}$$

4.2.4. Mechano-Acoustic Transducer (Ideal Gyrator)

This type of transducer occurs at a junction point between the mechanical and acoustical parts of an analogous circuit and it converts mechanical energy to acoustical energy by means of turns ratio equals to piston area S_D.

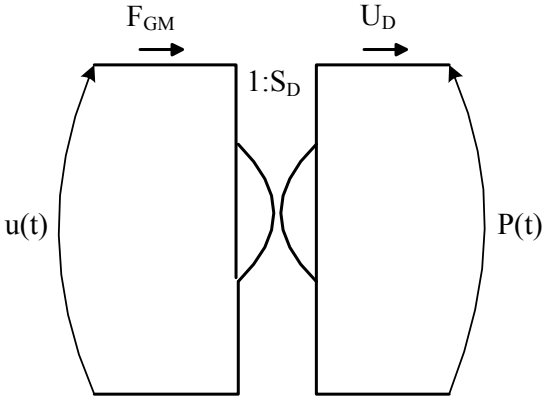

Fig. 4.8 Mechano-Acoustic Transducer (Gyrator)

Basic equations:

$$F_{GM}(t) = S_D P(t) \tag{4.11}$$

$$U_D(t) = S_D u(t) \tag{4.12}$$

4.2.5. Acoustical Circuit

In the acoustical part of the circuit pressure is the voltage (across variable) and volume velocity is the current through variable. The current U_D is volume velocity emitted by the driver cone.

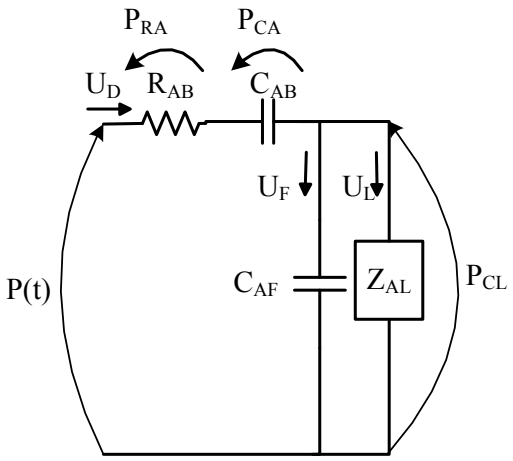

Fig. 4.9 Acoustical Circuit

Equations for the acoustical system:

$$P_{RA}(t) = R_{AB}U_D(t) \tag{4.13}$$

$$P_{CA}(t) = \frac{1}{C_{AB}}\int^{t} U_D(\tau)d\tau \tag{4.14}$$

$$P_{CL}(t) = \frac{1}{C_{AF}}\int^{t} U_F(\tau)d\tau = Z_{AL}U_L(t) \tag{4.15}$$

From Kirchoff's Voltage Law;

$$P(t) = P_{RA}(t) + P_{CA}(t) + P_{CL}(t) \tag{4.16}$$

$$U_D(t) = U_F(t) + U_L(t) \tag{4.17}$$

By using equations given above and known driver parameters are sufficient to determine diaphragm velocity, volume velocity of air and pressure fluctuation at throat. At this point, it should be noted that a generalized analysis of horn-loaded driver system is impossible because of the dependence of Z_{AL} (horn throat impedance) on the horn geometry and on frequency. More detailed calculation will not be given for electro-mechano-acoustical circuit, but it will be performed later while linear graph model of the driver is being analyzed.

4.2.6. System Efficiency

As Keele [87] stated, maximum efficiency occurs at the driver's resonance frequency. If driver mechanical losses are neglected, the maximum nominal efficiency can be obtained when the acoustic load resistance equals to the driver's voice-coil resistance and the maximum true efficiency occurs when the reflected acoustical load resistance is much higher than the driver's voice coil resistance. The system efficiency is defined in the mid-frequency range. Because the fact that while higher compression ratios will raise the high frequency efficiency, it may decrease mid-frequency range efficiency.

The nominal efficiency of horn-driver system is calculated by dividing the acoustic output power by the nominal electrical input power. True efficiency however is calculated by dividing the acoustic output power by the true electrical input power.

Nominal electrical input power (P_{NE}) for compression driver:

$$P_{NE} = \frac{e_g^{\,2}}{2R_E} \tag{4.18}$$

Since modern amplifiers exhibit very low output impedance, it provides constant-voltage operation regardless of loudspeaker impedance. Various simplifications can be made to determine the maximum efficiency. Keele [87] analyzed how to maximum efficiency change with the corresponding simplification and displayed the equations and results.

4.3. Linear Graph Modeling

As stated before several different types of analogies between variables and elements may be defined. In this section, generalized "through" (f) and "across" (v) variables have been applied to relate elements associated with the linear graph system representation. Linear graph allows to develop modeling methods that are similar to well known techniques for electrical circuit analysis. There is also *bond graph* modeling (Appendix 2, Fig. 1) similar to linear graph, based on the concepts of "effort" and "flow" variables a little bit different from "through" and "across" variables, such that for the first forces and electrical voltages are considered to be analogous, while in the *linear graph* method forces and electrical currents are considered to be analogous.

First, general theory of linear graph modeling will be given, and then application to horn-loaded compression driver will be shown. Finally, driver will be analyzed by using lumped parameter linear graph model in order to find diaphragm velocity or sound pressure at the throat.

4.3.1. One-Port Elements

One port pure elements can be defined as the pure elements possessing only one energy port for the energy exchange between their environments. According to their energetic behavior they can be divided into two main groups

a. Active Elements
b. Passive Elements

There exist two versions of active elements,

i. A-Type Active Elements

The generalized across-variable (v) is defined function of time $v_{21}=f(t)$ and is independent of through variable (f).

ii. T-Type Active Elements

The generalized through variable (f) is defined function of time f=f(t) and is independent of across-variable (v).

For the horn loudspeakers case, since it's driven by voltage source e_g, it can be considered as A-Type active elements. For the definitions of ideal source types refer to Appendix 2 (Table 1).

There are one dissipative (D-Type) and two storage passive elements. Storage elements are known as capacitive (A-Type) and inductive (T-Type).

i. D-Type Passive Elements (Energy Dissipators)

They are defined by an algebraic relationship between the across and through variables of the form:

$$v_{21} = F(f) \qquad \text{or} \qquad f = \phi(v_{21}) \tag{4.19}$$

where F and φ representing single valued function. Elemental equations of D-Type passive elements and their corresponding power dissipated equations can be seen in Appendix 2 in a tabular form (Table.2).

ii. A-Type Passive Elements (Capacitive Stores)

These elements are characterized by their energy storage feature by virtue of across variable associated with them. They are defined by a constitutive relationship between the integrated through (h) and the across variable (v_{21}) associated with as

$$h = \phi(v_{21}) \tag{4.20}$$

where ψ representing a single valued monotonic function. Elemental and constitutive equations of A-Type passive elements and their corresponding energy storage equations can be seen in Appendix 2 in a tabular form (Table.3).

iii. T-Type Passive Elements (Inductive Stores)

These passive pure elements are characterized by their energy storage feature by virtue of through variable associated with them.

$$x_{21} = \psi(f) \qquad (4.21)$$

where ψ representing a single valued monotonic function and x_{21} is the generalized integrated across-variable. Elemental and constitutive equations of T-Type passive elements and their corresponding energy storage equations can be seen in Appendix 2 in a tabular form (Table.4).

4.3.2. Two-Port Elements

The process of energy conversion between different domains is known as transduction and elements that convert the energy are defined as transducers. There are two ideal two-port transducers, namely transformer and gyrator.

i. Transformers

Either the integrated across variables of the two ports are related by single valued functions as

$$x_b = \phi(x_a) \qquad (4.22)$$

Or the integrated through variables of the two ports are related by single valued functions as

$$h_b = \psi(h_a) \qquad (4.23)$$

ii. Gyrators

Integrated across variable of one of the ports is related to the integrated through variable of the other port;

$$x_b = \phi(h_a) \tag{4.24}$$

or

$$h_b = \psi(x_a) \tag{4.25}$$

4.3.3. Linear Graph of Horn Loudspeaker System

For horn loaded loudspeaker, there is electrical, mechanical and electrical domain.

In the electric part, there is one A-Type active element V_g (driver voice coil input voltage), one T-Type passive element L_E (voice coil inductance) and one D-Type passive element R_E (voice coil resistance).

In the mechanical part, there is one A-Type passive element m_m (mechanical mass of driver diaphragm assembly), one T-Type passive element k_m (mechanical stiffness of suspension system) and one D-Type passive element b_m (damping coefficient of suspension system).

Finally, in the acoustical part, there are two A-Type passive elements C_B, C_F (back and front volume capacitance), two D-Type passive element R_B (back volume resistance), R_{AL} (resistance of the horn throat) and one A-Type passive elements M_{AL} (capacitance of the horn throat).

Voice coil loudspeakers are also energy transduction devices for transduction between electrical and mechanical translational system. Therefore, there is a transformer with a turns ratio (TR) equal to $1/(Bl)$. Furthermore, driver cone acts as a piston and provide transduction between mechanical translation and fluid systems. So, there is also gyrator with a turns ratio equal to the piston area S_D.
Complete linear graph of horn-loaded loudspeaker system is given Fig. 4.10.

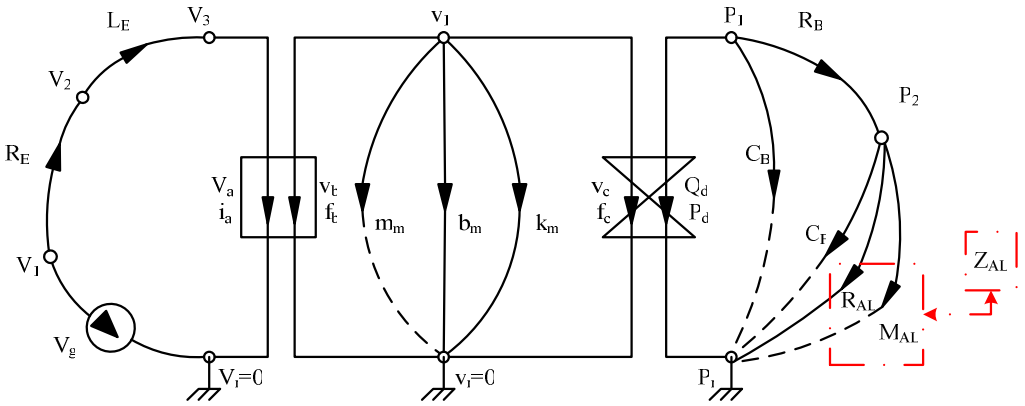

Fig. 4.10 Complete linear graph model of horn-loaded loudspeaker.

In this graph C_B and C_F act as a capacitance. Principle of conservation of mass requires;

$$\rho Q = \frac{d}{dt}(\rho V) = V\frac{d\rho}{dt} + \rho\frac{dV}{dt} \tag{4.26}$$

where V is the volume, ρ is the mass density of the fluid. Since there is no external flow (Q=0) into the volume box V_B and volume of front chamber V_F. Left side of the Equation 4.26 is zero. It's also known that

$$\frac{dV}{dt} = Q \tag{4.27}$$

And equation of state requires that;

$$d\rho = \frac{\rho}{\beta}dP \tag{4.28}$$

where β is the bulk modulus of elasticity [Pa] of the liquid. It's important to note that bulk modulus of gases can be expressed as

$$\beta = np \tag{4.29}$$

By using above equations, it can be found that

$$Q = \frac{V}{\beta}\frac{dp}{dt} = C_f\,\dot{p}_{21} \tag{4.30}$$

Therefore, acoustical compliance of air in box C_B and acoustical compliance of air in front chamber C_F are considered as capacitive (A-Type passive) elements.

Since the impedance of horn throat is hard to compute and dependent on the horn geometry and frequency. Its effect will be analyzed later with the help of acoustic finite element analysis software. For simplicity while finding cone velocity the coupling between voice coil motion and horn loading is overlooked. The widely used methods of direct-radiator loudspeaker system analysis, based on the pioneering work of Thiele and Small, neglect the radiation impedance components in deriving the system response functions [47-53]. Neglecting these components provides a very powerful simplification of the equivalent circuit that helps the designer in deriving the appropriate response functions and system relationships. One of the main effects of not including the radiation terms in the analysis is that all derived responses are high-pass functions. After simplifications, new linear graph (Fig. 4.11) will be analyzed. Diaphragm velocity, or acoustic pressure at the throat area will be found by means of linear graph model and this data will be used as input variable (source) for the acoustic analysis of FEM geometry of the horns.

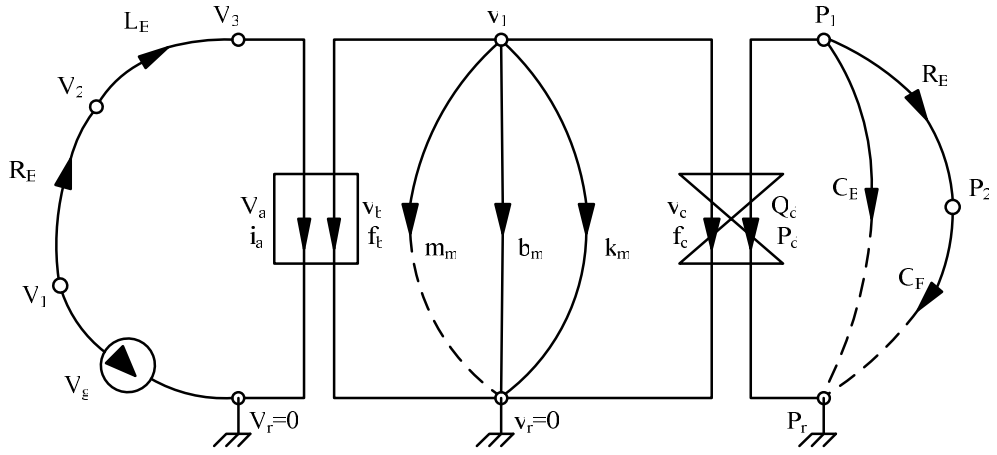

Fig. 4.11 Linear graph model of horn driver.

Number of branch (B) is equal to 13, number of node (N) is 7, and there is one A-type active element (A_a=1).

4.3.4. Analysis of Linear Graph Model

For the analysis of Fig. 4.11, first appropriate normal tree should be constructed. Procedure to form normal tree is

i. Entering all A-Type active elements
ii. Completing the tree by using maximum number of A-type passive elements
iii. If the not complete at step ii., complete it by using D-Type passive elements.

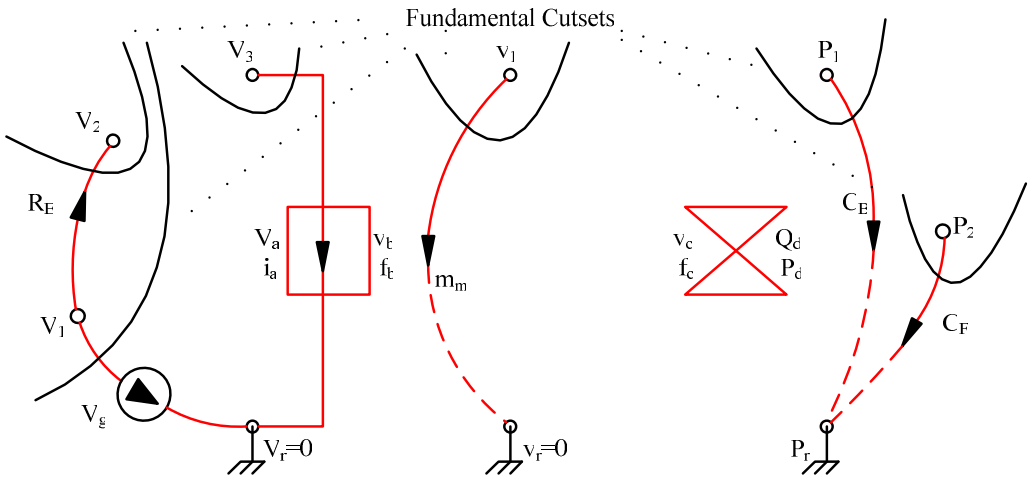

Fig.4.12. Normal tree and fundamental cutsets

With the normal tree, state equations can be derived for the systems with two port elements by choosing the *primary variables* as the across-variables on all branches of the normal tree and the through-variables on all normal tree links, including those associated with the two- port elements. The system *state variables* are the across-variables of the A-type passive elements in the normal tree, and the through-variables of the T-type passive elements in the normal tree links.

From the normal tree in Fig.4.12:

Primary Variables: $V_g(t)$, v_{mm}, P_{CB}, P_{CF}, V_a, v_c, P_d, V_{RE}, i_{LE}, f_b, f_{bm}, f_{km}, Q_{RB}

Secondary Variables: $i_g(t)$, f_{mm}, Q_{CB}, Q_{CF}, i_a, f_c, Q_d, i_{RE}, V_{LE}, v_b, v_{bm}, v_{km}, P_{RB}

State Variables: v_{mm}, P_{CB}, P_{CF}, i_{LE}, f_{km}

The B-A=12 elemental equations written in terms of primary variables are:

$$\frac{dv_{mm}}{dt} = \frac{1}{m_m} f_{mm} \tag{4.31}$$

$$\frac{dP_{CB}}{dt} = \frac{1}{C_B} Q_{CB} \tag{4.32}$$

$$\frac{dP_{CF}}{dt} = \frac{1}{C_F} Q_{CF} \tag{4.33}$$

Moving coil loudspeaker is considered as an ideal electro-mechanical transducer for which the following constitutive relationship can be written;

$$V_a = (Bl) v_b \tag{4.34}$$

$$f_b = -(Bl) i_a \tag{4.35}$$

Considering the combined fluid and mechanical system, coupled by driver, act as a hydraulic ram (piston). Thereby it's regarded as a gyrator and the following constitutive relationship can be written;

$$v_c = -\frac{1}{S_D} Q_d \tag{4.36}$$

$$P_d = \frac{f_c}{S_D} \tag{4.37}$$

$$V_{RE} = R_E i_{RE} \tag{4.38}$$

$$\frac{di_{LE}}{dt} = \frac{1}{L_E} V_{LE} \tag{4.39}$$

$$f_{bm} = b_m v_{bm} \tag{4.40}$$

$$\frac{df_{km}}{dt} = k_m v_{km} \tag{4.41}$$

$$Q_{RB} = \frac{1}{R_B} P_{RB} \tag{4.42}$$

The N-1=6 continuity equations are:

$$i_g(t) = -i_{RE} \tag{4.43}$$

$$i_{RE} = i_{LE} \tag{4.44}$$

$$i_a = i_{LE} \tag{4.45}$$

$$f_b = -f_{mm} - f_{km} - f_{bm} - f_c \tag{4.46}$$

$$Q_d = -Q_{CB} - Q_{RB} \tag{4.47}$$

$$Q_{RB} = Q_{CF} \tag{4.48}$$

The B-N+1=7 compatibility equations are,

$$V_{LE} = V_g(t) - V_a - V_{RE} \tag{4.49}$$

$$v_b = v_{mm} \tag{4.50}$$

$$v_{bm} = v_{mm} \tag{4.51}$$

$$v_{km} = v_{mm} \tag{4.52}$$

$$v_c = v_{mm} \tag{4.53}$$

$$P_d = P_{CB} \tag{4.54}$$

$$P_{RB} = P_{CB} - P_{CF} \tag{4.55}$$

There are 25 equations. On the other hand, the number of unknowns is equal to summation of two variables per passive element (2(B-A)=24) and one variable per active element (A=1). Hence, there are 25 (2(B-A)+A=25) unknowns which is the same as the supplied equations. The secondary variables can be directly eliminated from elemental equations and by direct substitution the twelve elemental equations can be reduced to five state equations and placed in the standard form. At this point before going on the manipulations, linear graph can be simplified more by using simplified mechanical model of compression driver (Fig. 4.13).

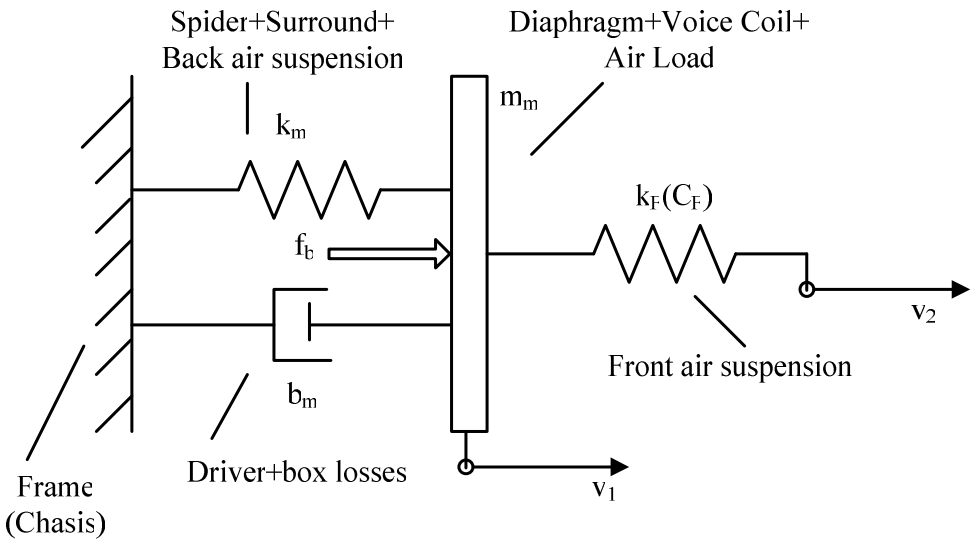

Fig. 4.13. Mechanical part of simplified model of a loudspeaker.

C_F (k_F) in the acoustical part and L_E in the electrical part will be omitted. In front of the diaphragm there is an air space with compliance C_F and at low to mid frequencies the air in this space behaves like an incompressible fluid, that is, ωC_F is small, and all air displaced by the diaphragm passes into the throat of the horn. The voice coil inductance L_E is neglected as in the most loudspeaker analyses for low to mid frequencies. When this is done, new linear graph can be constructed again, such as Fig. 4.14.

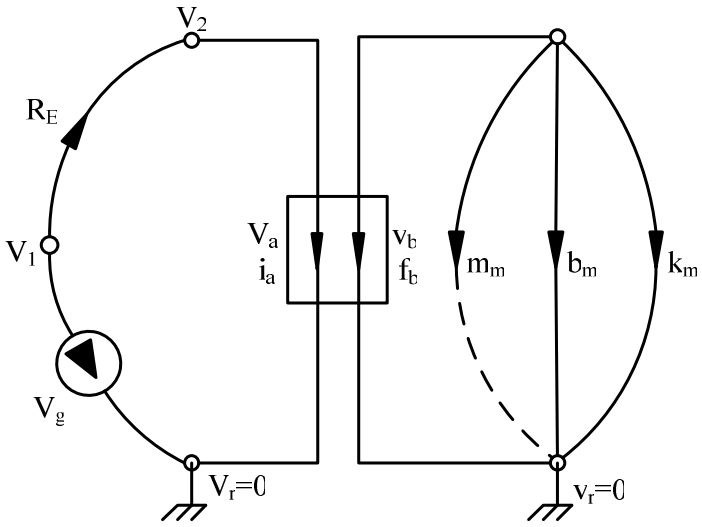

Fig. 4.14 Simplified linear graph of compression driver

Number of branch (B) is 7, number of node (N) is 4 and there is one A-type active element (A_a=1).

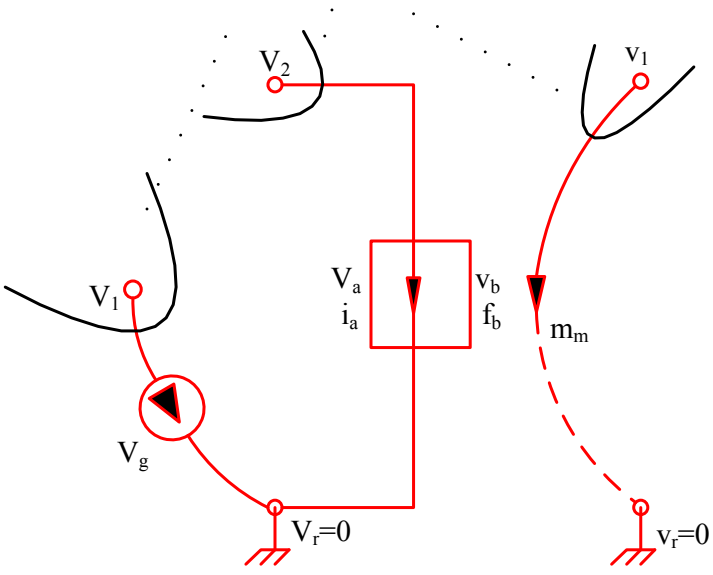

Fig. 4.15 Corresponding normal tree of the simplified linear graph.

From the normal tree in Fig. 4.15.:

Primary Variables: $V_g(t)$, v_{mm}, V_a, i_{RE}, f_b, f_{bm}, f_{km}

Secondary Variables: $i_g(t)$, f_{mm}, i_a, V_{RE}, v_b, v_{bm}, v_{km}

State Variables: v_{mm}, f_{km}

The B-A=6 elemental equations written in terms of primary variables are:

$$\frac{dv_{mm}}{dt} = \frac{1}{m_m} f_{mm} \tag{4.56}$$

$$V_a = (Bl)v_b \tag{4.57}$$

$$f_b = -(Bl)i_a \tag{4.58}$$

$$i_{RE} = \frac{V_{RE}}{R_E} \tag{4.59}$$

$$f_{bm} = b_m v_{bm} \tag{4.60}$$

$$\frac{df_{km}}{dt} = k_m v_{km} \tag{4.61}$$

The N-1=3 continuity equations are:

$$i_g(t) = -i_{RE} \tag{4.62}$$

$$i_a = i_{RE}$$

(4.63)

$$f_{mm} = -f_b - f_{km} - f_{bm} \tag{4.64}$$

The B-N+1=4 compatibility equations are,

$$V_{RE} = V_g(t) - V_a \tag{4.65}$$

$$v_b = v_{mm} \tag{4.66}$$

$$v_{bm} = v_{mm} \tag{4.67}$$

$$v_{km} = v_{mm} \tag{4.68}$$

The secondary variables can be directly eliminated from elemental equations:

$$\frac{dv_{mm}}{dt} = -\frac{1}{m_m}\left(f_b + f_{km} + f_{bm}\right) \tag{4.69}$$

$$V_a = (Bl)v_{mm} \tag{4.70}$$

$$f_b = -(Bl)i_{RE} \tag{4.71}$$

$$i_{RE} = \frac{V_g(t) - V_a}{R_E} \tag{4.72}$$

$$f_{bm} = b_m v_{mm} \tag{4.73}$$

$$\frac{df_{km}}{dt} = k_m v_{mm} \tag{4.74}$$

By direct substitution the six elemental equations can be reduced to two state equations and placed in the standard form.

$$\frac{d}{dt}\begin{bmatrix} v_{mm} \\ f_{km} \end{bmatrix} = \begin{bmatrix} \left(-\frac{(Bl)^2}{m_m R_E} - \frac{b_m}{m_m}\right) & -\frac{1}{m_m} \\ k_m & 0 \end{bmatrix}\begin{bmatrix} v_{mm} \\ f_{km} \end{bmatrix} + \begin{bmatrix} \frac{Bl}{m_m R_E} \\ 0 \end{bmatrix} V_g(t) \tag{4.75}$$

One way of solving the equation (4.75) is to use "Euler Method" applied to a system of first order differential equations and given initial condition, so that v_{mm}(t) and f_{km}(t) can be found at any time. The other way is to assume a sinusoidal input V_g(t) of frequency ω and amplitude V_{ga} and found the steady state response at varying frequencies.

$$V_g(t) = V_{ga}\sin(\omega t) \tag{4.76}$$

And the Laplace transform V_g(s) of this input can be written as;

$$V_g(s) = V_{ga}\left(\frac{\omega}{s^2 + \omega^2}\right) \tag{4.77}$$

Applying Laplace Transforms and gathering the outputs $v_{mm}(s)$ and $f_{km}(s)$ on the left side of the equation;

$$\begin{bmatrix} s+\dfrac{(Bl)^2}{m_m R_E}+\dfrac{b_m}{m_m} & \dfrac{1}{m_m} \\ -k_m & s \end{bmatrix}\begin{bmatrix} v_{mm}(s) \\ f_{km}(s) \end{bmatrix}=\begin{bmatrix} \dfrac{Bl}{m_m R_E} \\ 0 \end{bmatrix} V_{ga}\left(\frac{\omega}{s^2+\omega^2}\right) \tag{4.78}$$

Taking the inverse of the left most matrices and multiplying both sides with the inverse gives a general equation in the form of equation 4.79;

$$X(s)=G_{XY}(s)Y(s) \tag{4.79}$$

where X symbolizes the output (v_{mm}), Y symbolizes the input (V_g) and G_{XY} symbolizes the transfer function (G_v). After some manipulation, the transfer function G_v between v_{mm} and V_g takes the form, such as:

$$G_v(s)=\frac{s(Bl)}{s^2 m_m R_E+s\left((Bl)^2+b_m R_E\right)+k_m R_E} \tag{4.80}$$

At this point $\dfrac{\omega}{s^2+\omega^2}$ has not been added to the equation, since it will be accounted while obtaining complex frequency response $G(j\omega)$, such as

$$G(j\omega)=G_v(s)\big|_{s=j\omega}=\frac{j\omega(Bl)}{R_E\left(k_m-\omega^2 m_m\right)+j\omega\left((Bl)^2+b_m R_E\right)} \tag{4.81}$$

Amplitude (magnitude) of $G(j\omega)$ is given by

$$\left|G(j\omega)\right|=\frac{\sqrt{\left[\omega^2(Bl)\left((Bl)^2+b_m R_E\right)\right]^2+\left[\omega(Bl)R_E\left(k_m-\omega^2 m_m\right)\right]^2}}{\left[R_E\left(k_m-\omega^2 m_m\right)\right]^2+\left[\omega\left((Bl)^2+b_m R_E\right)\right]^2} \tag{4.82}$$

and the phase is defined as

$$\phi(\omega)=\tan^{-1}\left(\frac{R_E\left(k_m-\omega^2 m_m\right)}{\omega\left((Bl)^2+b_m R_E\right)}\right) \tag{4.83}$$

Then, the output expression (v_{mm}) at steady state can be calculated from

$$v_m(t) = V_{ga}\left|G(j\omega)\right|\sin\left(\omega t + \phi(\omega)\right) \tag{4.84}$$

Finally, by using equation (4.84) in the "Folded Horn Design" interface with the driver model equation algorithm, diaphragm ring (cone) velocity (Fig. 4.16) and phase angle can be found depending on the frequency. "Folded Horn Design" interface takes the essential driver design parameters of the chosen driver as inputs and calculates all the necessary data in conformity with the previously mentioned driver design procedures (Fig.4.17). Users have the possibility of changing driver design parameters easily by inserting desired values to the left panel on the interface. After the appropriate values inserted, primary calculation will start as soon as the click on the "Primary Design" button and at the right panel major parameters of the driver will be shown. The sample primary design parameters for compression driver are taken from the ElectroVoice Loudspeaker Company. In primary design stage while obtaining mechanical mass and stiffness of the driver corresponding Leach [24] equations will be used. At the right bottom table diaphragm (cone) velocity and phase angles can be seen after the "Major Design" button is pressed.

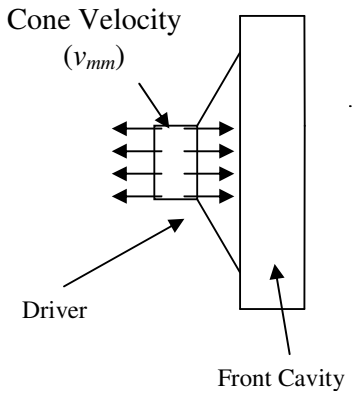

Fig. 4.16 Schematic view of the applied cone velocity

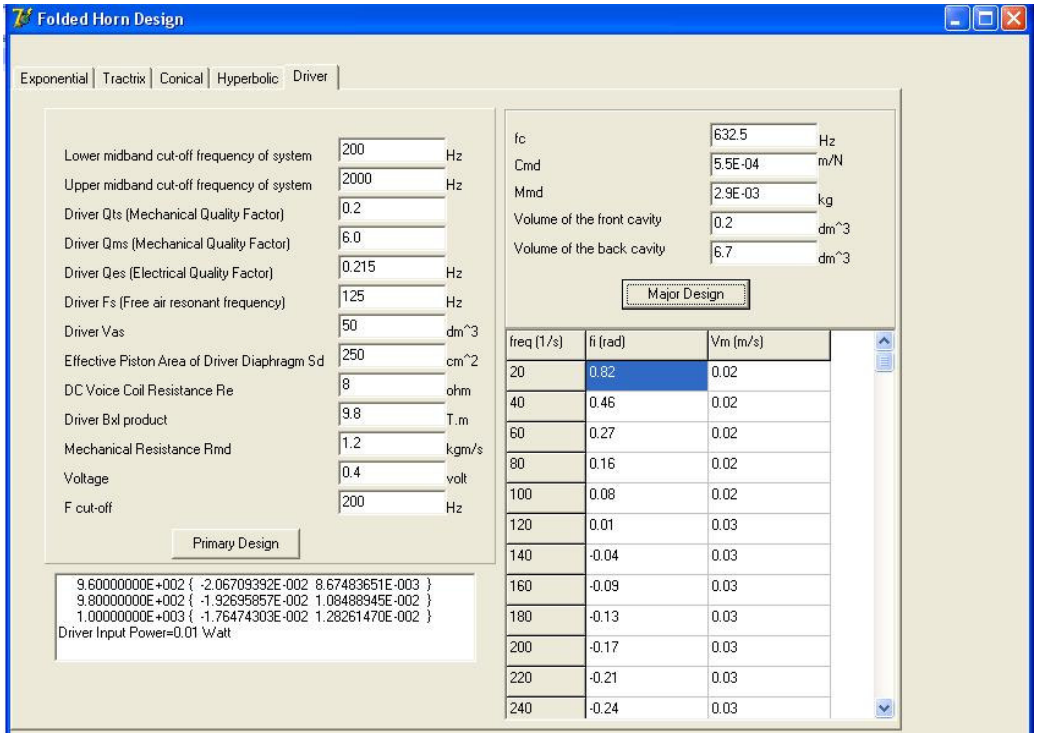

Fig. 4.17 Driver module of “Folded Horn Design” interface

CHAPTER 5

ACOUSTICAL FINITE ELEMENT ANALYSIS OF HORNS

After 3D model of horns are constructed automatically using MSC.Marc Mentat by parallel working with Folded Horn Design interface developed in Delphi software and diaphragm velocity (or pressure at the throat) is calculated, these data will be used as input variables (source) for the acoustic analysis of the horns FEM geometry. Natural frequencies of air inside the horn envelope along with the corresponding mode shapes as well as directivity characteristics and sound pressure level distributions for various types of horns can be analyzed and compared with each other. Effects of folding and flare rate will also be studied and evaluated. These analyses are carried by means of computational complete acoustic and vibro-acoustic software, MSC.Actran. In this part, the horns designed for a cut-off frequency of 200 Hertz and with square horn mouth shapes will be considered. The effect of front cavity C_{AF} is also taken into consideration by adding the finite element model of the front cavity into the finite element model of the horns. Diaphragm (cone) also attached to the complete model. Chosen diaphragm material is polypropylene and input material properties of polypropylene entered in the finite element model can be seen in Appendix 3.

Firstly, natural frequencies and corresponding mode shapes of cavities (Fig. 5.1-5.12) will be found. These frequencies give some helpful information about how the cavity behaves. The knowledge of number of natural frequencies and the way they are distributed in the frequency range of interest is very useful to evaluate performance of different horn shapes. This information will be listed in tabular (Table 5.1-5.4) forms.

Secondly, acoustic pressure in terms of its rms value will be calculated. Calculated frequencies and mode shapes are post processed by using the interface software MSC. Patran (Actran preference for MSC.Patran) and sound pressure levels (SPL) are compared for different type of horns in the frequency range of interest (Fig. 5.14-

5.19). Pressure predictions will be performed out of the horn cavity for two points. One of the points is taken on the lateral axis of the horn and 2 meter away from the mouth to find on-axis responses. The other one is again two meter away from the horn, but located at 30 degree angle with the lateral axis of the horn to find off-axis responses.

Thirdly, directivity characteristics of the horns will be calculated and compared with each other in the Fig. 5.21 to Fig. 5.35. Horns are desired to have directionally wide coverage. This will be evaluated at field points near the exit of the horn mouth for a radius of two meters.

Finally, general information (number of elements and nodes, calculation times, cpu specifications) for the computational analysis will be presented in tabular form in order to show feasibility of these analyses.

5.1. Natural Frequencies

Modal analysis by finite elements is a numerical method to determine natural frequencies and corresponding mode shapes of a dynamic system by discretization of the studied geometry. From natural frequency standpoint of cavity it can be said that the lower the number of natural frequencies in the working frequency range, the better the horn pressure transmission. In this part horns designed with respect to cut-off frequency of 200 Hz and upper frequency of 2000 Hz will be analyzed and their mode shapes at corresponding frequency will be illustrated. Actran uses Modal Extraction for Eigen value solver. Fig. 5.1 to Fig. 5.4 show a typical mode shapes for each non-folded horn shapes. Fig. 5.5 to Fig. 5.8 show a typical mode shapes for each single-folded horn shapes and lastly, Fig. 5.9 to Fig. 5.12 show a typical mode shapes for each double-folded horn.

These analyses are performed for the first 20 natural frequencies inside horn cavities. Then, comparison tables will be presented to show the differences in the behavior of natural frequencies from non-folded to double folded horns in Table 5.1-5.4.

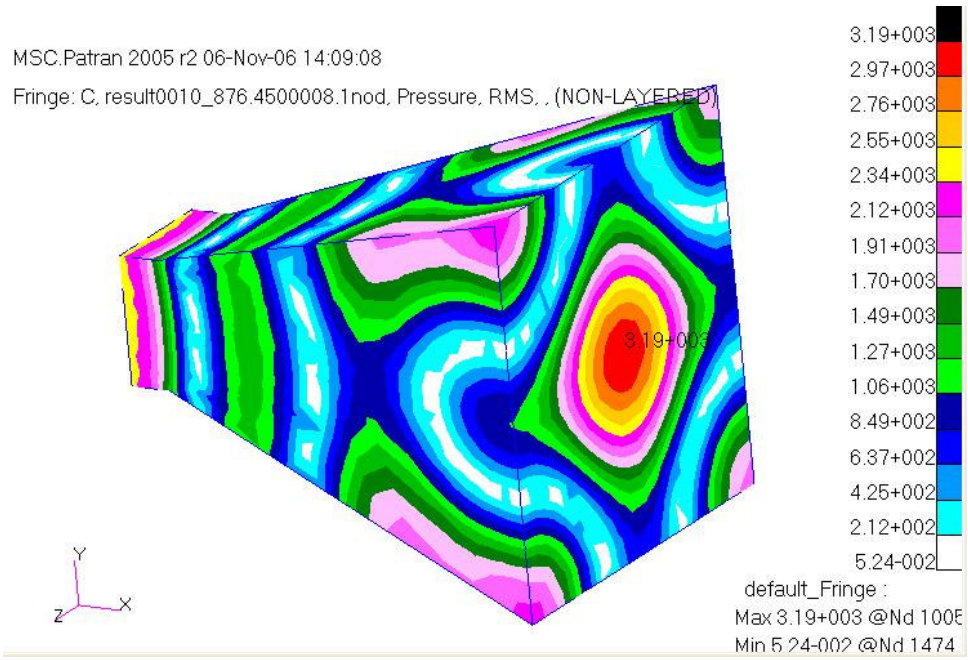

Fig. 5.1 A typical mode shape of the non-folded conical horn cavity at 876.5 Hz

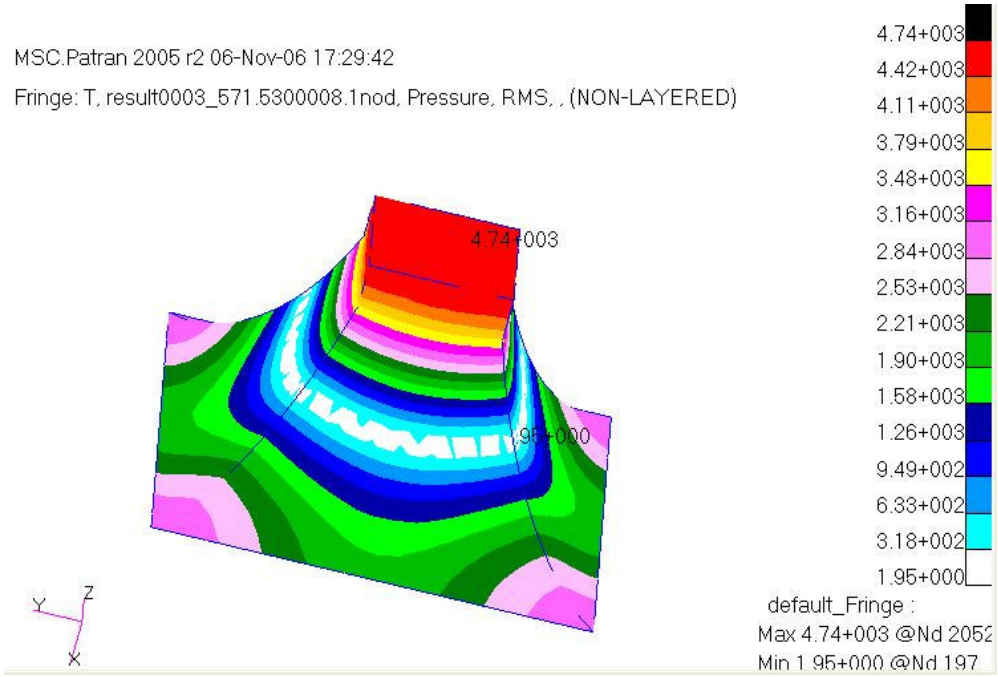

Fig. 5.2 A typical mode shape of the non-folded tractrix horn cavity at 571.5 Hz

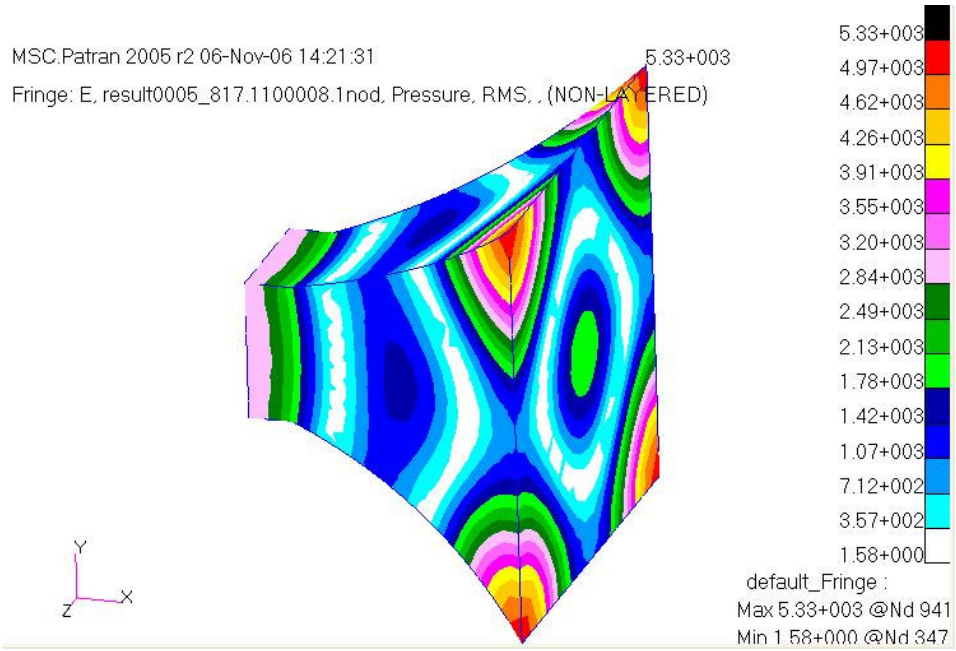

Fig. 5.3 A typical mode shape of the non-folded exponential horn cavity at 817.1 Hz

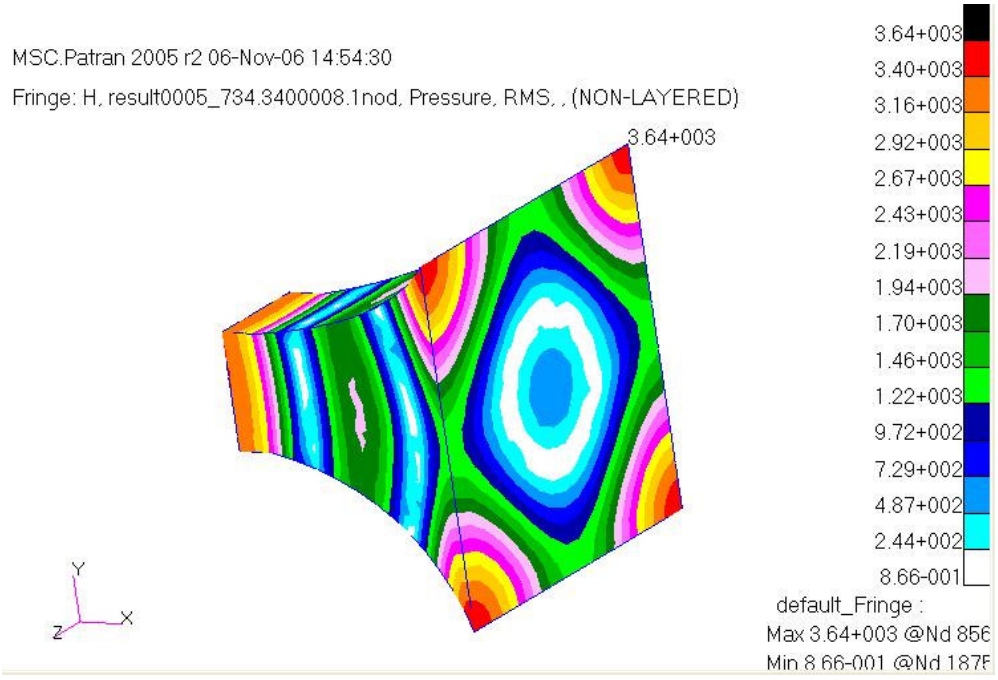

Fig. 5.4 A typical mode shape of the non-folded hyperbolic horn cavity at 734.1 Hz

The modal analysis gave the information on the number of natural frequencies in the frequency range of interest, i.e., 1 to 2000 Hz. Acoustically speaking the most prominent effect of these natural frequencies is coloration. Each horn speaker has its own characteristic coloration. Many bass horns have resonance problems. At natural frequencies unexpected pressure peaks are appear adversely affecting the response. Mode shapes figures can be viewed as 3D maps of the rms value of the pressure inside the horn cavities. Such data is especially important while interpreting the SPL values of the horns and directivity characteristics.

Table 5.1 to Table 5.4 show the series of harmonically related resonant peaks, different resonance frequencies of one kind of horns and for the all type (non-folded to double folded). As folding numbers increase, first natural frequencies getting smaller values and first 20 natural frequencies range retreats (drops) to range 0-1000 hertz, while in non-folded case 20^{th} resonances reach up to 1168-1569 Hz, in single folded case they only reach 954-1138 Hz and in double folded case they reach 783-910 Hertz. This is the proof of increasing the number of folding also increase the number of resonances (colorations).

In real life applications excessive vibration may be caused by acoustical modes triggered by structural defects. At the point where the sound comes out of the mouth of the horn, the edge of the mouth can vibrate in a bell mode. In this study horn walls are considered as rigid and thereby such defects are neglected.

For a bass horn can radiate at low frequencies, it should be long enough. Due to size limitations it should be folded. The net result is long, folded and slowly expanding tube that sounds more like a resonant tube than a wide band bass horn. Typical mode shapes of single folded horns are given below from Fig. 5.5 to Fig. 5.12. Horn geometries are cut from mid plane to be able to show the internal pressure distribution patterns.

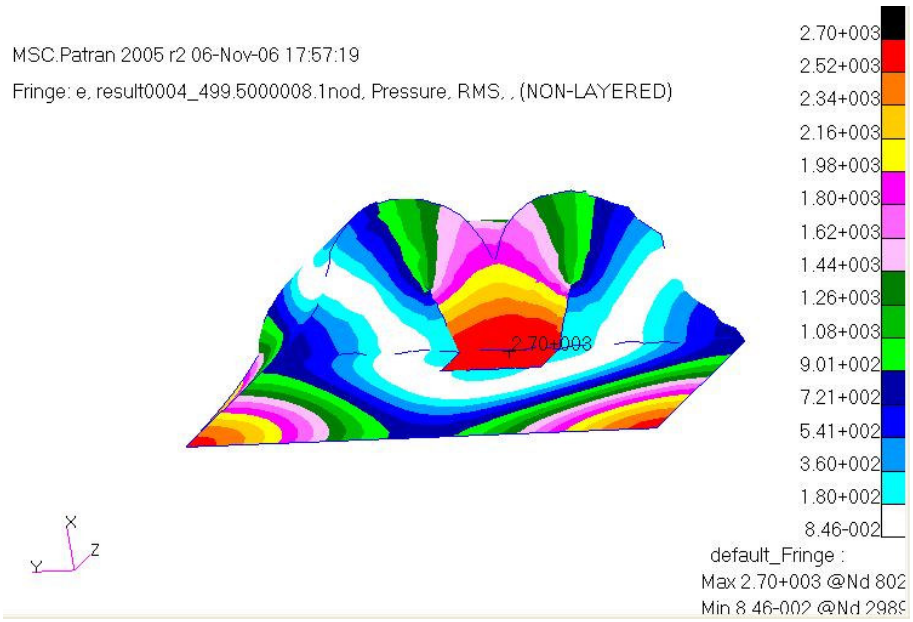

Fig. 5.5 Typical mode shape of the single folded exponential horn cavity at 499.5 Hz

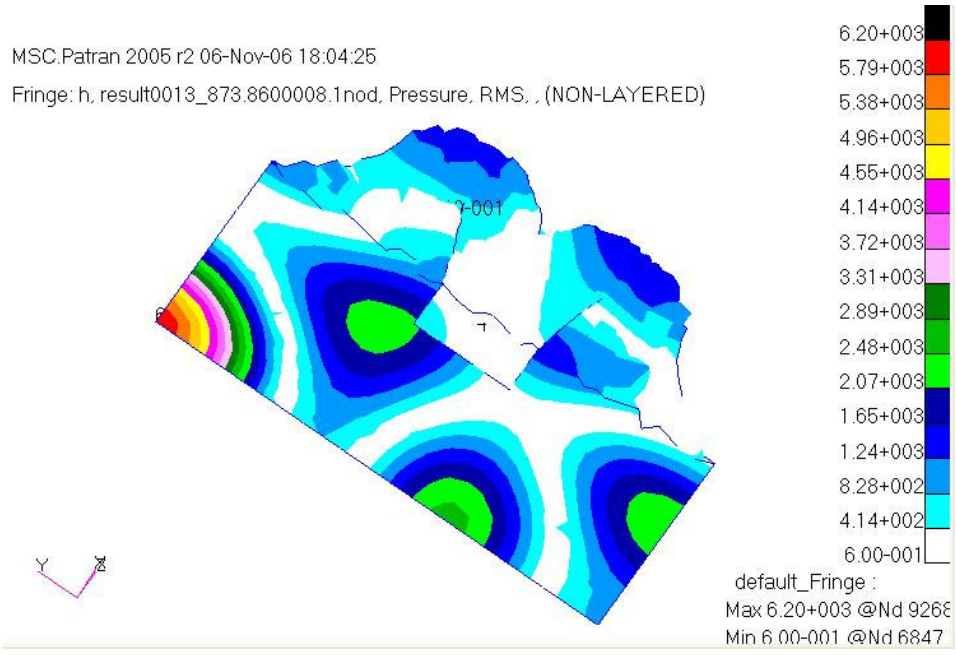

Fig. 5.6 A typical mode shape of the single folded hyperbolic horn cavity at 873.9 Hz

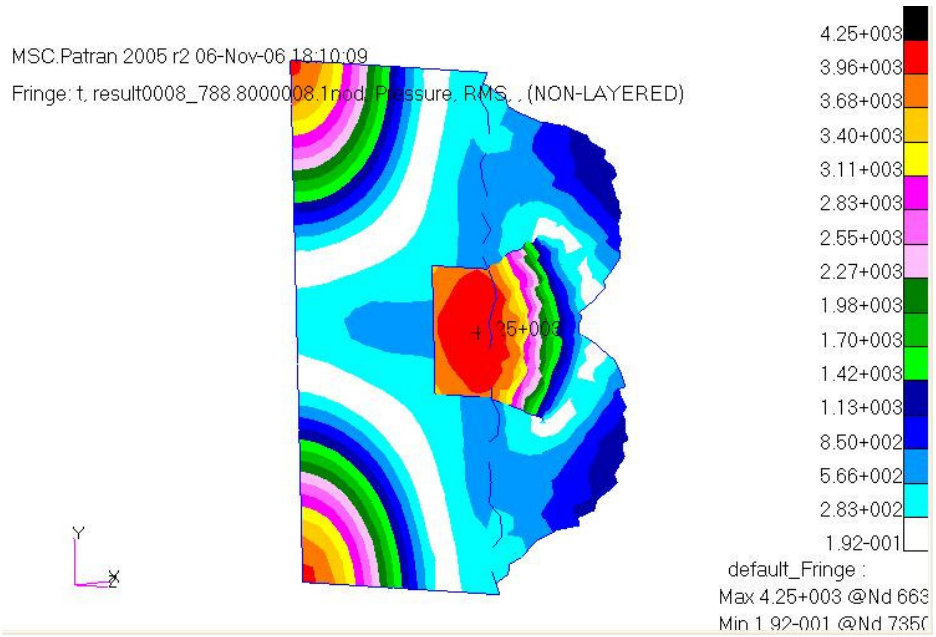

Fig. 5.7 A Typical mode shape of the single folded tractrix horn cavity at 788.8 Hz

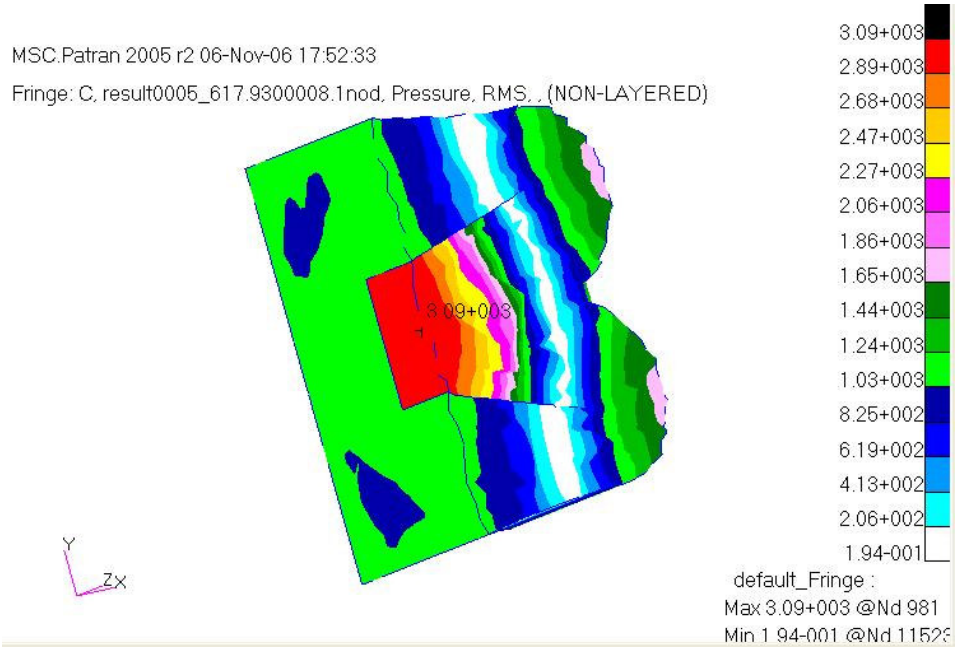

Fig. 5.8 A Typical mode shape of the single folded conical horn cavity at 617.9 Hz

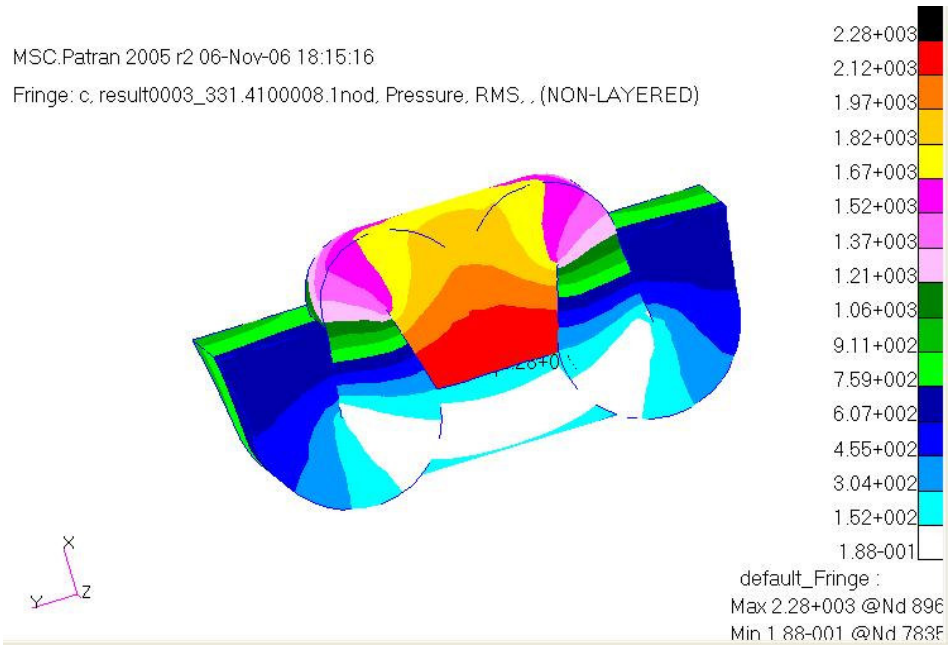

Fig. 5.9 A typical mode shape of the double folded conical horn cavity at 331.4 Hz

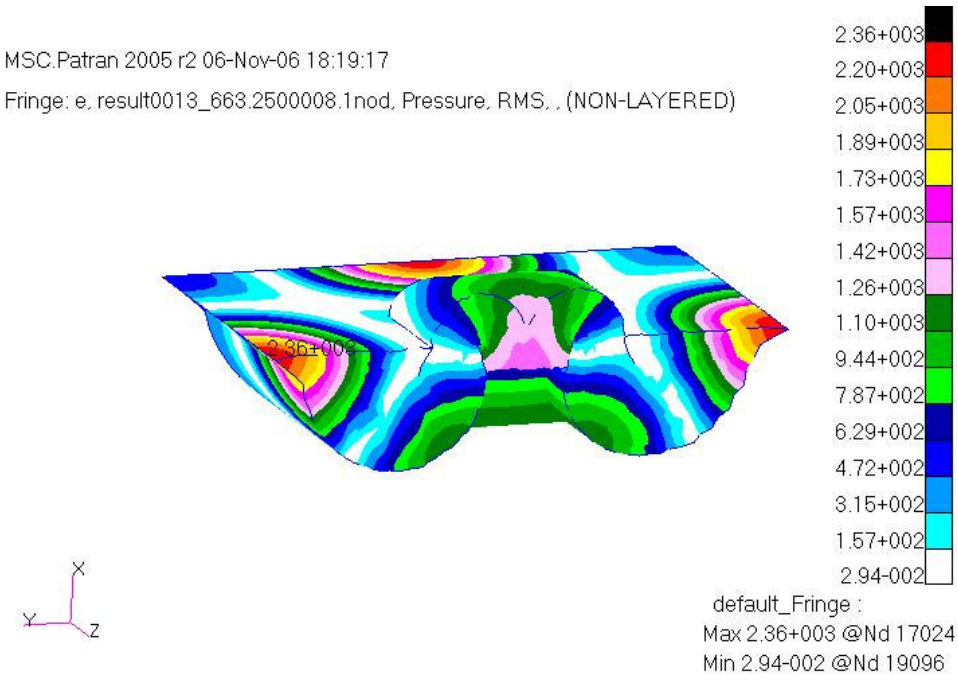

Fig. 5.10 A typical mode shape of the double folded exponential horn cavity at 663.3 Hz

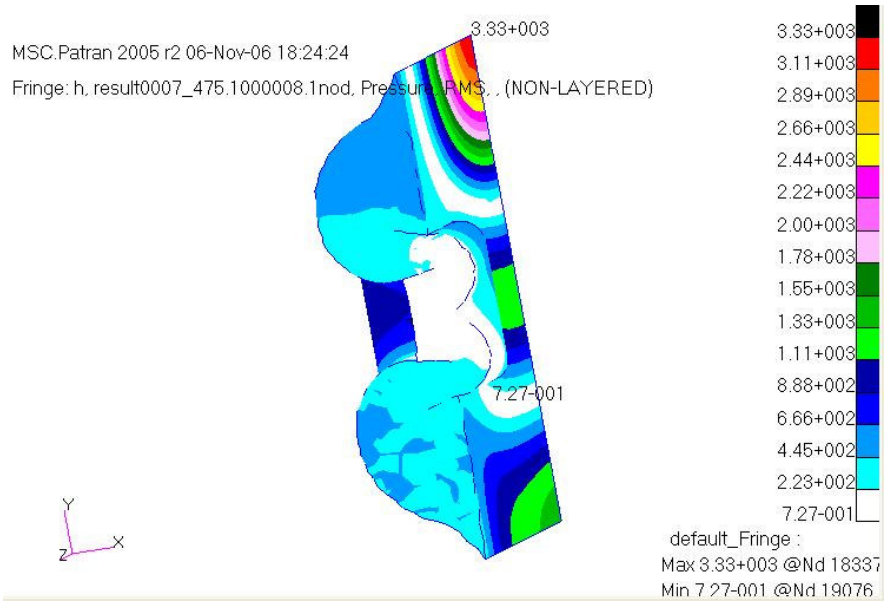

Fig. 5.11 A typical mode shape of the double folded hyperbolic horn cavity at 475.1 Hz

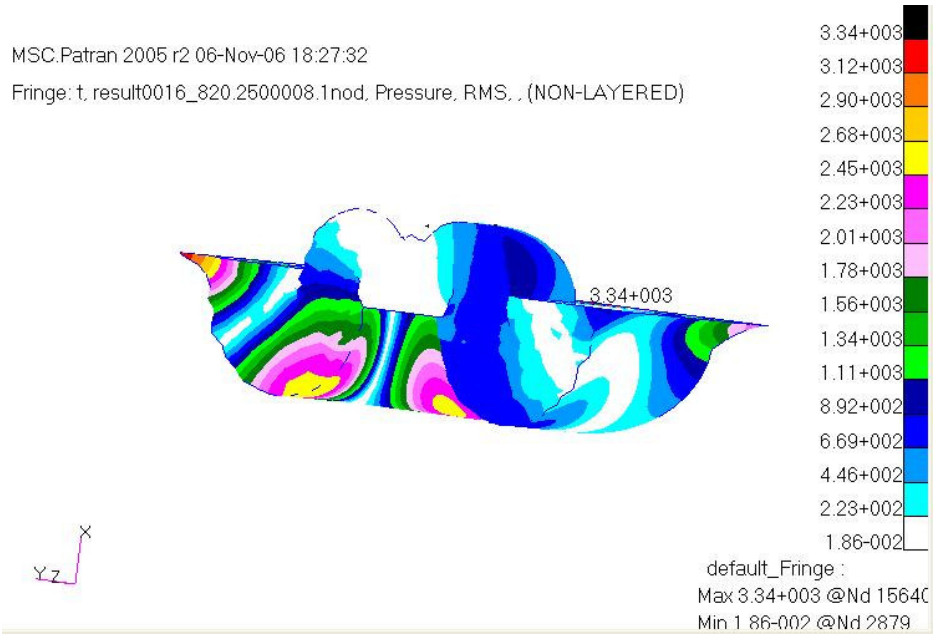

Fig. 5.12 A Typical mode shape of the double folded tractrix horn cavity at 820.3 Hz

Table 5.1 First 20 natural frequencies inside the conical horns cavities between the frequencies of 1-2000 Hz

#th Mode Shape	Non-Folded (Hz)	Single Folded (Hz)	Double Folded (Hz)
1	409.1	**331.1**	**250.1**
2	**434.0**	**331.2**	**250.1**
3	**434.1**	399.2	331.4
4	565.2	512.8	383.3
5	594.2	617.9	489.8
6	**728.1**	665.8	**551.2**
7	**728.4**	**676.2**	**551.3**
8	810.2	**676.3**	600.4
9	836.9	**798.8**	**615.9**
10	876.5	**799.0**	**616.1**
11	**917.8**	812.9	721.6
12	**918.7**	862.7	735.8
13	924.5	963.9	**765.8**
14	**971.3**	967.6	**765.9**
15	**973.1**	**989.1**	779.2
16	1121.4	**989.2**	827.4
17	1159.3	**1066.5**	840.2
18	**1163.8**	**1066.6**	874.3
19	**1164.5**	**1138.8**	**910.8**
20	1168.2	**1138.9**	**910.9**

Table 5.2 First 20 natural frequencies inside the exponential horns cavities between the frequencies of 1-2000 Hz

#th Mode Shape	Non-Folded (Hz)	Single Folded (Hz)	Double Folded (Hz)
1	**475.2**	**285.0**	**195.7**
2	**475.3**	**285.1**	**195.8**
3	476.4	406.8	286.5
4	630.3	499.5	362.0
5	817.1	572.4	399.5
6	900.7	**605.0**	**438.3**
7	**914.2**	**605.1**	**438.4**
8	**915.0**	681.1	503.9
9	1024.8	**741.5**	**568.1**
10	**1035.2**	**741.7**	**568.2**
11	**1037.2**	752.6	597.1
12	1155.1	778.9	638.9
13	1226.2	889.5	663.3
14	**1227.2**	**892.9**	**664.1**
15	**1228.2**	**893.0**	**664.2**
16	1366.3	933.8	734.8
17	1375.1	945.0	758.0
18	**1378.1**	**952.5**	**763.0**
19	**1378.9**	**952.8**	**763.1**
20	1400.8	954.5	783.3

Table 5.3 First 20 natural frequencies inside the hyperbolic horns cavities between the frequencies of 1-2000 Hz

#th Mode Shape	Non-Folded (Hz)	Single Folded (Hz)	Double Folded (Hz)
1	393.9	**289.3**	**210.8**
2	**474.3**	**289.4**	**210.9**
3	**474.6**	417.7	312.1
4	629.6	427.4	376.1
5	734.3	580.9	434.0
6	898.4	**601.3**	**475.0**
7	**900.1**	**601.4**	**475.1**
8	**900.7**	609.5	522.5
9	929.2	713.5	**618.5**
10	**1010.7**	**714.0**	**618.6**
11	**1011.2**	**714.1**	635.1
12	1135.7	739.5	696.2
13	**1169.9**	**873.8**	699.5
14	**1171.1**	**873.9**	**715.5**
15	1198.6	904.7	**715.6**
16	1239.9	921.7	780.0
17	**1312.0**	922.5	797.8
18	**1312.4**	949.0	**823.7**
19	1362.9	951.8	**823.8**
20	1369.3	955.8	838.7

Table 5.4 First 20 natural frequencies inside the tractrix horns cavities between the frequencies of 1-2000 Hz

#th Mode Shape	Non-Folded (Hz)	Single Folded (Hz)	Double Folded (Hz)
1	**526.9**	**323.8**	**225.1**
2	**527.1**	**323.9**	**225.2**
3	571.5	468.5	330.6
4	686.2	571.4	384.9
5	913.5	649.8	454.2
6	**987.6**	**707.7**	**499.6**
7	**988.2**	**707.8**	**499.7**
8	990.5	788.8	565.2
9	**1148.5**	**822.6**	**616.2**
10	**1149.9**	**823.7**	**616.4**
11	1225.0	826.2	679.3
12	1240.5	873.7	**724.9**
13	**1326.8**	**1014.4**	**725.1**
14	**1327.6**	**1014.7**	731.1
15	1373.3	1033.3	739.6
16	1475.6	1053.2	**820.2**
17	**1513.5**	1064.2	**820.3**
18	**1514.8**	**1072.3**	**820.4**
19	1536.0	**1072.5**	832.8
20	1569.1	1091.8	858.9

From Table 5.1 to Table 5.4 show the modal density of corresponding horns and their coloration frequencies. Frequencies, at which sound waves in a horn resonate, based on the horn dimensions. The acoustic modes will "color" the sound, i.e.

enhance certain frequencies and dull others. There are three types of modes. These are axial, tangential and oblique modes. Since the horns have three dimensional complex shapes, it's difficult to distinguish the one from the other. The primary "axial" resonances involve reflections from two opposing surfaces. Since the horns are axisymmetrical frequency pairs highlighted bold in table can be considered as axial modes shape frequencies. Coloration is important when considering sound propagation within the volume of horn. At these frequencies unexpected pressure peaks appear and can adversely affect the response. It has been observed that as the number of folding increase there appears more coloration in frequency range of 100 to 1000 Hz. These colorations frequencies will make sense while interpreting the SPL and directivity characteristics.

5.2. Acoustic Pressure, SPL

In real life applications, the levels and directivity of sound radiated through horn should be determined by measurements of sound levels at predefined points away from the horn mouths. Test procedures are developed to specify measurement conditions as well as locations of microphones. Measurement environment is often specified as anechoic space. In numerical studies to predict the sound levels and directivity characteristics radiation into free field is considered. Field points in the far field can be assigned to calculate these characteristics. They can be located anywhere inside any (acoustic or not) finite or infinite elements.

Analysis software MSC.Actran is capable of using finite and infinite elements together. Infinite elements allow for sound pressure levels calculation even far from the source. The discrete model of the surrounding air combines finite element modeling for the horn-shaped air cavity in the near field and infinite element modeling for the far field radiation. Fig. 5.13 shows the representation of the both domains covering the source.

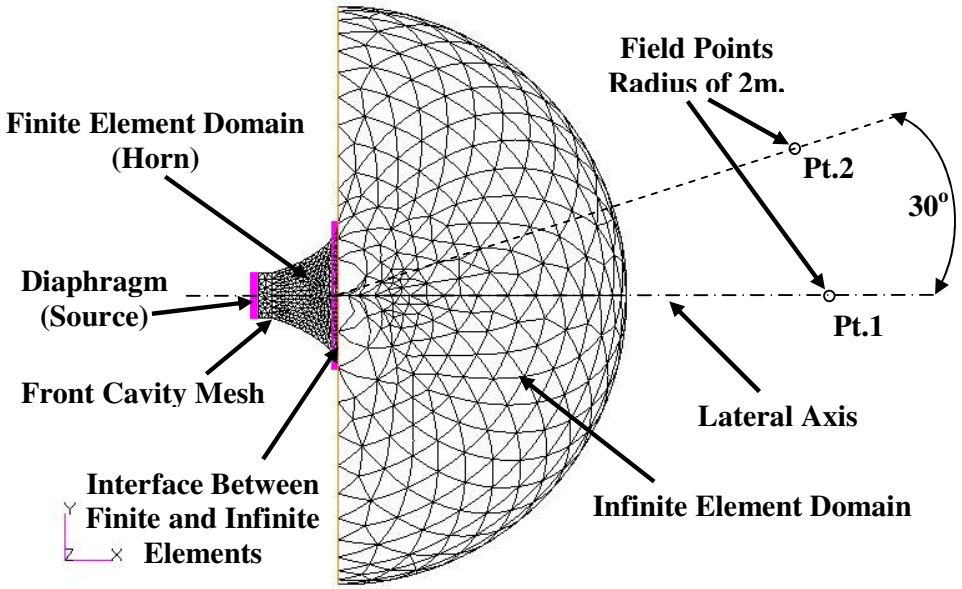

Fig. 5.13 Representation of the model for near to far field analysis

Frf (frequency response function) file of MSC.Actran can directly be plotted by any plotting tool (Patran) or loaded into Matlab or Excel (as ASCII file) in order to generate SPL vs. frequency curves. MSC.Actran uses direct sequential solver for the linear systems solver. There are three types of direct sequential solver are available. These are

i. Skyline
ii. Sparse
iii. Krylov

Analyses have been performed to found SPL values for two points, Pt.1 and Pt.2 as shown in Fig. 5.13 for each horn. One of the points is at 2 meter away from the center of the mouth plane which is on the lateral axis (on-axis) of the horn and the other point is again 2 meter away from the center of the mouth plane making 30 degree angle with lateral axis (off-axis). For these analyses, Krylov solver is used because of its high speed of analysis.

Used driver design parameters of the chosen driver to find the cone velocity for the analysis can be seen in the driver module of "Folded-Horn-Design" interface from Fig. 5.14. Applied input power of the driver is calculated from Equation 5.1 as 0.01 Watt.

$$P = \frac{V_{rms}^2}{R_E} = \frac{V^2}{2R_E} = \frac{0.4^2}{2\times 8} \tag{5.1}$$

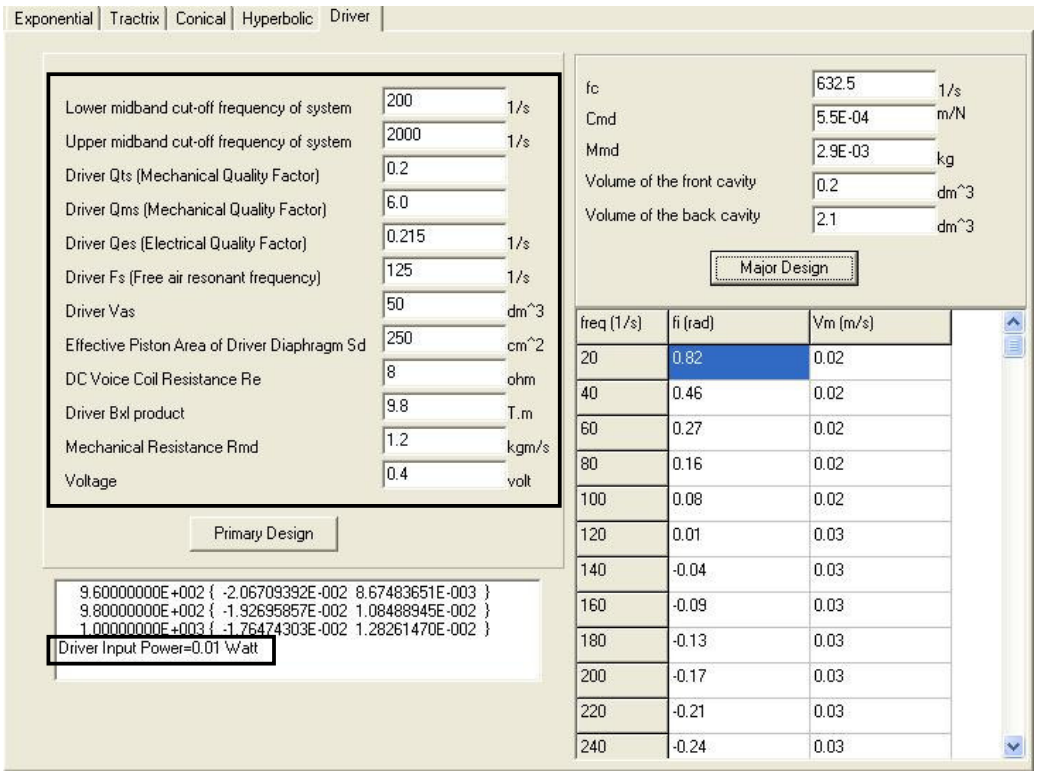

Fig. 5.14 Driver design parameters and input power

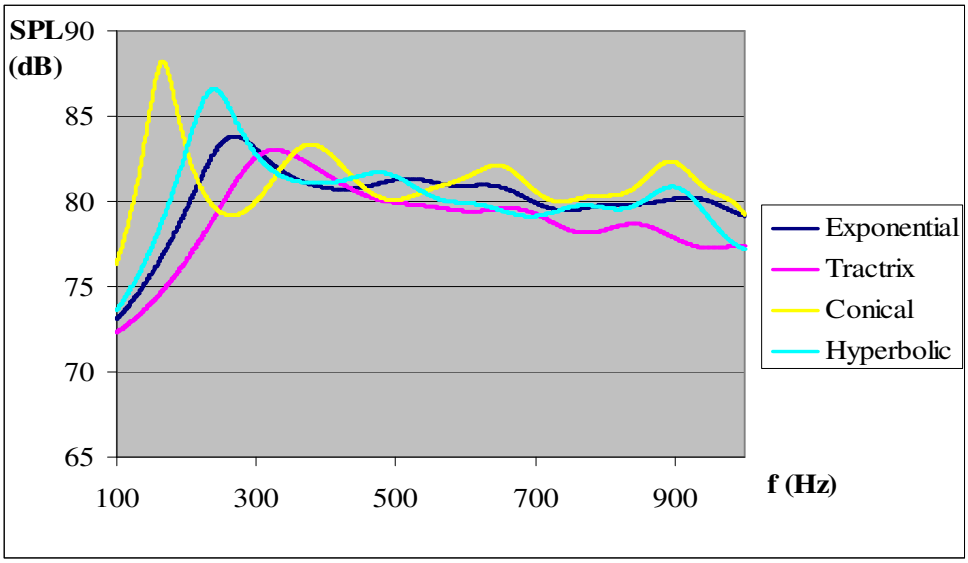

Fig. 5.15 SPL values at Pt.1 for non-folded horns

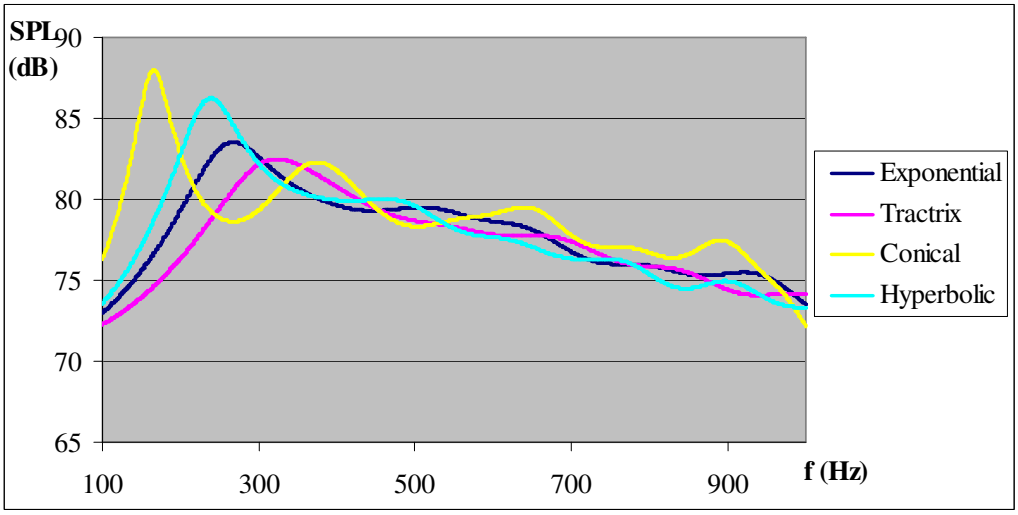

Fig. 5.16 SPL values at Pt.2 for non-folded horns

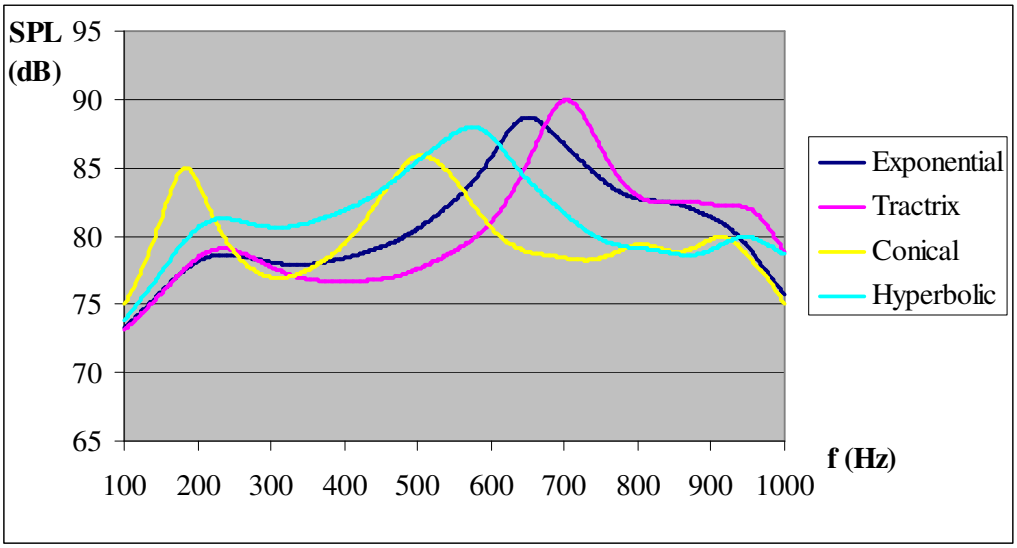

Fig. 5.17 SPL values at Pt.1 for single folded horns

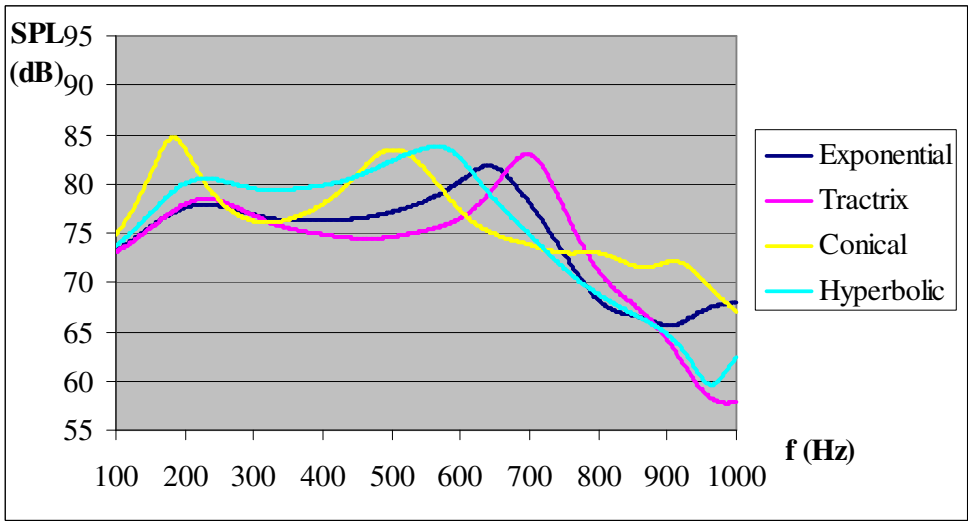

Fig. 5.18 SPL values at Pt.2 for single folded horns

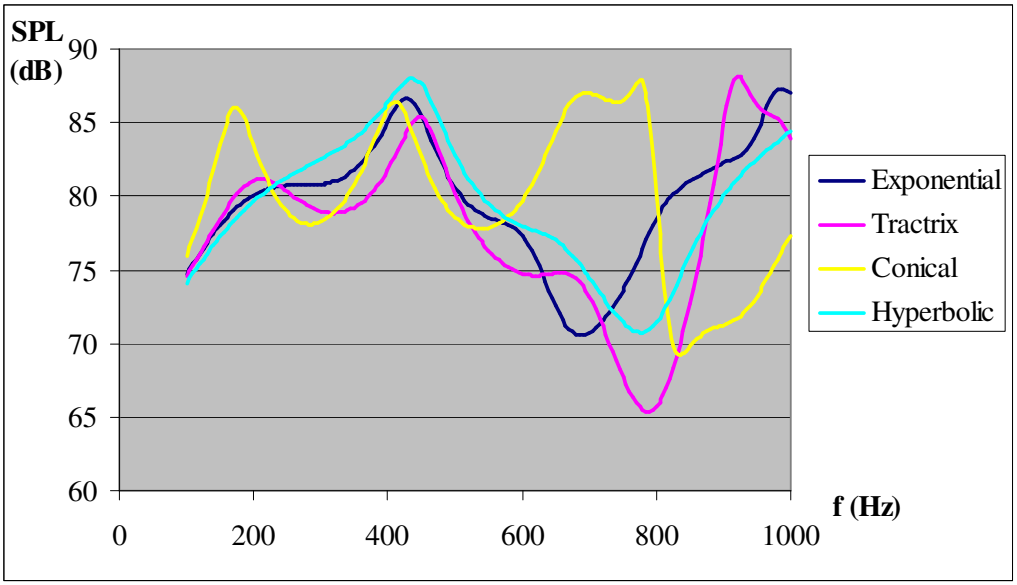

Fig. 5.19 SPL values at Pt.1 for double folded horns

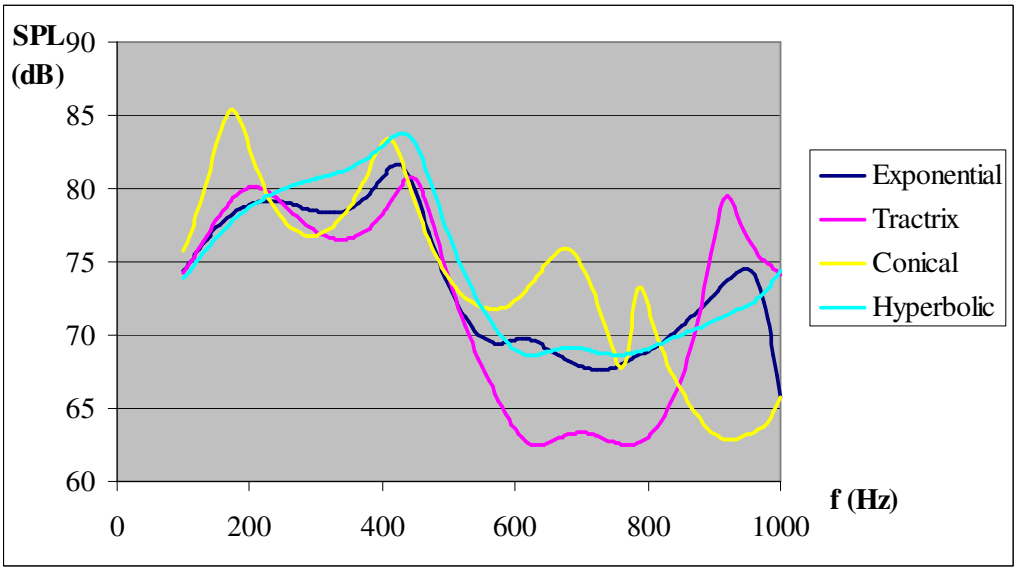

Fig. 5.20 SPL values at Pt.2 for double folded horns

Fig. 5.15 shows that in the frequency range between 300-1000 Hz hyperbolic and exponential non-folded horns yield better response than their counterpart since they

have smoother curve along the frequency range with generally higher average SPL. This implies these horns are more efficient and free from coloration in the specified frequency range.

In Fig. 5.16 all the horn responses show similar characteristics with no significant difference at all between each other. Responses decrease with increasing frequency as the frequency increase.

When these figures are compared it seems very difficult to predict the best horn flares types. The sharp peaks and dips need to be interpreted together with the natural frequencies. For example, there is sharp increase in the tractrix curve in Fig. 5.17 around 710 Hertz which may be attributed to pair of axial mode frequencies of 707.7 and 707.8 Hz (Table 5.4). In Fig. 5.18 the steady decrease on the SPL values of the hyperbolic horn frequencies 900-960 Hz can be observed. This drop may also be attributed to the mode shapes (there is 6 mode shapes) in this range (900-960 Hz). Coloration in this range can trigger the decrease on the SPL values. Similar observations can be also viewed in the other curves and graphs. Again, conical horn curve increases sharply at around 720 Hz and drops suddenly at around 840 Hz in Fig. 5.19. These frequencies are also coloration frequencies 728.1, 728.4, 810.2 and 836.9 Hz as shown in Table 5.1.

There have been no significant differences on SPL responses between each different flare horn. So it is also preferred to compare non-folded and folded cases besides making a comparison between different flare rates. Bends caused more distortions and affected SPL adversely. From below graphs (Fig. 5.21-5.28), the effects of folding can be observed and compared for each horn separately. All the non-folded horns show more uniform responses. Less fluctuation is observed at conical horns with folding (Fig.5.21 and Fig.5.22), while tractrix responses worsen much more than the others with the folding (Fig. 5.27 and 5.28).

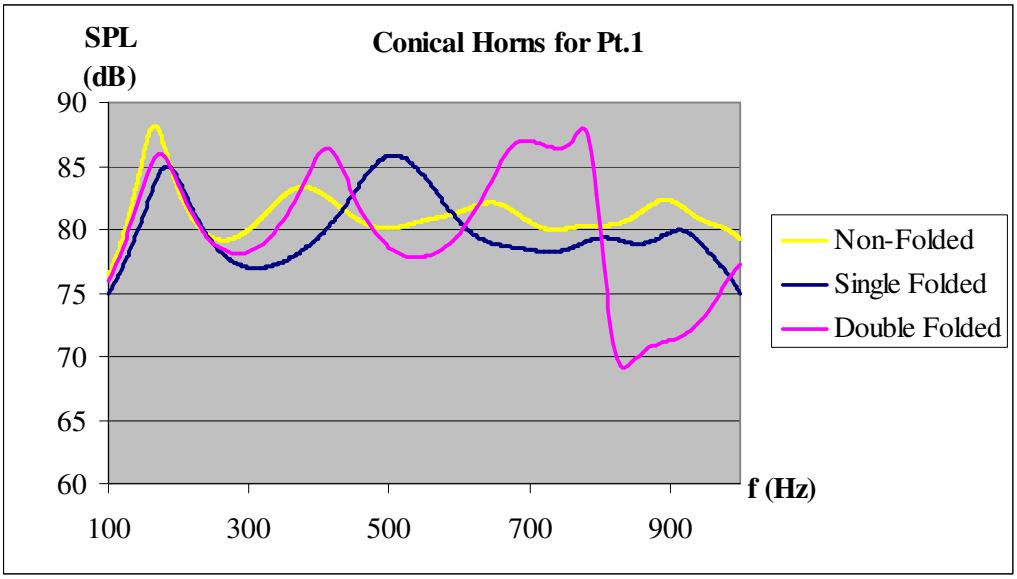

Fig. 5.21 Responses of conical horn types at Pt.1

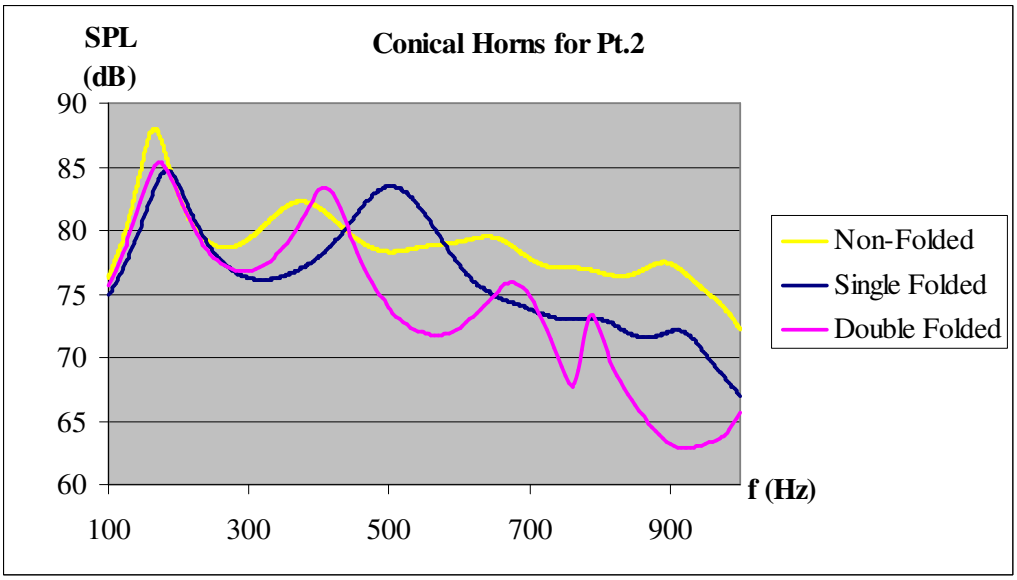

Fig. 5.22 Responses of conical horn types at Pt.2

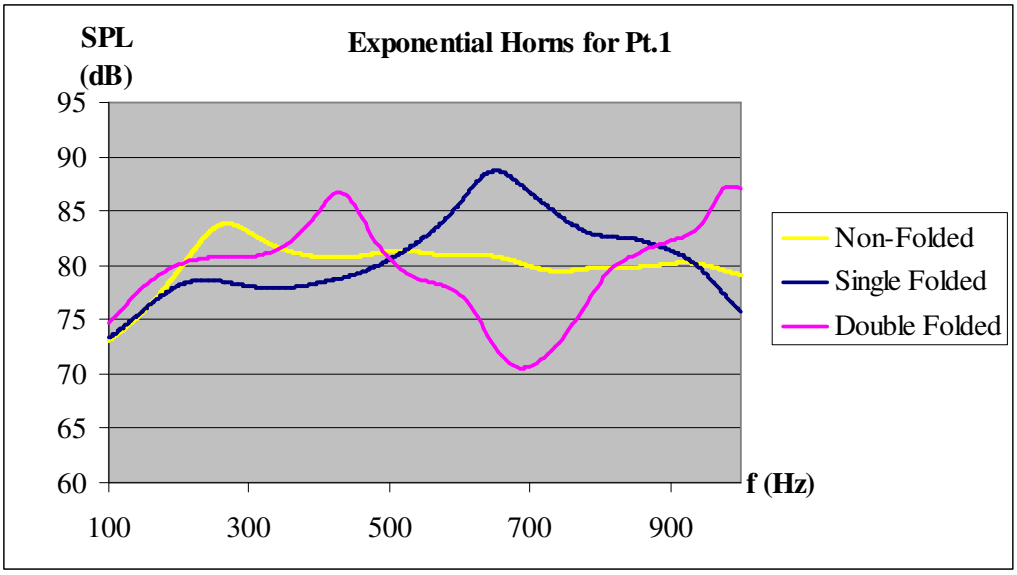

Fig. 5.23 Responses of exponential horn types at Pt.1

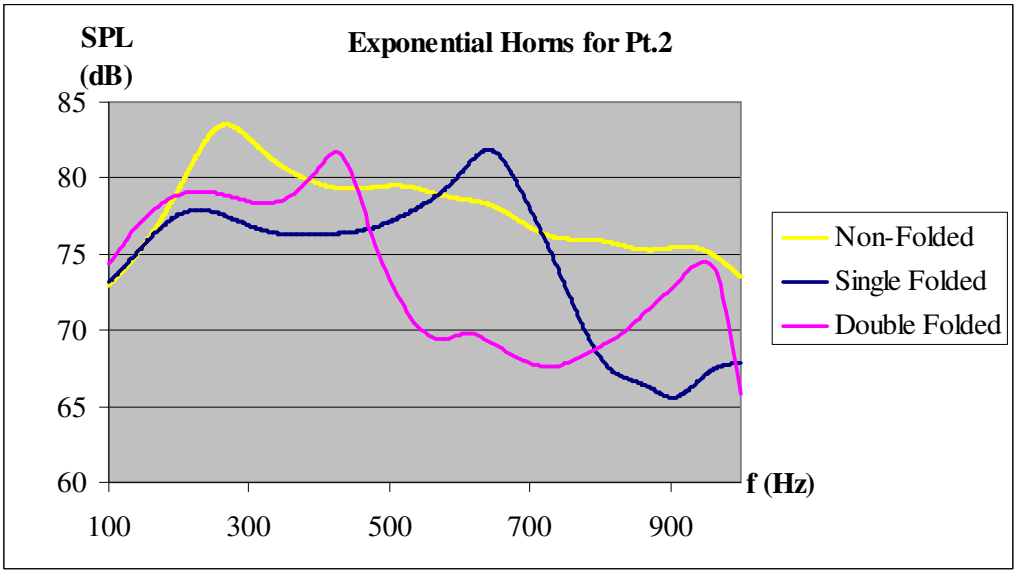

Fig. 5.24 Responses of exponential horn types at Pt.2

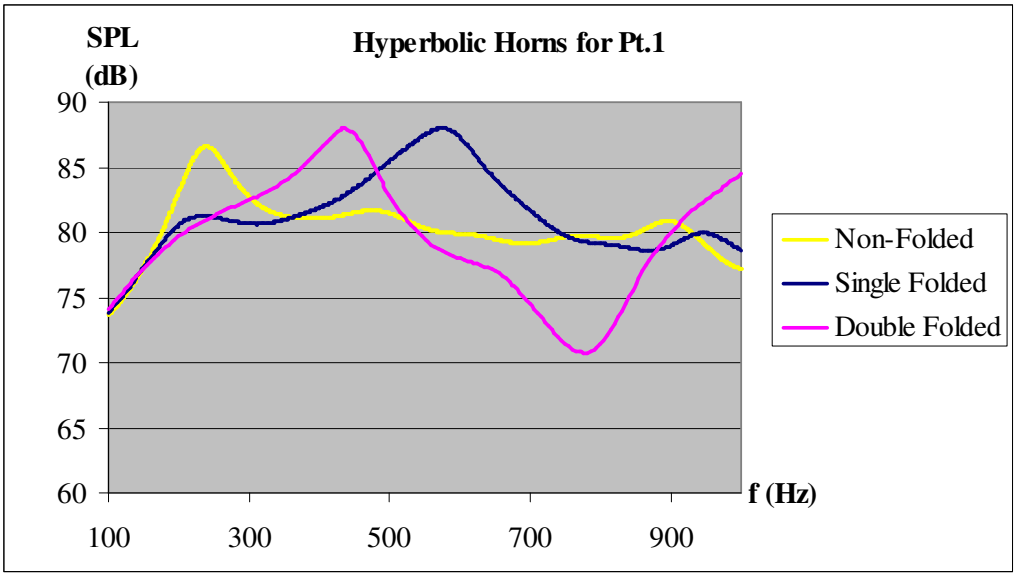

Fig. 5.25 Responses of hyperbolic horn types at Pt.1

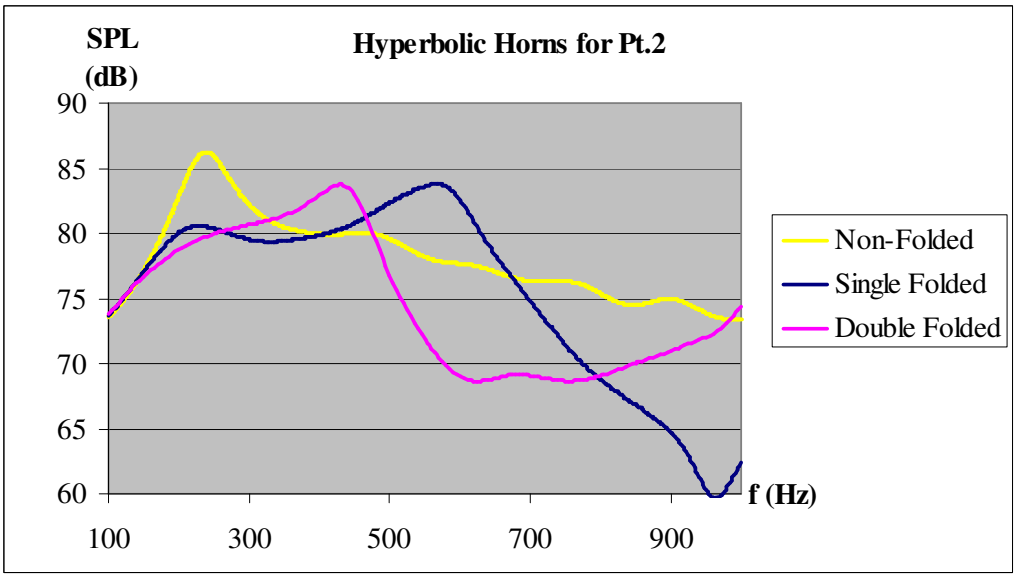

Fig. 5.26 Responses of hyperbolic horn types at Pt.2

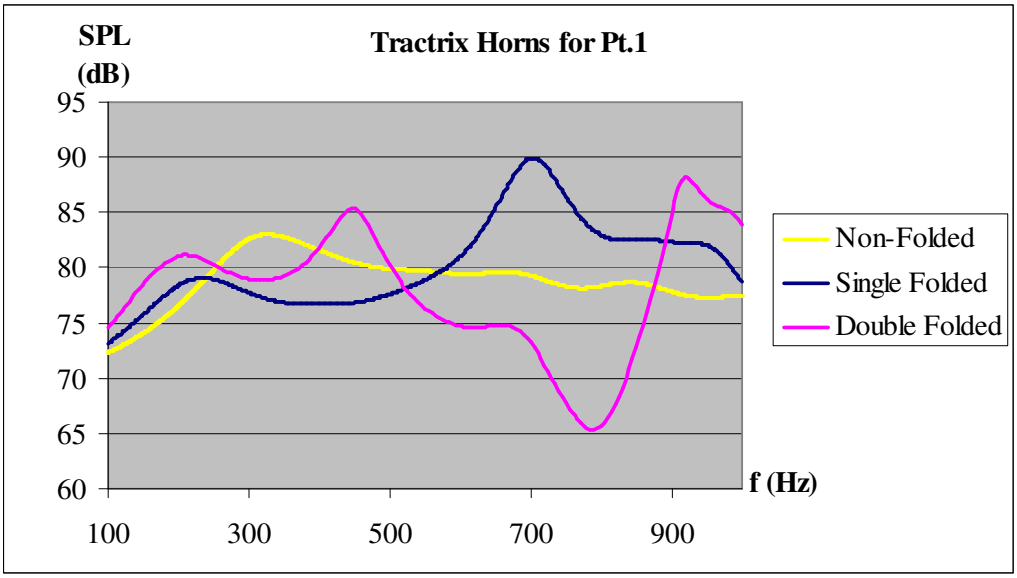

Fig. 5.27 Responses of tractrix horn types at Pt.1

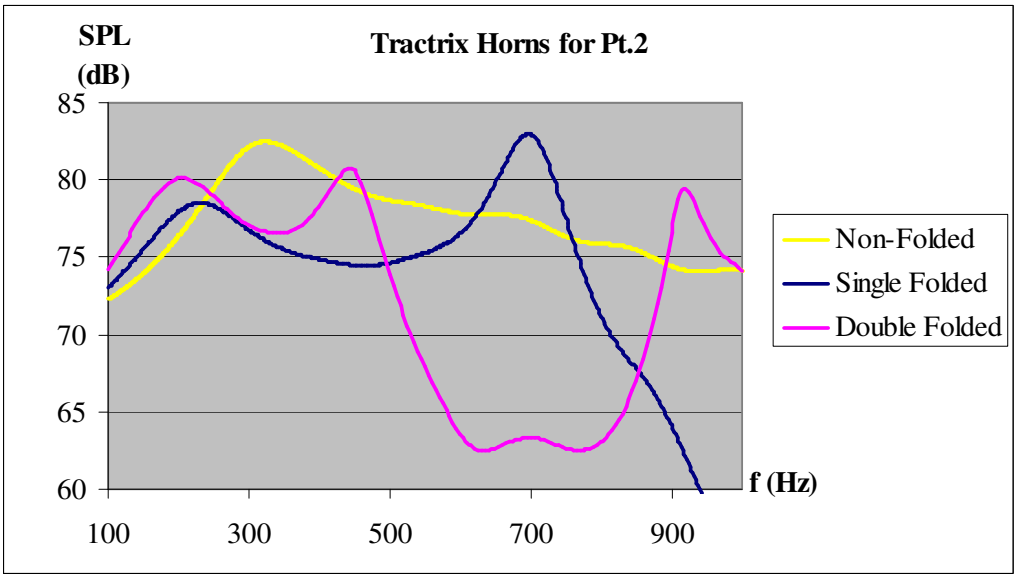

Fig. 5.28 Responses of tractrix horn types at Pt.2

Since the effective length increase with the foldings, SPL values can be higher in some ranges of frequencies because they behave more like infinite horns and transmission efficiency increases a bit. But because of higher extent of coloration, responses are not uniform and fluctuate considerably from uniform behavior. For horns with finite lengths, resonance results from reflection waves from mouth (also from bordering enclosures), causing irregularities in the SPL characteristics. It's also observed that on axis SPL behaviors (at Pt.1) do not deteriorate as much as the one off-axis SPL behaviors (at Pt.2). Average on-axis SPL values are listed in Table 5.5.

These values are lower than the real life situations, because input driver voltage has been taken as 0.4 Volt (then V_{rms}=0.28 Volt) and driver coil resistance has been taken as 8 ohm. These values correspond to 0.01 Watt, 100 times smaller than the standard applications driver input power value (1 Watt). In order to find corresponding values of SPL for 1 Watt power, sensitivity ratings can be used. Ratings based on the sound pressure level for a given input voltage or power is known as sensitivity ratings. The sensitivity is usually defined as (dB/W·m) decibels output for an input of one nominal watt or a specified input voltage. The rms value of voltage used is often 2.83V, which happens to be 1 watt at a nominal 8 ohms. Measurements taken with this reference are quoted as (dB/2.83V·m).

Table 5.5 Average on-axis SPL values of all kinds of horns

Horn Type	Average SPL Values (dB)
Non-Folded Conical	81.3
Non-Folded Exponential	80.3
Non-Folded Hyperbolic	80.5
Non-Folded Tractrix	78.9
Single Folded Conical	80.0
Single Folded Exponential	80.8
Single Folded Hyperbolic	81.4
Single Folded Tractrix	80.4
Double Folded Conical	79.9
Double Folded Exponential	79.6
Double Folded Hyperbolic	79.5
Double Folded Tractrix	77.9

Since the SPL analyses are performed at 2 meters away (r_2) from the mouth, firstly corresponding average SPL (SPL_1) values at 1 meter (r_1) should be found. The inverse square distance law in the free field for the sound pressure p is inverse-proportional to the distance r of a point sound source. The pressure at 2 meter is p_2 and pressure at 1 meter is p_1, then p_1 can be calculated in terms of p_2 (Equation 5.2). By using SPL equation (Equation 5.3) p_2 values can be found from average SPL values.

$$\frac{p_1}{p_2} = \frac{r_2}{r_1} = 2 \tag{5.2}$$

$$SPL = 10\log_{10}\left(\frac{p^2}{p_o^2}\right) = 20\log_{10}\left(\frac{p}{p_o}\right) \tag{5.3}$$

where p is either p_1 or p_2 and p_o is the reference sound pressure (=$1x10^{-6}$ Pascal), and SPL_1 is SPL values at 1 meter.

After calculations all the SPL values 1 meter away from the mouth can be found and given in Table 5.6. It is also derived from Equation (5.3) that doubling the pressure corresponds to an increase of 6 dB in SPL.

Table 5.6 SPL values at one and two meter away from the horn mouths

Horn Type	Average SPL Values at 2 meter (dB)	Average SPL Values at 1 meter (dB)
Non-Folded Conical	81.3	87.3
Non-Folded Exponential	80.3	86.3
Non-Folded Hyperbolic	80.5	86.5
Non-Folded Tractrix	78.9	84.9
Single Folded Conical	80.0	86.0
Single Folded Exponential	80.8	86.8
Single Folded Hyperbolic	81.4	87.4
Single Folded Tractrix	80.4	86.4
Double Folded Conical	79.9	85.9
Double Folded Exponential	79.6	85.6
Double Folded Hyperbolic	79.5	85.5
Double Folded Tractrix	77.9	83.9

Finally, normalization is needed for the input electrical power. Initial power (P_1=0.01 watt) is modified for 1 watt power input (P_2). This implies an increase of 100 times. Then, new SPL values (SPL_2) can be calculated from equation (5.4). Corresponding SPL values for 1 watt driver input (electrical) power are listed in Table 5.7.

$$SPL_2 = 10\log_{10}\frac{P_2}{P_r} = 10\log_{10}\frac{100P_1}{P_r} = 10\log_{10}\frac{P_1}{P_r} + 10\log 100 = SPL_1 + 20 \qquad (5.4)$$

Table 5.7 Corresponding normalized SPL values for 1 watt driver input power (Sensitivity Ratings, SR)

Horn Type	SPL_2 (dB) or SR (dB/W.m)
Non-Folded Conical	107.3
Non-Folded Exponential	106.3
Non-Folded Hyperbolic	106.5
Non-Folded Tractrix	104.9
Single Folded Conical	106.0
Single Folded Exponential	106.8
Single Folded Hyperbolic	107.4
Single Folded Tractrix	106.4
Double Folded Conical	105.9
Double Folded Exponential	105.6
Double Folded Hyperbolic	105.5
Double Folded Tractrix	103.9

5.3. Directivity Characteristics

Complete directivity analysis start with finding sound pressure levels (SPL) at all points on a sphere surrounding the loudspeaker system. In other words, the loudspeaker is at the center of that sphere, and the distance between the loudspeaker and the surface of this sphere would be equal at all points and should be large when compared to the loudspeaker's dimensions. In order to achieve this, a field point mesh has been generated and it is used for the analysis of directivity. Because while measuring directivity, there should be circular shape of field points on x-y plane (or x-z plane), which is perpendicular to mouth plane of the horns (Fig.5.29). It can be performed for different axial distance from the throat. Measurements have been made certain frequencies from 250 Hertz to 2000 hertz and for the radius of 2 meters.

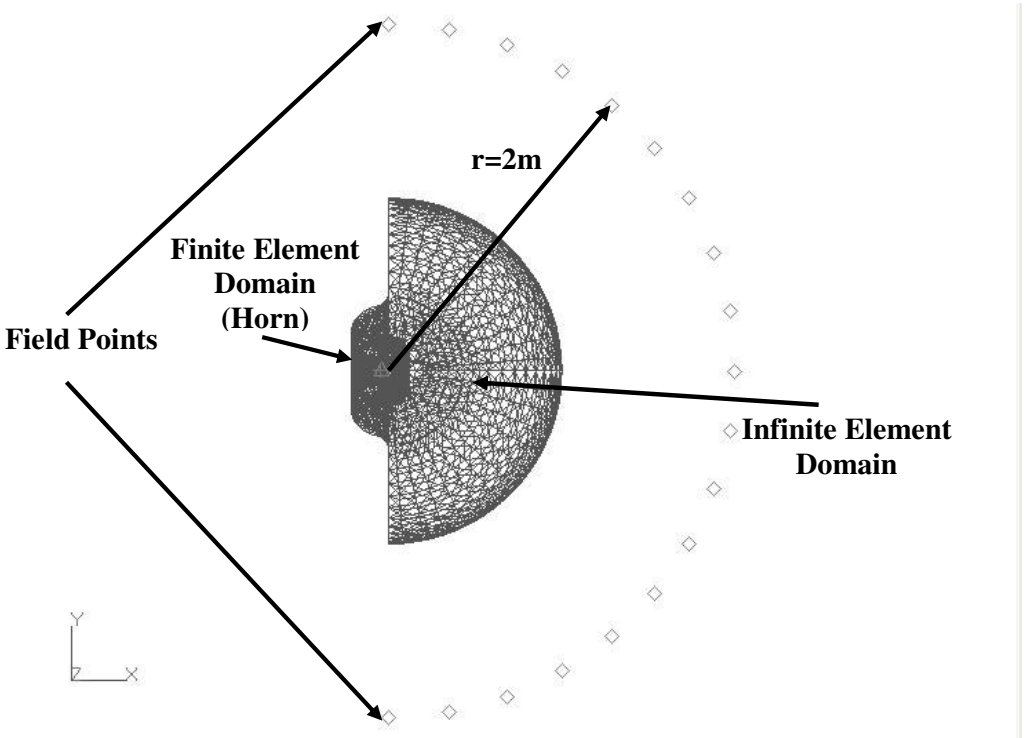

Fig. 5.29 Complete finite element model for prediction of Directivity Characteristics

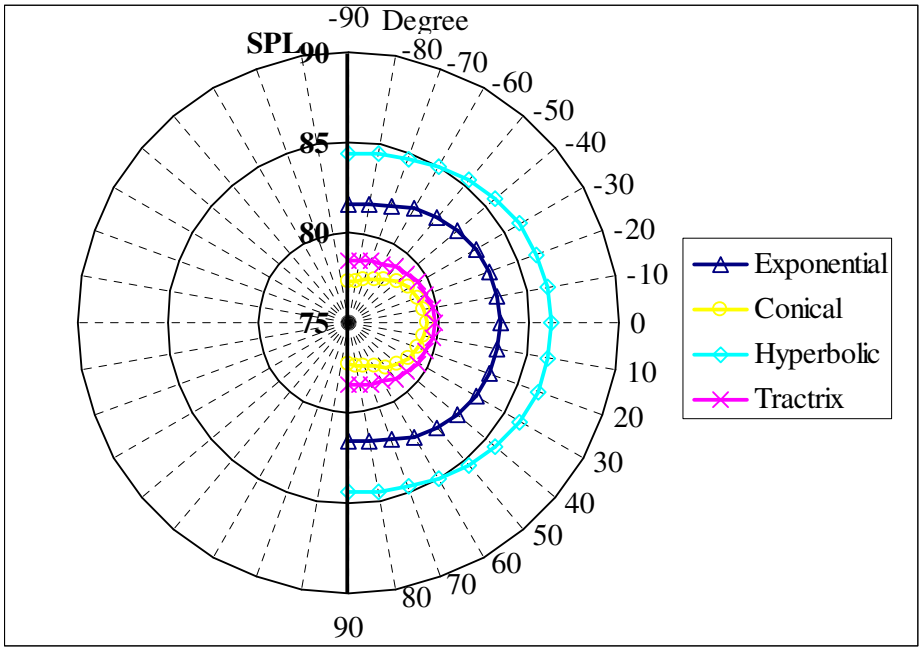

Fig. 5.30 Directivity patterns of non-folded horns at 250 Hz

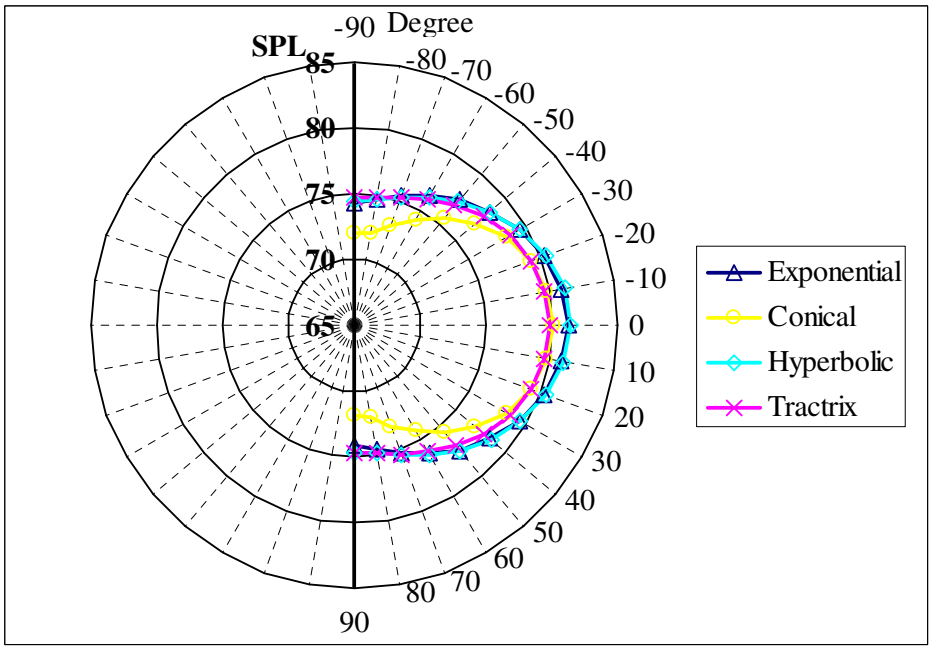

Fig. 5.31 Directivity patterns of non-folded horns at 500 Hz

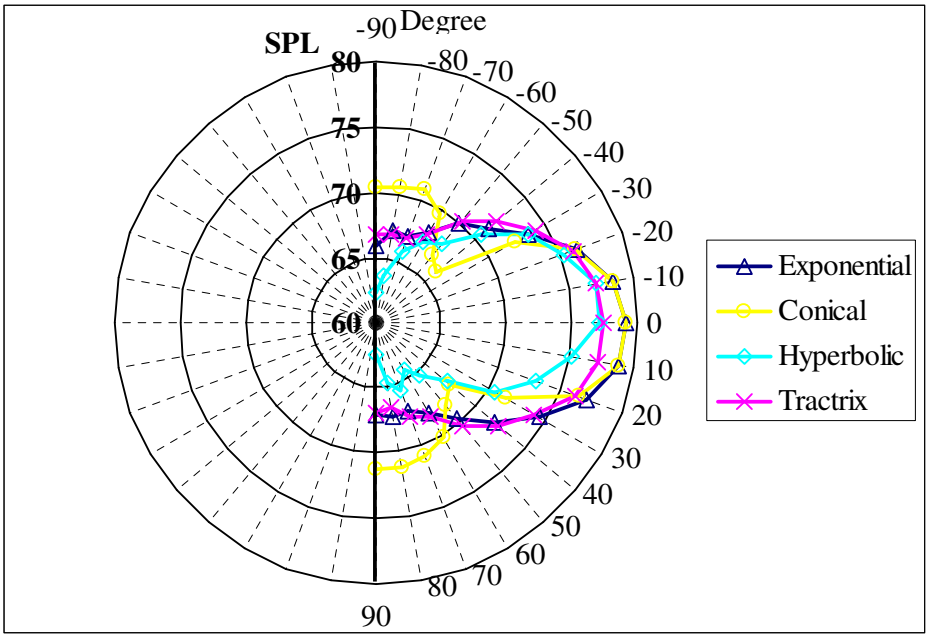

Fig. 5.32 Directivity patterns of non-folded horns at 1000 Hz

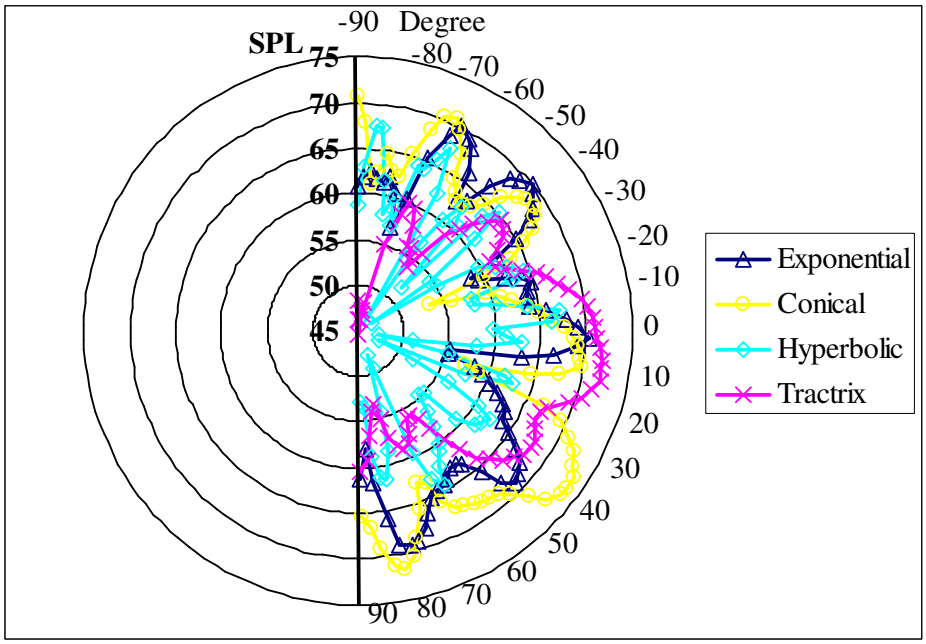

Fig. 5.33 Directivity patterns of non-folded horns at 2000 Hz

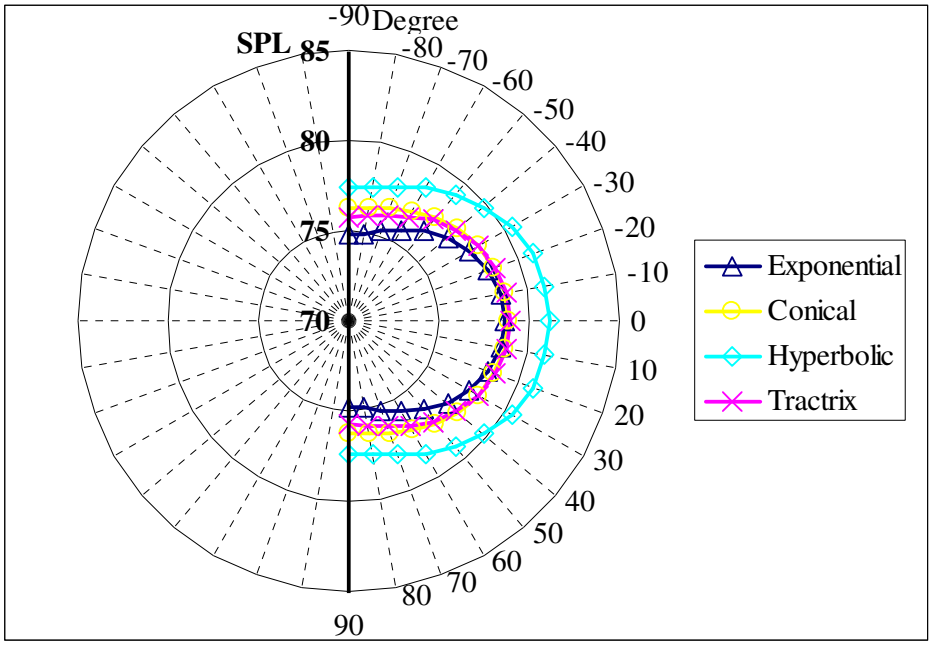

Fig. 5.34 Directivity patterns of single folded horns at 250 Hz

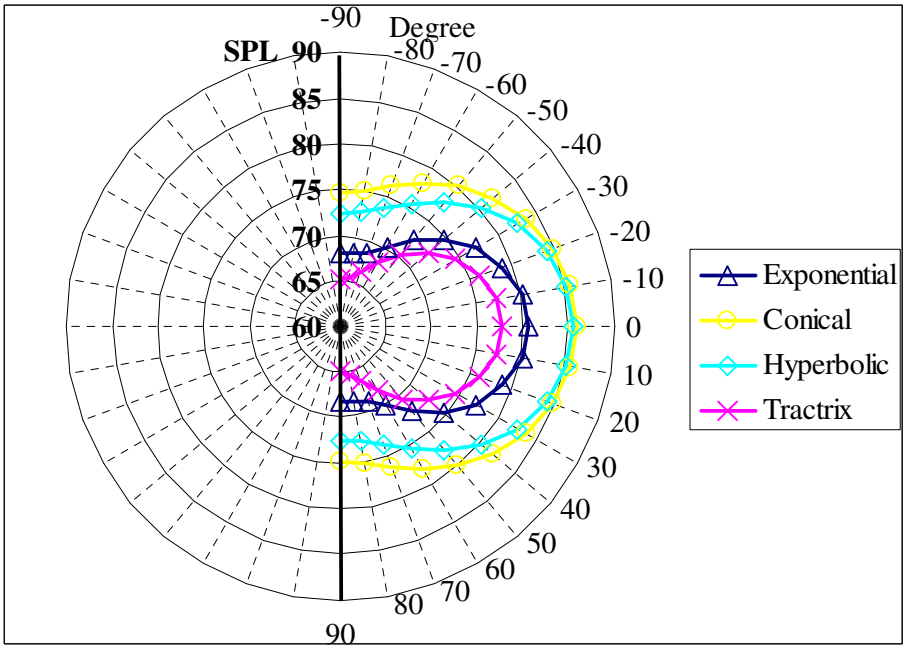

Fig. 5.35 Directivity patterns of single folded horns at 500 Hz

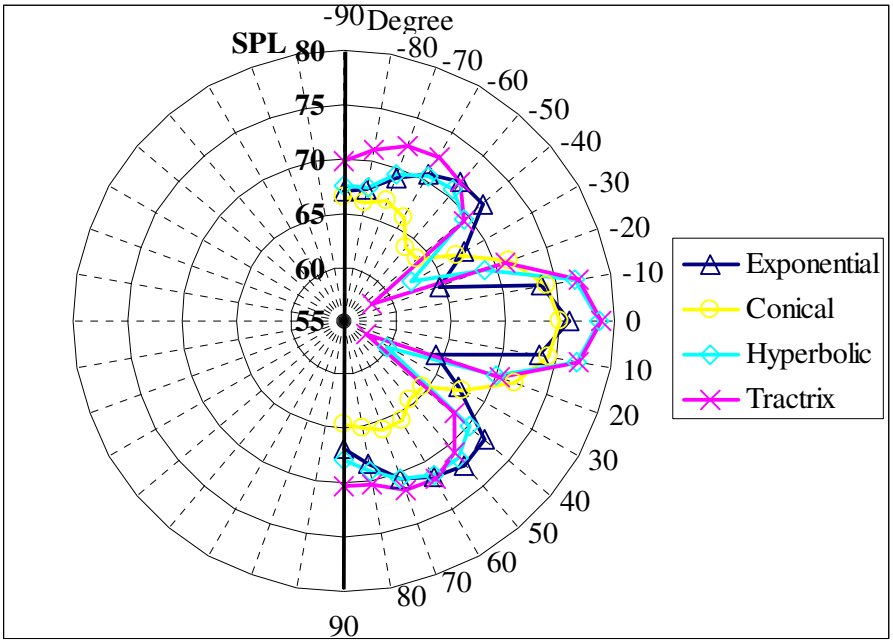

Fig. 5.36 Directivity patterns of single folded horns at 1000 Hz

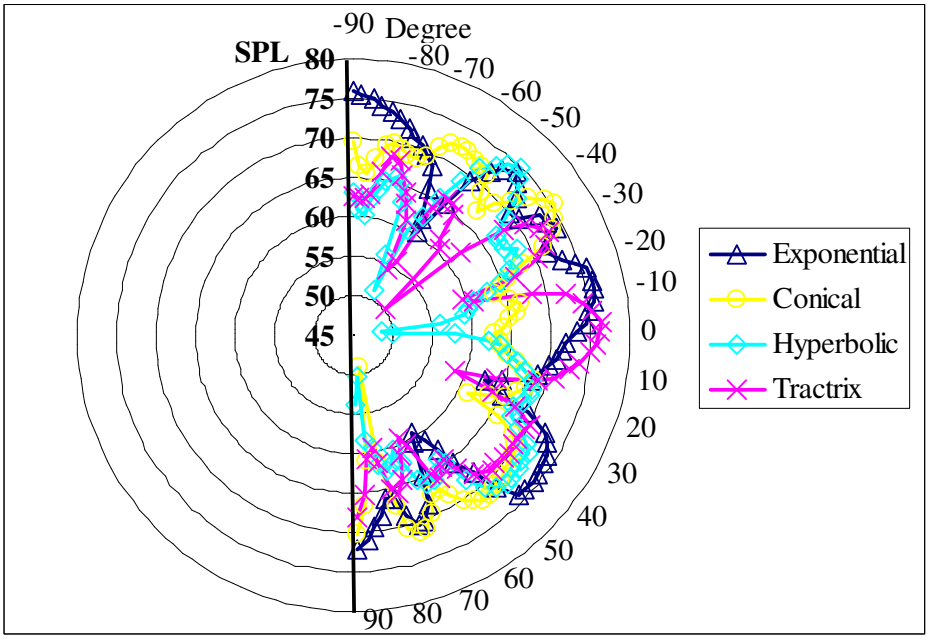

Fig. 5.37 Directivity patterns of single folded horns at 2000 Hz

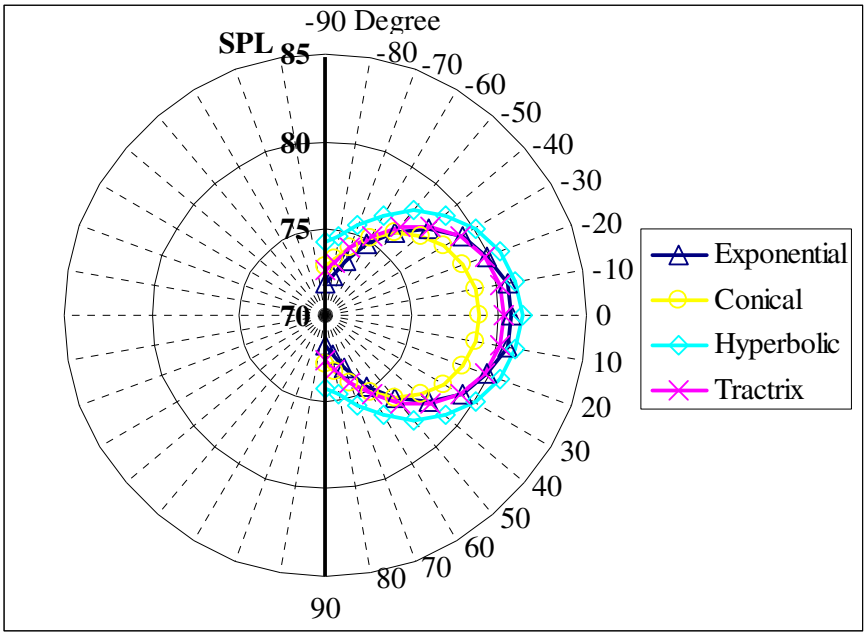

Fig. 5.38 Directivity patterns of double folded horns at 250 Hertz

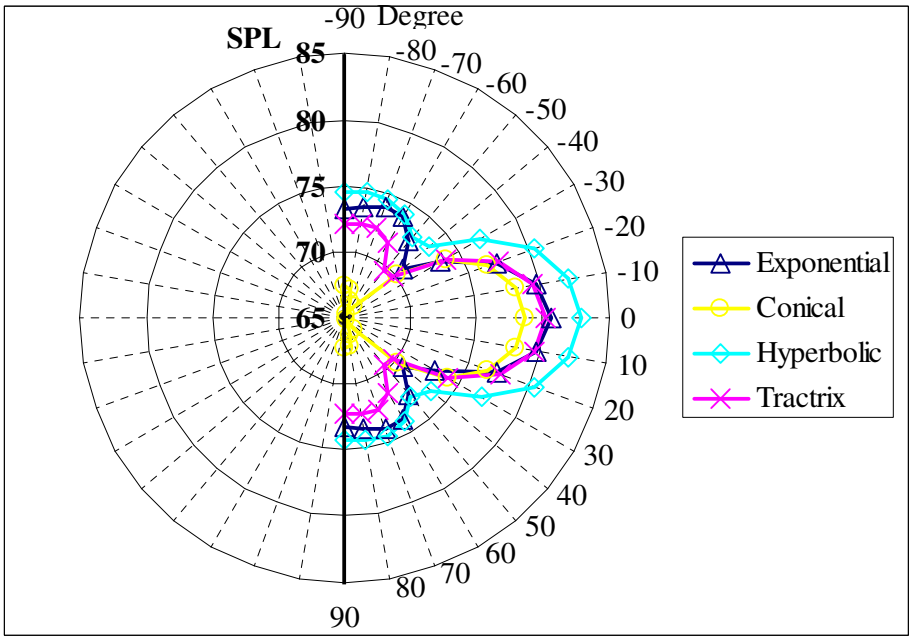

Fig. 5.39 Directivity patterns of double folded horns at 500 Hertz

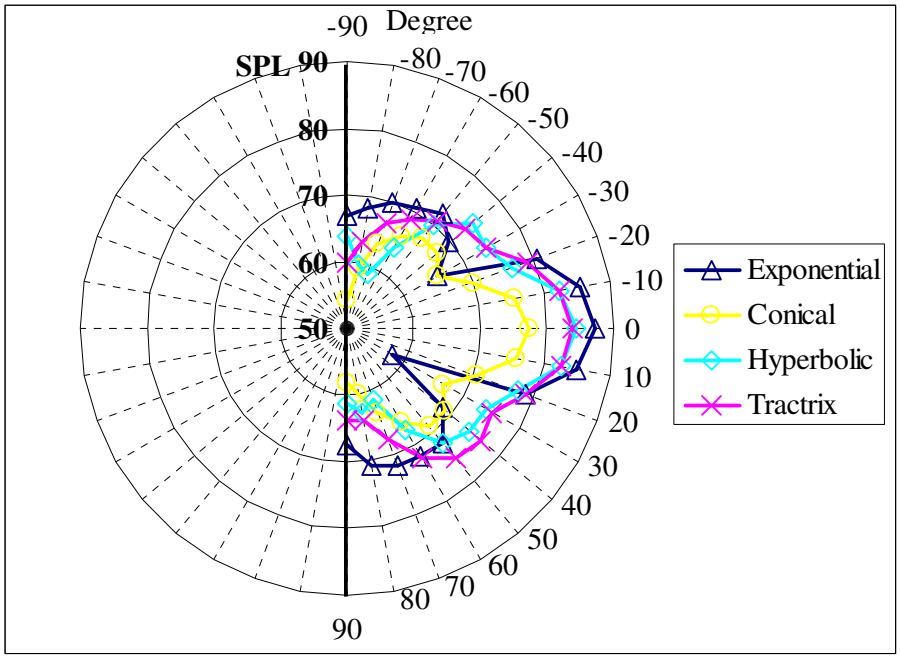

Fig.5.40 Directivity patterns of double folded horns at 1000 Hertz

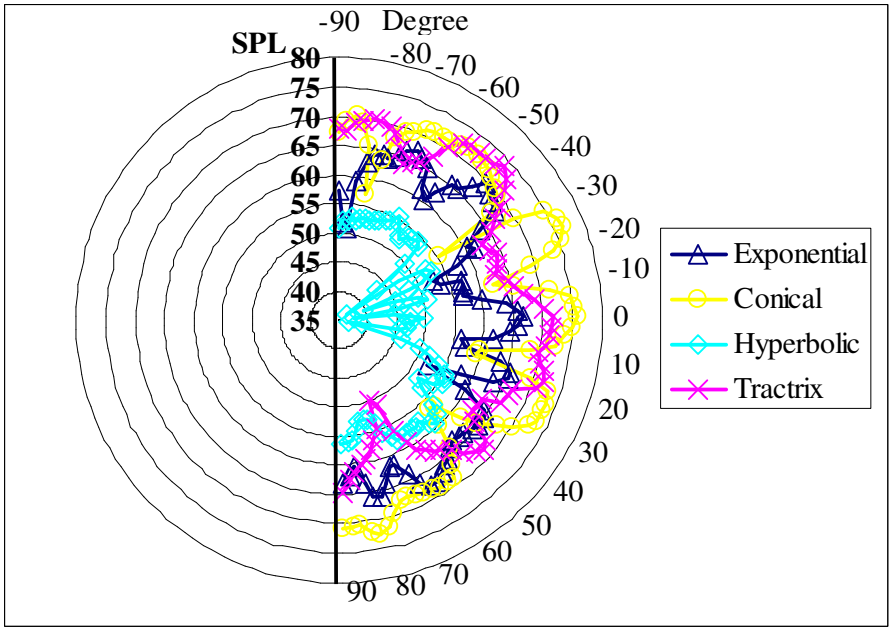

Fig.5.41 Directivity patterns of double folded horns at 2000 Hertz

By looking at the directivity characteristics plots (from Fig.5.30 to Fig.5.41), it can be deduced that the higher the frequency the worse is the directivity characteristics. There appear more lobes in directivity characteristics. With regard to higher frequencies, non-linearities become more apparent especially after four times the cut-off frequencies. This rule of thumb comes from the phenomenon of air overload distortion and Beranek [16, Fig.9.12] showed the percentage of distortion change according to different f/f_c. In this case, f_c equals to 200 Hz and $4xf_c$ equals to 800 Hz and above 800 Hz (at 1000 Hz and 2000 Hz) directivity characteristics heavily distort. Distortion also increases with folding(s) since the wavefronts at the higher frequencies can be distorted at bends. Furthermore, at high frequencies the vibration of a loudspeaker cone takes complex shape, so that normal variations in the uniformity of cones result in substantial differences in the radiation. This effect may result to a very irregular and unpredictable response curve and directivity pattern at high frequencies such as 1000 Hz and 2000 Hz.

As mentioned in the previous section, dB values are evaluated for a driver having 0.01 watt input power. For this reason in evaluation of plots relative levels are considered instead of the absolute values. It is also possible to add 20 dB to each point to normalize the results.

5.4. CPU Times and Computer Specifications

All of these calculations have been performed at the computer specifications given blow:

RAM: 1 Gb (512x2) TwinMos Dual DDR 400 MHz
Processor: AMD Athlon 64 3000+ VENICE (1.8GHz, 512K, S939)
Motherboard: MSI K8N Neo4 Platinium

Table 5.8 Element and node numbers of all type horns

Horn Type	Finite Element #	Infinite Element #	Total Node #	Total Element #
Non-Folded Conical	9044	21420	5854	30465
Non-Folded Exponential	9605	25150	6612	34756
Non-Folded Hyperbolic	9264	12977	4453	22242
Non-Folded Tractrix	9129	39050	8916	48180
Single Folded Conical	54380	25550	16073	79929
Single Folded Exponential	53350	25549	15681	78900
Single Folded Hyperbolic	58072	25548	16718	83621
Single Folded Tractrix	47643	26268	14517	73912
Double Folded Conical	96090	25526	24976	121617
Double Folded Exponential	93779	24266	23537	118046
Double Folded Hyperbolic	102748	24669	25494	127418
Double Folded Tractrix	85208	25015	22115	110224

Note: There is also one source element and field points (extra nodes)

For natural frequency analysis there is no infinite elements, these type of analysis are just performed for finite elements. Table 5.6 shows the required CPU times for corresponding horns and memory usage. All the three dimensional elements are tetrahedral and two dimensional elements are triangular in the finite element model.

Table 5.9 Required CPU Times for the natural frequency analyses
for frequency of 1 Hz to 2000 Hz

Horn Type	MEM Usage	CPU Times (minutes)
Non-Folded Conical	700	3.4
Non-Folded Exponential	700	4.1
Non-Folded Hyperbolic	700	3.8
Non-Folded Tractrix	700	3.7
Single Folded Conical	700	15.2
Single Folded Exponential	700	15.1
Single Folded Hyperbolic	700	15.9
Single Folded Tractrix	700	16.8
Double Folded Conical	700	28.8
Double Folded Exponential	700	28.1
Double Folded Hyperbolic	700	31.2
Double Folded Tractrix	700	27.6

While obtaining SPL values of single folded horn in the frequency range 100-1000 Hz, due to time limitations frequency increase steps have been taken as 2. So that, direct computation for 451 frequencies (100, 102, 104 ...1000 Hz) have been performed. In a similar manner Frequency increase steps have been taken as 5 for the double folded horn shapes and by doing that direct computation for 181 frequencies (105, 110, 115 ...1000 Hz) have been performed (Table 5.7). The higher the node and element number, the more CPU times are required and/or more memory allocation.

Since the CPU memory is limited to RAM of computer that the analyses are performed, time is an important criteria and in order to decrease required time one should decrease steps as told above. All the SPL analyses have included to total elements (finite and infinite) and nodes.

Table 5.10 Required CPU times for the SPL analyses for the frequencies of 100 Hz to 1000 Hz

Horn Type	MEM Usage	CPU Times (hours)	Frequency Number
Non-Folded Conical	700	1.6	901
Non-Folded Exponential	700	1.7	901
Non-Folded Hyperbolic	700	1.2	901
Non-Folded Tractrix	700	2.2	901
Single Folded Conical	700	12.5	451
Single Folded Exponential	700	12.2	451
Single Folded Hyperbolic	700	13.1	451
Single Folded Tractrix	700	11.8	451
Double Folded Conical	700	25.2	181
Double Folded Exponential	700	24.6	181
Double Folded Hyperbolic	700	25.1	181
Double Folded Tractrix	700	23.7	181

Finally, directivity analyses have been performed for different frequencies. These are 250, 500, 1000, 2000 Hz. In order to achieve these analyses field points (extra nodes) should be added to the geometry. For the frequencies of 250 Hz to 1000 Hz, only 19 field points have been used while for the frequency of 2000 Hz 73 field points have been used in order to have more accurate graphs. Since at high frequencies there are much more loops and it requires more field numbers to be able to indicate these lobes. Table 5.8 shows the average required times for just one frequency.

Table 5.11 Required time range for each directivity plot analyses

Horn Type	MEM Usage	CPU Times (minutes)	Frequency Number
Non-Folded Conical	700	3.2-3.5	1
Non-Folded Exponential	700	2.5-2.8	1
Non-Folded Hyperbolic	700	2.1-2.4	1
Non-Folded Tractrix	700	3.5-3.9	1
Single Folded Conical	700	12.5-16.2	1
Single Folded Exponential	700	11.8-15.9	1
Single Folded Hyperbolic	700	14.2-16.7	1
Single Folded Tractrix	700	14.5-15.2	1
Double Folded Conical	700	18.2-19.5	1
Double Folded Exponential	700	18.5-19.8	1
Double Folded Hyperbolic	700	21.4-25.4	1
Double Folded Tractrix	700	23.4-26.3	1

CHAPTER 6

SUMMARY AND CONCLUSIONS

6.1 Summary

Computer aided auto-construction of various types of folded horns and acoustic analysis of coupled horn and driver systems have been presented in this thesis. A new procedure has been developed for auto construction of folded horn shapes.

A computer interface called as “Folded Horn Design” has been developed in Delphi to facilitate the construction of the horn geometry by reducing the geometrical modeling time in a commercial FEA program. By arranging the primary design parameters four different types of horns have been analyzed. To obtain folded to double folded horns, different axial length limitations were designated. After all, horn geometry consisting of linear (conical), exponential, hyperbolic and tractrix shapes were automatically constructed by activating the interface of “Folded Horn Design”. FEM geometries of horn were constructed in MSC.Marc-Mentat and then these geometries were exported to acoustic finite element analysis software, MSC.ACTRAN, to calculate mode shapes, natural frequencies, directivity patterns and resulting sound pressure level (SPL) in the free field. Since radiated sound field expression depends on the velocity distribution on the loudspeaker vibrating diaphragm, the velocity distribution should have been determined. In order to model the loudspeaker linear graph modeling, which has the ability to manage complex relationships between inputs and outputs, was preferred. The electrical and mechanical properties of the horn driver were modeled with lumped elements for the linear graph modeling technique. Finally, driver cone ring velocity (source) and finite element models of horns were coupled. The walls bordering horn contours were considered rigid in the analysis. Cone geometry and front cavity were also included in the model.

6.2 Conclusions

Acoustically speaking the most prominent effect of natural frequencies associated with air entrapped in the horn boundaries is coloration. Each horn speaker has its own coloration characteristic. Coloration enhances certain frequencies and dulls others. Many bass horns have resonance problems. At natural frequencies unexpected pressure peaks appear adversely affecting the response. It has been observed that as the number of foldings increase, first natural frequencies getting smaller values and first 20 natural frequencies range has retreated to the range of 0 Hz to 1000 Hz. In non-folded case 20^{th} resonance has reached up to 1168-1569 Hz, whereas in single folded case they have only reached to 954-1138 Hz and in double folded case they have reached to 783-910 Hz. This is the proof of increasing the number of folding also increase the number of natural shapes (colorations). From standpoints of natural frequencies and corresponding mode shapes, non-folded horns have been the best. Non-folded and single folded tractrix and exponential horns have been observed to have less number of coloration than conical and hyperbolic. For the double folded case, the situation has differed a bit and the conical horn has exhibited the less extent of coloration. Then, the tractrix, hyperbolic and exponential horns have exhibited colorations in ascending order. These colorations have affected the SPL responses. In relation with the coloration frequencies, sharp peaks and dips on the SPL curves have been experienced.

Because of the increase in the effective length with the foldings, horns behave more like infinite horns and transmission efficiency rises a bit. It has been observed that SPL values of folded horns were higher than non-folded horns in some ranges of frequencies. But responses were not uniform and fluctuated considerably from uniform behavior because of higher extent of coloration. On the other hand, for horns with finite lengths, coloration results from reflection waves from mouth (also from bordering enclosures), causing unexpected irregularities in the SPL characteristics.

As expected from the coloration characteristics, non-folded tractrix and exponential horns have result more uniform on-axis response of pressure distribution at one

meter away from the horn mouth, again exponential type horns are better. It's known that throat resistance for the tractrix and hyperbolic horn reaches the value of unity quicker than the other type of horns. This condition could have affected the results for the sake of hyperbolic and tractrix horns. However, non-linear distortion is higher for the Tractrix and Hyperbolic as Beranek [16] stated, because these horns have a tube that flares very little until it gets to the end where it flares suddenly. The problem with such a long tight flare is that as sound pressures increase, the restricted passage for the air causes it to begin to compress and this causes distortion. It's called as second harmonic distortion at throat. Therefore, second harmonic distortion at throat could have affected the hyperbolic and tractrix horn adversely. It has been also noted that there has been no significant differences on SPL responses between each different flare horn. So it was preferred to compare non-folded and folded cases instead of making a comparison between different flare rates. Bends caused more distortions and affected SPL adversely. All the bends were π radian but not sharp. It's important for sound transmission arranging lateral dimension (axial length) of horn up to bend is not at half wavelengths. In order to achieve smooth transmission, at bends cross-sectional area continue to change in a similar manner i.e. at the same rate the area as change before the bends.

There are several important factors causing distortion and nonuniformity in the directivity characteristics. These are nonuniformity of the velocity distribution in the cone especially at high frequencies and nonlinearity of air. It was concluded that, the higher the frequency is, the worse the directivity characteristics will be. Non-linearity became more apparent especially after four times of the cut-off frequencies. Beranek [16, Fig.9.12] had showed the percentage of distortion change according to different f/f_c. In this case, f_c was equal to 200 Hz for all kind of horns and $4xf_c$ was equal to 800 Hz. Above 800 Hz (at 1000 Hz and 2000 Hz) directivity characteristics have heavily distorted. Distortion also increased with folding(s) since the wavefronts at the higher frequencies could have been distorted at bends. Furthermore, at high frequencies the vibration of a loudspeaker cone takes complex shapes, so that normal variations in the uniformity of cones have resulted in substantial differences in the

radiation. This effect may result to a very irregular and unpredictable response curves, and directivity patterns at high frequencies such as 1000 Hz and over.

SPL values are evaluated for a driver having 0.01 watt sine input power. For this reason sensitivity ratings gave more logical information about how the designed horns would response. These ratings calculated and tabulated for the average SPL values of horns and it was seen that the values of sensitivity ratings have been in the range of 103.9 to 107.4 (dB/W.m). These values were obtained for one meter distance and for 1 watt driver sine input power.

6.3 Future Works

One possible future work is, in addition to auto construction of horn geometry, auto analysis can be achieved. Furthermore, acoustical analyses have been performed for rigid and non-absorbing enclosure assumption. The absorption of sound by the walls and the effect of their stiffness introduce attenuations. Vibration of the walls distorts the frequency characteristic and introduces reverberation. These can be also studied and appropriate boundary conditions can be specified between horn cavity and walls and their effects can be analyzed. The effect of wall materials and thickness can also be observed.

Another future work involves slight modifications in the algorithms to accommodate different bending for one type horn. Different function and relations can be developed while switching the coordinates, i.e. from rectangular to polar. Comparisons can be made between the folding techniques and folding functions. In addition, it may very insightful to evaluate the restriction of horn width at a bend to specific number times the highest wavelength and the axial length that folding(s) can be attempted.

While horn mouths with different width to height ratio can be constructed by using designed interface, analyses have been only performed for the width to height ratio of 1 and for rectangular mouth shapes. Analysis can be performed for horn mouths

with different width to height ratio. Then these analyses can be compared for the optimum shape of the horn mouths.

Horns with two different flare sections (permutation forms) can also be constructed by a small modification in the algorithm. In practice, these types of horns are commonly considered as horns with good loading and directivity control.

Finally, all the designed and constructed horns can be manufactured to test in an anechoic chamber to compare and validate the results of FEA obtained.

REFERENCES

[1] Strutt, J. W. (Lord Rayleigh), *The Theory of Sound*, 2nd Edition, London, Macmillan, 1926 (1st Ed., 1877).

[2] Webster, A.G., "Acoustical impedance and the Theory of Horns and of the Phonograph", Proc. Natl. Acad. Sci., Vol.6, 1919.

[3] Hanna, C. R. & Slepian, J., "The Function and Design of Horns for Loudspeaker", J. Amer. Institute of Electrical Engineers Vol. 23, Feb. 1924.

[4] Flanders P. B., British Patent No.245, 415, March 1927.

[5] Kellogg, E. W. and Rice, C. W., "Notes on the Development of a New Type of Hornless Loud Speaker", J. American Institute of Electrical Engineers, vol. 44, pp. 982-991, (1927).

[6] Ballantine, S., "On the Propagation of Sound in the General Bessel Horn of infinite Length", J. Franklin Inst., pp. 85-103, 1927.

[7] Wilson, P. & Webb, A. G., *Modern Gramophones and Electrical Reproducers*, Cassel 1929.

[8] Crandall, I. B., *Vibrating Systems and Sound*, van Nostrand, 1926

[9] Voigt, P. G. A. H., British Patent Nos. 278,098 (1927), 351,209 (1930), 404,037 (1934), 435,042 (1935).

[10] Bos, H. J. M., "Recognition and wonder: Huygens, tractional motion and some thoughts on the history of mathematics", *Tractrix* **1**, 3-20, 1989.

[11] Lindsay, R. B., “Connectors in Acoustical Conduits”, Amer. Phys. Soc. Physical Review vol. 34, pp. 808-816, sept. 1929.

[12] Freehafer, J.E., “An Acoustical Impedance of an Infinite Hyperbolic Horn”, J. Acoustic Soc. Am., Vol. 11, pp. 467-476, April 1940.

[13] Salmon, V., “Generalized Plan Wave Horn Theory”, J. Acoustic Soc. Am., Vol. 17, pp. 199-221, January 1946.

[14] Salmon, V., “A New Family of Horns”, J. Acoustic Soc. Am., Vol. 17, pp. 212-218, January 1946.

[15] Mawardi, O. K., “Generalized Solutions of Webster’s Horn Theory”, J. Acoust. Soc. Am, Vol. 21, pp. 323-330, July 1949.

[16] Beranek, L.L., *Acoustics*, McGraw-Hill, 1954.

[17] Olson, H. F., *Elements of Acoustical Engineering*, van Nostrand, 1957.

[18] Eisner, E., “Complete Solutions of the “Webster” Horn Equation”, J. Acoustic Soc. Am., 41, pp. 1126-1145. (Apr. 1967)

[19] Bernoulli, D., “Physical, Mechanical, and Analytic Researches on Sound and on the Tones of Differently Constructed Organ Pipes,” (in French) Mémoires de l’Academie Scientifique, pp. 431-485. (1764)

[20] Wente, E. C. and Thuras, A. L., “Auditory Perspective – Loudspeakers and Microphones”, Jour. Trans. AIEE, Vol. 53, pp. 17-24, Jan. 1934; reprinted J. Audio Eng. Soc., Vol. 26, pp. 518-525, July-August 1978.

[21] Klipsch, P.W., "A Low-Frequency Horn of Small Dimensions", J. Audio Eng. Soc., March 1979, Vol. 27, No. 3, p.141-148. (Reprint of article from J. Acoust. Soc. Am, Vol. 13, pp. 137-144, 1941 October)

[22] Klipsch, P. W., *La Scala*, Audio Engineering Society Preprint No. 372, April, 1965.

[23] Plach, D.J. "Design Factors in Horn-Type Speakers", J. Audio Eng. Soc., Vol. 1, pp. 276-281, October 1953.

[24] Leach, W. M. Jr., "On the Specification of Moving-Coil Drivers for Low-Frequency Horn-Loaded Loudspeakers", J. Audio Eng. Soc., Vol. 27, No. 12, pp. 950-959, 1979 December.

[25] Leach, W. M. Jr., "Author's Reply to Comments by E. F. McClain", J. Audio Eng. Soc., Vol. 29, pp. 523-524, 1981.

[26] Edgar, B., "The Show Horn", Speaker Builder 2/90, 1990.

[27] Olson, H. F. and Massa, F., "A High-Quality Ribbon Receiver", Jour. Acous. Soc. Am., Vol. 8, No. 1, 1936, pp. 48-52.

[28] Hilliard, J. K., "A Study of Theatre Loud Speakers and the Resultant Development of the Shearer Two-Way Horn System", Tech. Bul. Acad. Res. Conv., March, 1936, pp. 1-15.

[29] Keele, D.B.,Jr., "What's So Sacred about Exponential Horns", presented at the 51st Convention of the Audio Eng. Soc., Vol. 23, p.492, 1975 July/Aug.

[30] Keele, D.B.,Jr., "Optimum Horn Mouth Size" presented at the 46th Convention of the Audio Eng. Soc., Vol. 21, p.748, 1973 November.

[31] Henricksen, C. A. & Ureda, M. S., “The Manta Ray Horns”, Loudspeakers Vol. 2 An Anthology, pp. 30-35, 1977.

[32] Ohtsuki, S. “Calculation Method for the Nearfield of a Sound Source with Ring Function”, J. Acoust. Soc. Japan., 1974, 30(2), 76–81.

[33] Backman, J. “Computation of Diffraction for Loudspeaker Enclosures”, Loudspeakers, Volume 3, An Anthology of Articles on Loudspeakers from the Journal of The Audio Engineering Society, (1984–1991), Vol. 32–Vol. 39, 65–83.

[34] Kaddour, A., Rouvaen, J. M. and Belbachir, M. F., “Simulation and visualization of loudspeaker's sound fields”, Electronic Journal “Technical Acoustics”, http://www.ejta.org, 2003, 21.

[35] Klippel, W., “Modeling the nonlinearities in horn loudspeakers”, J. Audio Eng. Soc. 44(6), 470–480, 1996.

[36] Klippel, W., “Nonlinear system identification for horn loudspeakers”, J. Audio Eng. Soc. 44(10), 811–820, 1996.

[37] Sheerin, J. H., “Acoustic Wavefront Mapping in Horn Bends”, JHS Audio (http://ldsg.snippets.org/HORNS/index.php), 1999.

[38] Dinsdale, J., “Horn Loudspeaker Design”, Wireless World, pp. 19-24, Mar 1974.

[39] Benade, A. H, Jansson, E. V., “On Plane and Spherical Waves in Horns with Nonuniform Flare I. Theory of Radiation, Resonance Frequencies, and Mode Conversion”, Acustica 31(2): 80-98, 1974.

[40] Rienstra, S. W., “The Webster Equation Revisited”, 8th AIAA/CEAS Aeroacoustics Conference, June 2002.

[41] Geddes, E.R, “Acoustic waveguide theory”, AES Preprint 2547, 83rd Convention, Oct 16-19 1987.

[42] Putland, G. R., “Every One-Parameter Acoustic Field Obeys Webster's Horn Equation”, Journal of the AES, Vol. 41, No. 6, pp. 435-448 (June 1993)

[43] Smith, B. H., “An Investigation of the Air Chamber of Horn Type Loudspeakers”, J. Acoustic Soc. Amer., Vol. 25 No.2, December 1952.

[44] Holland, K. R., Fahy, F. J. and Morfey, C. L., “Prediction and Measurement of the One-Parameter Behavior of Horns,” J. Audio Eng. Soc., 39, pp. 315-337. (May 1991)

[45] Firestone, F. A., “A new analogy between mechanical and electrical systems”, J. Acoust. Soc. Amer., vol. 4, pp. 249–267, 1933.

[46] Novak, J. F., “Performance of enclosures for low resonance high compliance loudspeakers”, Journal of the Audio Engineering Society, vol. 7, pp. 29-37, 1959.

[47] Small, R. H., “Closed-box loudspeaker systems, part i: Analysis”, Journal of the Audio Engineering Society, vol.20(10), pp. 798-808, December 1972.

[48] Small, R. H., “Direct-radiator loudspeaker system analysis”, Journal of the Audio Engineering Society, vol.20(5), pp. 383-395, June 1972.

[49] Small, R. H., “Closed-box loudspeaker systems, part ii: Synthesis”, Journal of the Audio Engineering Society, vol.21(1), pp. 11-18, February 1973.

[50] Small, R. H., “Simplified loudspeaker measurements at low frequencies”, Journal of the Audio Engineering Society, vol.20(1), pp. 28-33, January-February 1972.

[51] Thiele, A. N., “Loudspeakers in vented boxes: Part 1”, Journal of the Audio Engineering Society, vol.19(5), pp. 382-391, May 1971.

[52] Thiele, A. N., “Loudspeakers in vented boxes: Part 2”, Journal of the Audio Engineering Society, 19(6):471, June 1971.

[53] Thiele, A. N., “Loudspeakers, enclosures and equalizers. In Proceedings of the Institution of Radio and Electronics Engineers”, vol. 34, pp. 425-448, November 1973.

[54] Howard, R. C., “Acoustical Circuits Revisited,” Journal of the Audio Engineering Society, Vol. 20, No. 3., pp. 185-197, 1972.

[55] Werner, R. E. and Carrel, R. M., “Application of Negative Impedance Amplifiers to Loudspeaker Systems”, Journal of the Audio Engineering Society, vol. 6, no. 4, pp. 240-243, Oct.1958.

[56] Keele, D. B. Jr., “Low Frequency Horn Design Using Thiele/Small Design Parameters”, AES Preprint #1250, 1977.

[57] Tappan, P. W., “Analysis of a low-frequency loudspeaker system”, Journal of the Audio Engineering Society, vol.7(1), pp.38-46, January 1959.

[58] Kaizer, A. J. M., “Modeling of the nonlinear response of an electrodynamic loudspeaker by a volterra series expansion”, Journal of the Audio Engineering Society, vol.35(6), pp.421-433, June 1987.

[59] Klippel, W., “Dynamic measurement and interpretation of the nonlinear parameters of electrodynamic loudspeakers”, Journal of the Audio Engineering Society, vol. 38(12), pp. 944-955, December 1990.

[60] Klippel, W., “Nonlinear large-signal behavior of electrodynamic loudspeakers at low frequencies”, Journal of the Audio Engineering Society, vol. 40(6), pp.483-496, June 1992.

[61] Klippel, W., “The mirror filter-a new basis for reducing nonlinear distortion and equalizing response in woofer systems”, Journal of the Audio Engineering Society, vol.40(9), pp. 675-691, September 1992.

[62] Klippel, W., “Direct feedback linearization of nonlinear loudspeaker systems”, Journal of the Audio Engineering Society, vol. 46(6), pp.499-507, June 1998.

[63] Leach, Jr., W. M., “Electroacoustic-Analogous Circuit Models for Filled Enclosures”, J. Audio Engineering Soc., vol. 37, pp. 586–92, July/Aug 1989.

[64] Putland, G. R., “Modeling of Horns and Enclosures for Loudspeakers”, Department of Electrical and Computer Engineering University of Queensland, December 1994.

[65] Arai, M., “Study on Acoustic Filters by an Electric Simulator”, J. Acoustical Soc. of Japan, vol. 16, pp. 16–28. English abstract, 1960.

[66] Sherman, C. H. and Butler, J. L., “Analysis of harmonic distortion in electroacoustic transducers”, J. Acoustic Soc. Am. 98, 1596–1611, 1995.

[67] Sherman, C. H., Butler, J. L. and Butler, A. L., “Analysis of harmonic distortion in electroacoustic transducers under indirect drive conditions”, J. Acoustic Soc. Am. 101, 297-314, 1997.

[68] Schurer, H., Berkhoff, A. P., Slump, C. H. and Herrmann, O. E., “Modeling and compensation of nonlinear distortion in horn loudspeakers”, J. Audio Eng. Soc. 43 (7/8), 592–598, 1995.

[69] Al-Ali, K.M., “Loudspeakers: Modeling and Control”, University of California at Berkeley, 1999.

[70] Keele, D. B. Jr. “Low-frequency Loudspeaker Assessment by Nearfield Sound Pressure Measurement”, Loudspeakers, An Anthology of Articles on Loudspeakers from the Journal of The Audio Engineering Society, (1953–1977), Vol. 1–Vol. 25, 344–352.

[71] Kates, J. M. “Radiation from a Dome”, Loudspeakers, An Anthology of Articles on Loudspeakers from the Journal of The Audio Engineering Society, (1953–1977), Vol. 1–Vol. 25, 413–415.

[72] Suzuki, H., Tichy, J. “Radiation and Diffraction Effects by Convex and Concave Domes”, Loudspeakers, Volume 2, An Anthology of Articles on Loudspeakers from the Journal of The Audio Engineering Society, (1978–1983), Vol. 26–Vol. 31, 292–300.

[73] Suzuki, K., Nomoto, I. “Computerized Analysis and Observation of the Vibration Modes of a loudspeaker Cone”, Loudspeakers, Volume 2, An Anthology of Articles on Loudspeakers from the Journal of The Audio Engineering Society, (1978–1983), Vol. 26–Vol. 31, 301–309.

[74] Bruneau, A. M., Bruneau, M. “Electrodynamic Loudspeaker with Baffle: Motional Impedance and Radiation”, Loudspeakers, Volume 4, An Anthology of Articles on Loudspeakers from the Journal of The Audio Engineering Society, (1984–1991), Vol. 32– Vol. 39, 54–64.

[75] Kyouno, N., Sakai, S., Morita, S. “Acoustic radiation of a Horn loudspeaker by the Finite Element Method Acoustic characteristics of a Horn Loudspeaker with an Elastic Diaphragm”, Loudspeakers, Volume 2, An Anthology of Articles on Loudspeakers from the Journal of The Audio Engineering Society, (1978–1983), Vol. 26–Vol. 31, 364–373.

[76] Porterand, J., Tang, Y. “A Boundary–Element Approach to Finite-Element radiation Problems”, Loudspeakers, Volume 4, An Anthology of Articles on Loudspeakers from the Journal of The Audio Engineering Society, (1984–1991), Vol. 32–Vol. 39, 65–83.

[77] Kaizer, A. J. M., Leeuwestein, A. “Calculation of the Sound Radiation of a Nonrigid Loudspeaker Diaphragm Using the Finite-Element Method”, Loudspeakers, Volume 4, An Anthology of Articles on Loudspeakers from the Journal of The Audio Engineering Society, (1984–1991), Vol. 32–Vol. 39, 11–123.[19] Locanthi, B., “Application of Electric Circuit Anologies to Loudspeaker Design Problems” IEEE Trans Audio, Vol. PGA-6 (1952 March); reprinted in Loudspeakers (Audio Eng. Soc., New York, 1980), pp. 217-224.

[78] Stahl, K. E., “Synthesis of Loudspeaker Mechanical Parameters by Electrical Means: A New Method for Controlling Low-Frequency Loudspeaker Behavior”, Journal of the Audio Engineering Society, vol. 29, no. 9, pp. 587-596, Sept. 1981.

[79] Normandin, R., “Extended Low-Frequency Performance of Existing Loudspeaker Systems”, Journal of the Audio Engineering Society, vol. 32, no. 1/2, pp. 18-22, Jan. 1984.

[80] Bortoni, R., “Damping Factor: An Introductory Treatment”, IV. Brazilian AES Convention, São Paulo, Brazil, June 2000.

[81] Bortoni, R., Filho, S. N., Seara, R., "Comparative Analysis of Moving-Coil Loudspeakers Driven by Voltage and Current Sources", Audio Eng. Society, 115th Convention, New York, Oct. 2003.

[82] Behler, G. K. and Makarski, M., "Two-port representation of the connection between horn driver and horn", JAES, 51(10), 2003.

[83] Makarski, M., "Determining Two-Port Parameters of Horn Drivers using only electrical Measurements", Audio Eng. Society, 116th Convention, May 2004.

[84] Sakai, S., Kagawa, Y. & Yamabuchi, T., "Acoustic Field in an Enclosure and Its Effect on Sound-Pressure Responses of a Loudspeaker", J. Audio Engineering Soc., vol. 32, pp. 218–27, April 1984.

[85] Kinsler, L. E., Frey, A. R., Coppens, A. B. And Sanders, J. V., *Fundamentals of Acoustics*, New York, NY: John Wiley and Sons, Inc., 1999.

[86] King, M. J., "Mathematical Model for the One Dimensional Exponential Horn", Quarter Wavelength Loudspeaker Design Gallery, Aug. 2004.

[87] Keele, D., B., Jr., "Maximum Efficiency of Compression Drivers", Audio eng. Soc., 117th Convention, California, Oct. 2004.

[88] Atherton, M. A. and Bates, R. A., "Bond Graph Analysis in Robust Engineering Design", Qual. Reliab. Eng. Int. 2000; 16:325-335.

[89] Platin, B. E., Çalışkan, M. and Özgüven H. N., *Dynamics of Engineering Systems*, METU, Ankara, June 1988.

Appendix A

Sample Codes Written in Pascal Language

Code A.1

```
Sx:=St;        (dummy variable)
Lt:=0.01;      (mm)
while Sx<Sm do
begin
Sx:=St*sqr(cosh(Lt/x0)+T4*sinh(Lt/x0));
Lt:=Lt+0.01;
end;
```

Code A.2

```
L1:=2/5*Lt;                (Length of horn until the bending part)
LF:=1/5*Lt;                (Length of bending part)
R2:=R1;

Repeat                     (Calculation of R2)
err:=RM*Ln((RM+Sqrt(RM* RM-RT* RT))/ RT)-Sqrt((RM*RM - RT*RT))-
RM*Ln((RM +Sqrt(RM * RM -R2*R2))/R2)+Sqrt((RM*RM-R2*R2))-L1-LF;
R2:=R2+0.001;
until abs(err)<0.01;
RM2:=LF/pi;                (transformation eqn. from the Cartesian to the polar coord.)

For i:= 40 To 59 do
begin
R2[i]:=R2-(R2-R1)*(59-i)/19;
d[i]:=(Rm2+Sqrt(Rm2*Rm2-R2[i]*R2[i]))/R2[i];
x1[i]:=Rm2*Ln((Rm2+Sqrt(Rm2*Rm2-Rt2*Rt2))/Rt2)-Sqrt((Rm2*Rm2-Rt2*Rt2))-
(Rm2*Ln(d[i])-Sqrt((Rm2*Rm2-R2[i]*R2[i])))-L1;
```

```
                                    (x1 is the arc length calculated from tractrix formulae)
teta[i]:=x1[i]/RM2;                 (appropriate bend angle for the arc length)
x[i]:= L1+R2[i]*sin(teta[i]);       (x coordinates of horn contour during the bend)
R22[i]:=sqrt(pi*sqr(R2[i]))/2;
y[i]:= R22[40]-R22[i]*cos(teta[i]); (y coordinates of horn contour during the bend)
z[i]:= R22[40]-R22[i]*cos(teta[i]); (z coordinates of horn contour during the bend)
end;
```

Appendix B

Bond Graph Model of Loudspeaker

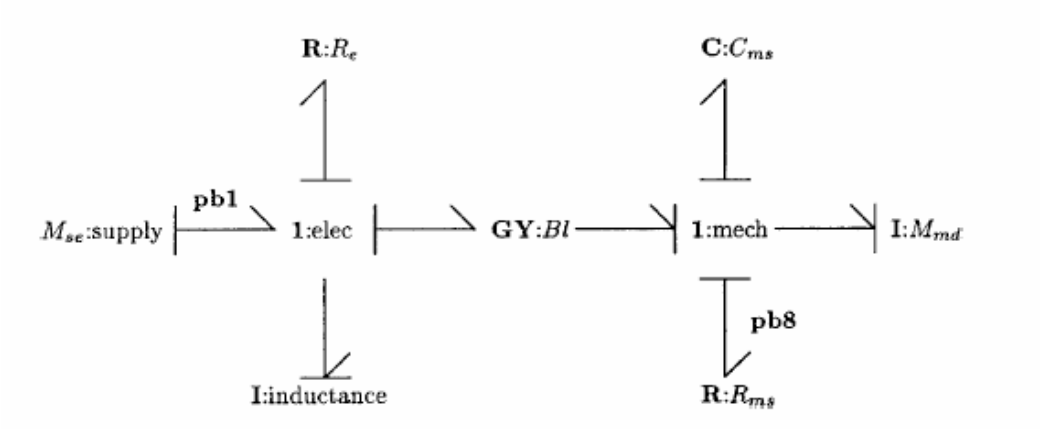

Fig. B.1 Example of a bond graph model of a loudspeaker. [88, Fig. 3]

Appendix C

Definitions and Equations for Linear Graph Modeling

Table C.1 Definition of ideal source type [89, Table 2.1]

Energy Domain	A-Type Active Elements	T-Type Active Elements
	Across Variable v_{21}	Through Variable f
Mechanical Translation	Velocity v(t)	Force f(t)
Mechanical Rotation	Angular velocity ω(t)	Torque T(t)
Electrical	Voltage e(t)	Current i(t)
Fluid	Pressure p(t)	Flow Q(t)

Table C.2 Elemental relationships for ideal D-Type element. [89, Table 2.2]

Element	Elemental Equations		Power Dissipated
	$f = \frac{1}{R} v_{21}$	$v_{21} = Rf$	$P = \frac{1}{R} v_{21}^2 = Rf^2$
Translational Damper	$F = bu$	$u = \frac{1}{b} F$	$P = bu^2 = \frac{1}{b} F^2$
Rotational Damper	$T = b_r \omega$	$\omega = \frac{1}{b_r} T$	$P = b_r \omega^2 = \frac{1}{b_r} T^2$
Electrical Resistance	$i = \frac{1}{R} e$	$e = Ri$	$P = \frac{1}{R} e^2 = Ri^2$
Fluid Resistance	$Q = \frac{1}{R_f} p$	$p = R_f Q$	$P = \frac{1}{R_f} p^2 = R_f Q^2$

Table C.3 Elemental relationships for ideal A-Type elements. [89, Table 2.2]

Element	Constitutive Equations	Elemental Equations	Energy Stored
	$h = Cv_{21}$	$f = C\frac{dv_{21}}{dt}$	$E = \frac{1}{2}Cv_{21}^{2}$
Translational Mass	$p = mv$	$F = m\frac{dv}{dt}$	$E = \frac{1}{2}mv^{2}$
Rotational Inertia	$h = J\omega$	$T = J\frac{d\omega}{dt}$	$E = \frac{1}{2}J\omega^{2}$
Electrical Capacitance	$q = Ce$	$i = C\frac{de}{dt}$	$E = \frac{1}{2}Ce^{2}$
Fluid Capacitance	$V = C_f p$	$Q = C_f \frac{dp}{dt}$	$E = \frac{1}{2}C_f p^{2}$

Table C.4 Elemental relationships for ideal T-Type elements. [89, Table 2.2]

Element	Constitutive Equations	Elemental Equations	Energy Stored
	$x_{21} = Lf$	$v_{21} = L\frac{df}{dt}$	$E = \frac{1}{2}Lf^2$
Translational Spring	$x = \frac{1}{k}F$	$v = \frac{1}{k}\frac{dF}{dt}$	$E = \frac{1}{2k}F^2$
Rotational Spring	$\theta = \frac{1}{k_r}T$	$\omega = \frac{1}{k_r}\frac{dT}{dt}$	$E = \frac{1}{2k_r}T^2$
Electrical Inductance	$\chi = Li$	$e = L\frac{di}{dt}$	$E = \frac{1}{2}Li^2$
Fluid Inductance	$\Gamma = I_f Q$	$p = I_f\frac{dQ}{dt}$	$E = \frac{1}{2}I_f Q^2$

Appendix D

Typical Properties of Polypropylene

Density: 0.905 g/cm^3

Tensile Strength: 4800 psi / 33.1 MPa

Tensile Modulus: 195000 psi / 1344.5 MPa

Tensile Elongation at Yield: 12 %

Flexural Strength: 7000 psi / 48.3 MPa

Flexural Modulus: 180000 psi / 1241.1 MPa

Compressive Strength: 7000 psi / 48.3 MPa

Hardness Rockwell R: 92

IZOD Notched Impact: 1.9 ft-lb/in / 101.4 J/m